Public University of Navarra

Department of Electric and Electronic Engineering

New multiplexing structures for fiber optic sensors

PhD dissertation by

Daniel Leandro González

Advisors

Prof. Dr. Manuel López-Amo Sainz

Dr. Silvia Díaz Lucas

Pamplona, 2016

Reconocimientos

Este trabajo se ha llevado a cabo gracias a las aportaciones económicas recibidas de los siguientes organismos y proyectos:

- Universidad Pública de Navarra mediante la ayuda de investigación predoctoral, la ayuda para movilidad y las ayudas complementarias a tesis doctorales.
- Proyecto de investigación TEC2010-20224-C02-01 del Ministerio de Economía y Competitividad de España
- Proyecto de investigación *TEC2013-47264-C2-2-R* del Ministerio de Economía y Competitividad de España a través del Fondo Europeo de Desarrollo Regional (FEDER).
- Acción Europea "*COST- TD1001: Novel and Reliable Optical Fibre Sensor Systems for Future Security and Safety Applications (OFSeSa)"*
- Proyecto INTERREG SUDOE Project "*ECOAL-MGT - Ecological Management of Coal Waste Piles, SOE3/P2/P714"*
- Ministerio de Economía y Competitividad de España a través del Proyecto campus de excelencia-Iberus (Innocampus).
- Grupo de investigación Comunicaciones Ópticas y Aplicaciones Electrónicas de la Universidad Pública de Navarra mediante la financiación de material y participación en congresos.

Introduction

Abstract

Fiber optic technology has been subject of an intense evolution during last decades due to their high capacities in communication applications. Taking advantage of this scientific and technical development, fiber optic sensors have emerged as a flexible solution to overcome some of the main limitations of conventional sensors. E.g., fiber optic is chemically inert and electromagnetically passive; accordingly, fiber optic sensors can operate in explosive environments such as fuel tanks or under high electric fields. Other important properties of fiber optic sensors include compactness, small size, light weight and low intensity noise among others. These properties have been exploited in multiple applications, being particularly successful the sensing solutions based on fiber Bragg gratings and interferometric fiber optic gyroscopes.

Numerous sensing approaches based on fiber optic sensors have been presented up to date, using different transducer mechanisms, interrogation or multiplexing techniques, etc. However, there are still some aspects to be improved. Possibly the most important drawback of fiber sensors is the relatively high cost compared with other well stablished technologies. Taking this into consideration, multiplexing techniques are especially important due to their inherent cost reduction per sensing element. Several multiplexing techniques can be employed depending on the type of sensor and the requirements of the application. For example, fiber Bragg gratings are particularly well suited for wavelength division multiplexing, while interferometric sensors usually require more complex approaches. In addition to reducing the cost, other factors of fiber optic sensors should be improved as well, such as signal-to-noise ratio, resolution, stability and remote long-distance operation among others.

In this framework, this thesis intends to contribute to the development of new optical fiber sensor networks, particularly focusing on the multiplexing capability. In accordance, interferometric and fiber Bragg grating sensors have been multiplexed in a variety of fiber optics networks. These networks comprise multiple approaches that can be divided in two main groups: passive networks for interferometric sensor multiplexing and active networks based on fiber lasers. Besides multiplexing capability, multiple factors are also investigated in the different contributions, such as single-longitudinal mode operation, remote interrogation or high-resolution measurements. Additionally, the properties of random distributed feedback fiber lasers have been analyzed for sensing applications.

The work performed during this thesis has been developed in the Optical Communication group at the *Universidad Pública de Navarra* (UPNA) under the doctorate program *Communication Technology*, for the degree of Doctor of Philosophy (Ph.D.) in Telecommunication Engineering. It should be mentioned that this work has been partially developed during a research stay performed at City London University under the guidance of Prof. Dr. Tong Sun.

Resumen

El campo de la fibra óptica ha sufrido una rápida evolución durante las últimas décadas debido a sus buenas prestaciones en aplicaciones de telecomunicaciones. Aprovechando este avance científico y técnico en componentes fotónicos, los sensores de fibra óptica han emergido como una solución flexible para solventar algunas de las principales limitaciones sufridas por los sensores convencionales. Por ejemplo, la fibra óptica es químicamente inerte y electromagnéticamente pasiva. Por lo tanto, puede trabajar en entornos explosivos como depósitos de combustible, o con campos eléctricos intensos. Otra cualidad importante de los sensores de fibra óptica es que son compactos, pequeños, ligeros e inducen un bajo ruido de intensidad. Estas propiedades se han aprovechado en diferentes aplicaciones, siendo particularmente exitosos los giróscopos de fibra óptica y las soluciones basadas en redes de difracción de Bragg.

Se han presentado hasta la fecha numerosos planteamientos para interrogar sensores de fibra óptica, utilizando diferentes mecanismos de transducción, técnicas de multiplexación o interrogación, etc. Sin embargo, todavía quedan algunos aspectos que mejorar. Posiblemente, el mayor inconveniente de los sensores de fibra, comparados con otras tecnologías asentadas, sea su coste relativamente alto. Teniendo esto en cuenta, las técnicas de multiplexación de sensores son especialmente importantes debido a que supone la reducción del coste por cada sensor. Se pueden utilizar diferentes técnicas de multiplexación dependiendo del tipo de sensor y de los requisitos de la aplicación. Por ejemplo, las redes de difracción de Bragg son especialmente adecuadas para utilizarse en multiplexación por longitud de onda, mientras que los sensores interferométricos normalmente requieren soluciones más complejas. Además de reducir el coste, hay otros factores de los sensores de fibra óptica que pueden mejorarse, como la relación señal-ruido, la resolución, la estabilidad y la interrogación remota a largas distancias entre otros.

En este contexto, esta tesis pretende contribuir al desarrollo de nuevas redes de sensores, haciendo especial hincapié en nuevas técnicas y topologías de multiplexación. De esta manera, se han multiplexado sensores interferométricos y redes de difracción Bragg siguiendo nuevos esquemas. Estas redes incluyen diferentes planteamientos, que pueden dividirse en dos grandes grupos: redes pasivas con multiplexación de sensores interferométricos y redes activas basadas en láseres de fibra. Además de las técnicas de multiplexación, también se han explorado otras alternativas, como la operación mono-frecuencia, la interrogación remota a largas distancias o la realización de medidas de alta resolución. Asimismo, se han analizado las capacidades de los láseres de fibra con reflectores distribuidos *random* para interrogación de sensores.

El trabajo realizado durante esta tesis se ha desarrollado en el Grupo de Comunicaciones Ópticas de la Universidad Pública de Navarra (UPNA), dentro del programa de doctorado de Tecnología de las Comunicaciones para la obtención del título de doctor en Ingeniería de Telecomunicación. Parte de este trabajo ha sido desarrollado durante una estancia de investigación en la *City London University* bajo la tutela de la Catedrático Dr. Tong Sun.

Thesis structure and personal contributions

The manuscript starts with this brief *Introduction* where a general overview of the research line is presented. In addition, the detailed contribution of the author to each work is shown. Following, the main body of the manuscript is divided in four chapters.

Chapter 1 summarizes the main principles and technologies used in the research work. Initially, the main types of fiber optic sensors are described, followed by the most important multiplexing techniques. A brief explanation of the main amplification types is also included due to their importance in the design of fiber lasers. Finally, it is incorporated the principle of operation and main types of fiber lasers.

In *Chapter 2*, a study about the multiplexing capabilities and adaptation to all-polarization maintaining of high-birefringence fiber loop mirror interferometers (HiBi FLM) is carried out. Initially, an introduction to the operating principle and interrogation techniques of fiber loop mirrors is included, followed by three original contributions:

- PAPER A: In this work two multiplexing structures based on HiBi FLM are validated as sensor networks by means of a fast Fourier transform interrogation technique. This author supervised the experiment, analyzed the experimental data and wrote the article.
- PAPER B: All polarization-maintaining versions of simple and two-section HiBi FLM structures are demonstrated theoretically and experimentally for high-resolution measurements. This author conceived the idea, performed the experiment, the simulations, analyzed the results and wrote the article.
- PAPER C: Multi-section HiBi FLM structures are validated as sensor networks without crosstalk, theoretically and experimentally. This author conceived the idea, performed the experiment, the simulations, analyzed the results and wrote the article.

Chapter 3 presents multiple schemes for exploiting the properties of fiber lasers in fiber optic sensing applications, mainly focusing on single-longitudinal mode and remote ultra-long operation. Firstly, a brief analysis of the use of fiber lasers in sensing applications is performed. Afterward, four original contributions are included:

- PAPER D: An erbium-doped fiber laser is designed to multiplex the temperature and strain information in the amplitude and wavelength of a single emission line. This author conceived the idea, performed the experiment, analyzed the results and wrote the article.
- PAPER E: A multi-wavelength single-longitudinal mode erbium-doped fiber laser is validated in L-band for sensing purposes showing improved stability. This author supervised the experiment and collaborated in the analysis of the results and the writing of the article.
- PAPER F: The versatility of DWDMs in the design of fiber lasers is shown by validating two fiber laser schemes: a multi-wavelength single-longitudinal mode erbium-doped fiber laser and a Raman multi-wavelength fiber laser for remote sensor monitoring (100 km). This author conceived the idea, supervised the experiment, analyzed the results and wrote the article.

- PAPER G: A fiber laser for remote sensor monitoring (155 km) based on Raman, Brillouin and erbium-doped fiber amplification is demonstrated as multiplexing scheme. This author performed the experiment, analyzed the results and collaborated writing the article.

In *Chapter 4* the particular properties of random distributed feedback fiber laser with respect to conventional fiber lasers are analyzed and exploited for sensing applications. The principle of operation of random fiber lasers and main properties are described in the first section, followed by three original contributions:

- PAPER H: In this work, a narrow-linewidth random fiber laser is presented, improving the linewidth of the narrowest random laser reported in almost ten times. This author conceived the idea, performed the experiment, analyzed the results and wrote the article.
- PAPER I: Based on the previous contribution, a narrow-linewidth random fiber laser is validated as high-resolution temperature and strain sensor. This author conceived the idea, supervised the experiment, analyzed the results and wrote the article.
- PAPER J: In this work, hybrid TDM/WDM sensor multiplexing in a 200 km-long sensor network is achieved, relying on optical time domain reflectometry in a lasing cavity. This scheme presents superior multiplexing flexibility than other long-range measurement systems in terms of position, wavelength and type of sensors multiplexed. This author conceived the idea, performed the experiment, analyzed the results and wrote the article.

Finally, the manuscript concludes with the main *conclusions and future research lines* where a brief summary of the research is reported. An appendix is included at the end of the document where all the *author contributions* are listed. Besides the main articles [PAPER A]-[PAPER J] mentioned in the thesis, additional journal articles [JOUR 11]-[JOUR 12] and conference contributions [CONF 1]-[CONF 15] are also referenced.

List of figures

List of acronyms

ASE	Amplified spontaneous emission
BOTDA	Brillouin optical time-domain analysis
CDM	Coherence-division multiplexing
CW	Continuous wave
DCF	Dispersion compensation fiber
DFB	Distributed feedback
DMUX/MUX	Wavelength-division demultiplexer/multiplexer
DWDM	Dense wavelength division multiplexing
EDF	Erbium-doped fiber
EDFA	Erbium-doped fiber amplifiers
EDFL	Erbium-doped fiber lasers
FBG	Fiber Bragg grating
FDM	Frequency division multiplexing
FFT	Fast Fourier transform
FLM	Fiber loop mirror
FOG	Fiber optic gyroscope
FPI	Fabry-Pérot interferometer
FRR	Fiber optic ring resonators
FSR	Free spectral range
FWHM	Full width at half maximum
FWM	Four Wave Mixing
HiBi	High-birefringence
LPG	Long period grating
MI	Michelson interferometer
MOF	Microstructured optical fiber
MZI	Mach-Zehnder interferometer
OADM	Optical add and drops multiplexers
OCDR	Optical coherence domain reflectometry
OFDR	Optical frequency-domain reflectometry
OSNR	Optical signal-to-noise ratio

OTDR	Optical time-domain reflectometry
PC	Polarization controller
PCF	Photonic crystal fiber
PM	Polarization maintaining
PS-FBG	Phase-shifter fiber Bragg grating
RDFL	Random distributed feedback fiber lasers
RFL	Raman fiber lasers
RS	Rayleigh scattering
SBS	Stimulated Brillouin scattering
SDM	Spatial division multiplexing
SFDM	Spatial-frequency division multiplexing
SLM	Single-longitudinal mode
SLM	Single-longitudinal mode
SMF	Single-mode fiber
SNR	Signal-to-noise ratio
SOA	Semiconductor optical amplifiers
SRS	Stimulated Raman scattering
TDM	Time-division multiplexing
TOF	Time of flight
WDM	Wavelength-division multiplexing

Chapter 3. Sensor schemes based on fiber lasers

Chapter 4. Investigation on random distributed feedback lasers for sensing applications

Chapter 1

Overview of the technologies employed

In this chapter, an overview of the basic technologies employed during the Ph.D. work is presented. Initially, the main properties and types of fiber optic sensors are described, followed by a brief introduction to sensor multiplexing. Next, the amplification processes employed in the lasers designed in this work are explained. Finally, a description of the operating principle, main properties and classification of fiber lasers is included.

1.1 Fiber optic sensors

1.1.1 Main properties

A fiber optic sensor can be defined as an optical fiber element that translates external changes of a measurand (physical, chemical, biological, etc.) into a modulation of one or several parameters of the light. Those changes are finally received at a detector which measures the variations. In this manner, a sensing system comprises four main elements:

- *Light source*: Typically laser or broad-band light sources are used to inject the light required for the sensor interrogation.
- *Optical communication channel*: Different fiber types and ranges can be used depending on the sensing approach. In some applications such as distributed sensing, the optical fiber can serve as both the channel and the transducer. In others, the optical fiber is just a communication channel, which can range from a few meters to hundreds of kilometers [1].
- *Optical transducer*: The fiber optic-based sensor itself. There are many types of sensors depending on the magnitude to be measured, the transduction nature, the modulation generated and the spatial distribution as presented in Table 1.1 [2].
- *Detector*: It is responsible of detecting the changes induced by the transducer in the input light. Again this time, the complexity greatly varies depending on the sensing solution/system.

The interest in fiber optic sensors relies on the fact that they overcome some of the main drawbacks of conventional sensors [3]. In addition, they open new possibilities in sensor monitoring including distributed temperature or strain sensing along tens of kilometers, which would be unaffordable using conventional techniques. Some of the key advantages of fiber optic sensors can be summarized as [4]:

- *Electromagnetically passive*: As a consequence they can be used in applications under high magnetic fields, radiation, or in explosive environments such as fuel tanks.
- *Chemically and biologically inert*: That implies that fiber optic sensors are immune to most chemical agents allowing them to work in harsh and corrosive environments. In addition, the biocompatibility and small size make fiber optic sensor suitable for biomedical applications.
- *Small size*: Due to the size and weight of optical fibers, small and light sensors can be designed, simplifying their integration in many applications.
- *High performance*: The sensitivity, resolution and dynamic range that fiber optic sensors can reach are potentially greater than the achieved by conventional sensors.
- *Remote monitoring*: Fiber optic sensors can be interrogated hundreds of kilometers away without external power supply due to the low loss of optical fiber. This is of special interest for sensors located at isolated or hostile places.
- *Multiplexing capability*: Depending on the sensor type, tens, hundreds or even thousands of sensors can be multiplexed in a single network, considerably reducing the cost of the system.

Nonetheless, fiber optic sensors also present some disadvantages that have to be taken into account. The main one is that even the cost is decreasing; it is generally higher than in other conventional technologies. In some other cases, optical sensors suffer from cross-sensitivity between measurands. This is evident for example in fiber Bragg gratings or distributed Brillouin-based sensing, which are affected by both temperature and strain. As a consequence, if strain monitoring is required, two sensors have to be used to discriminate temperature from strain changes. Taking all this into consideration, optical fiber sensors have found place in some market niches such as medicine, large composite and concrete structures, the electrical power industry, defense, aerospace, offshore, chemical sensing, gas and oil industry [5]. However, even presenting a higher performance, fiber optic sensors still have to compete against well-developed technologies in other fields [6].

In the next subsections, the most significant fiber optic sensors employed in this Ph.D. work are briefly described: fiber Bragg gratings, interferometric sensors and sensors based on microstructured and photonic crystal fiber.

FIBER OPTIC SENSORS			
Measurand	**Transduction nature**	**Induced modulation**	**Spatial distribution**
Electromagnetic	Intrinsic	Intensity	Point
Mechanical	Extrinsic	Phase	Distributed
Thermal		Wavelength	Quasi-distributed
Radiation		Polarization	
Chemical			
Flow, turbulence			
Biomedical			

Table 1.1. Classification of fiber optic sensors.

1.1.2 Fiber Bragg gratings

A fiber Bragg grating (FBG) is an optical device that presents a periodic variation of the refractive index along the fiber length (see Fig. 1.1). Depending on the nature of the FBG, they can behave as an optical filter in reflection, transmission or both. They have also been validated as fiber optic sensors for several parameters including as axial strain, temperature, vibrations, pressure, dynamic electric or magnetic fields and some chemical agents among others.

The principle of operation of a FBG is based on the Fresnel reflection, by which light traveling between two media is partially reflected. The central wavelength reflected in a FBG is defined by two times the effective refractive index of the core n_{eff} and the pitch Λ (period of the refractive index variation) as follows:

$$\lambda_B = 2\, n_{eff} \Lambda \qquad (1.1)$$

In this manner, light with wavelength λ_B entering the FBG will be reflected while every other wavelength will be transmitted as depicted in Fig.1.2. Other parameters of particular interest in a FBGs are the difference between the refractive index variations Δn of the core and the number of refractive index variations N. In general terms, higher Δn and N implies higher peak reflection; however, the bandwidth of the FBG is also proportional to Δn so achieving narrow and high-reflective gratings is not straightforward. Many types of FBGs can be designed depending on the length, the periodic structure of the refractive index variations (uniform, chirped, tilted, etc.) or the shape of the variations (positive-only, apodized, phase shifted, etc.). Extended information about FBGs can be found in [7]. Regarding the sensing capabilities of fiber Bragg gratings, their most important sensing applications are as temperature and axial strain sensor.

Taking into account that the Bragg wavelength is given by (1.1), changes induced in both n_{eff} and Λ by temperature or strain can be detected just by monitoring λ_B. In the case of axial strain, it directly affects the pitch Λ of the FBG but it also modifies the effective refractive index n_{eff} due to photo-elastic effects.

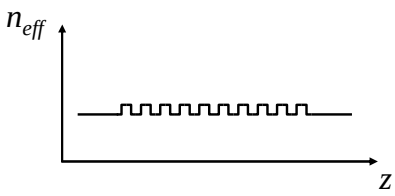

Fig.1.1. Refractive index profile of a fiber Bragg grating.

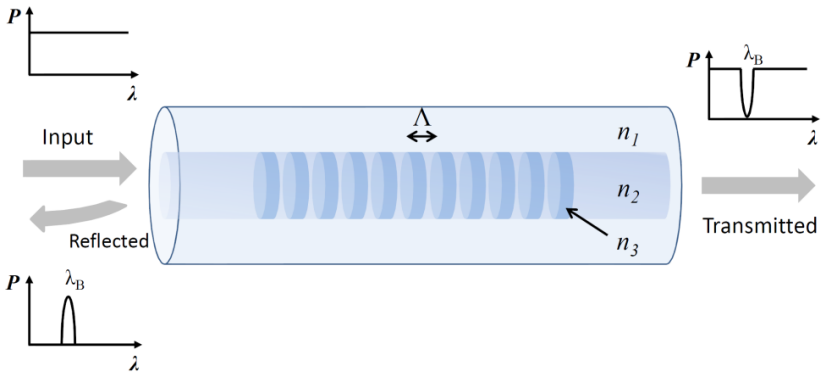

Fig. 1.2. Basic operating principle of a fiber Bragg grating.

As a result, the relative wavelength shift $\Delta\lambda_B$ induced by an axial strain variation $\Delta\varepsilon$ can be expressed as:

$$\Delta\lambda_B = \lambda_B\left(1-\rho_\alpha\right)\Delta\varepsilon \tag{1.2}$$

Being ρ_α the photo-elastic coefficient:

$$\rho_\alpha = \frac{n^2}{2}\left[\rho_{12}-\upsilon\left(\rho_{11}+\rho_{12}\right)\right] \tag{1.3}$$

Where n is the refractive index of the core, ρ_{12} and ρ_{11} are components of the optical fiber strain-optic tensor and υ is the Poisson's ratio. Common values for those constants are ρ_{12} = 0.252, ρ_{11}=0.113 and υ = 0.16. Consequently, it can be derived from (1.2) and (1.3) a sensitivity around 1.2 pm/με for standard single-mode fiber in the C-band (around 1550 nm) [8].

Equivalently, the response to temperature of a FBG can be also derived from:

$$\Delta\lambda_B = \lambda_B\left(\alpha+\xi\right)\Delta T \tag{1.4}$$

Where α represents the thermal expansion coefficient and ξ is the thermo-optic coefficient; being this last the most influential parameter in the sensitivity of FBGs to temperature. Typical values for temperature sensitivities are around 10 pm/°C at 1550 nm [9].

As previously mentioned, one of the main problems of some fiber optic sensors is the crosstalk between measurands. It is evident considering (1.4) and (1.2), that there is cross-sensitivity between temperature and strain since both parameters modify the pitch and the effective refractive index of the FBG. The complete relationship between Bragg wavelength, temperature and strain can be written as:

$$\Delta\lambda_B = \lambda_B\left[\left(\alpha+\xi\right)\Delta T+\left(1-\rho_\alpha\right)\Delta\varepsilon\right] \tag{1.5}$$

Consequently, it is not possible to directly discriminate between Bragg wavelength shifts induced by temperature, strain, or both of them. Much research has been done in this respect using photonic crystal fibers combined with FBGs [10], long period gratings (LPGs) [11], multimode fibers combined with FBGs [12], superstructured-gratings formed by writing FBG on a long-period gratings [13] among many others.

Even though conventional FBGs are the most extended because of their wide applicability [9], there are many other types of fiber Bragg gratings with significantly different properties such as sensitivity, spectrum shape, bandwidth, etc. Two particular classes will be briefly described due to the importance in this Ph.D. work.

Phase-shifted fiber Bragg gratings

The concept of phase-shifted FBGs (PS-FBGs) originated from a technique used to tailor the transmission spectrum of distributed feedback semiconductor lasers and it was firstly proposed in 1976 by Haus and Shank [14]. This approach was also validated to design fiber Bragg gratings in 1994 by Agrawal and Radic [15].

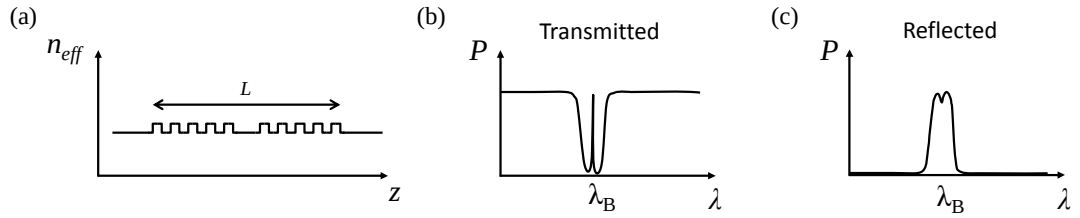

Fig. 1.3. (a) Refractive index profile of a phase-shifted fiber Bragg grating and its (b) transmitted and (c) reflected optical spectrum.

The main difference with simple FBGs is that the periodic index variation in the fiber core presents one or several phase shifts that modify the transmitted/reflected spectrum of the device. As a consequence, depending on the phase change and position, different narrow transmission peaks (bandwidth of several picometers) will arise in the rejected band of the transmitted spectrum. In the simplest case a Pi phase shifted can be included in $L/2$, supposing that L is the total length of the FBG as depicted in Fig. 1.3(a). As a result, a narrow transmission peak will appear in the middle of the notch band as represented in Fig. 1.3(b) and (c). Other configurations can be written in the FBG in order to attain a determined number of transmission peaks. For example, three transmission peaks can be achieved by including three phase shifts at the positions $L/4$, $L/2$ and $3L/4$ [15].

In the same manner as simple FBGs, PS-FBGs can also operate as fiber optic sensor but they are especially interesting used as narrow filters when combined with other filtering devices. In this work, the narrow bandwidth of π PS-FBGs will be used as wavelength selector (and high-resolution sensor) in fiber lasers.

Long period gratings

This particular type of fiber Bragg grating has a different operating principle than conventional FBGs like the described above. It was explained that FBGs have a sub-micron period so they couple light from the forward-propagating mode of the optical fiber to a backward counter-propagating mode [7]. However, in the case of long period gratings (LPGs), the period of the refractive index perturbations is much greater, in the range of 100 μm to 1 mm. Instead of reflecting back the light, they induce coupling between the propagating core mode and the co-propagating modes of the cladding. Due to the high losses of the cladding modes, attenuation bands appear at spectral regions given by the coupling at each cladding mode [16]. The attenuation bands will appear at a wavelength λ when the following condition is satisfied [17]:

$$\lambda = \left[n_{eff}(\lambda) - n^{i}_{clad}(\lambda) \right] \Lambda \qquad (1.6)$$

Where n_{eff} is the effective refractive index of the propagating core mode at wavelength λ, n^{i}_{clad} is the refractive index of the i-th cladding mode and Λ is the pitch of the LPG.

The transmitted spectrum will present attenuation bands at the different cladding modes-coupling, being the bandwidth of the filter of several nanometers; clearly overpassing typical bandwidth values of less than a nanometer for simple FBGs. As depicted in Fig. 1.4 there is not reflected light in the LPG response.

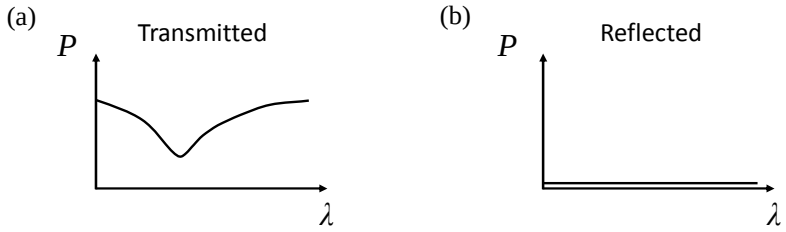

Fig. 1.4. (a) Transmitted and (b) reflected spectrum of a long-period grating.

Referring to the applicability of LPGs as sensors, they present different behavior than conventional FBGs. Even though the mechanisms that affect the wavelength of the LPG are the same (pitch variations, thermo-optic and strain-optic effects), the contributions of those variables vary depending on the order of the coupling modes. As a consequence, by an adequate choice of the LPG period it is possible to balance the contributions and obtain temperature or strain-insensitive sensors [18]. On the other hand, the sensitivities can be enhanced to achieve temperature or strain responses much higher than the offered by conventional FBGs (e.g. 2.75 nm/°C in [19]).

1.1.3 Interferometric fiber optic sensors

Interferometric fiber optic sensors have emerged as the natural advance of well-developed measurement devices in bulk optics [20]. This sensing technique relies on the principle of superposition to combine electromagnetic waves so the result of this combination somehow represents the relative phase between the waves. For example, the combination of two waves with equal frequency and dissimilar phase will result in an interference pattern dependent on the relative phase between them. Using different approaches, this relative phase can be modified by external agents including strain, vibration, temperature, etc. Consequently, interferometric fiber optic sensors can be exploited in a variety of sensing applications such as real time monitoring of deformation, fiber optic gyroscopes, magnetometers, etc. [21]. Compared to other technologies, this solution offers large dynamic ranges, and high accuracy and sensitivity [22].

Diverse interferometric approaches have been reported up to date, being the most important: Fabry-Pérot, Mach-Zehnder, Michelson, ring resonator and Sagnac interferometer. Before briefly describing the types it must be said that in every case it is considered that the coherence time of the laser source is much higher that the differential delay between waves.

Fabry-Pérot interferometer

A fiber Fabry-Pérot interferometer (FPI) is typically composed by two reflecting parallel surfaces with some space between them. As explained in the Fabry-Pérot cavity subsection in fiber lasers, interference arises due to the multiple combinations of the reflected and transmitted waves between the reflectors. Two main classes of FPI sensors can be defined [22]:

- Extrinsic: It employs the reflection from an external cavity created out of the optical fiber [23] as depicted in Fig. 1.5(a) for an air cavity. High finesse values can be attained by using high reflecting mirrors [24]. Additionally, extrinsic FPI are relatively simple and cost-effective. On the other hand, they present low coupling efficiency, require alignment and their packaging is not simple [25].

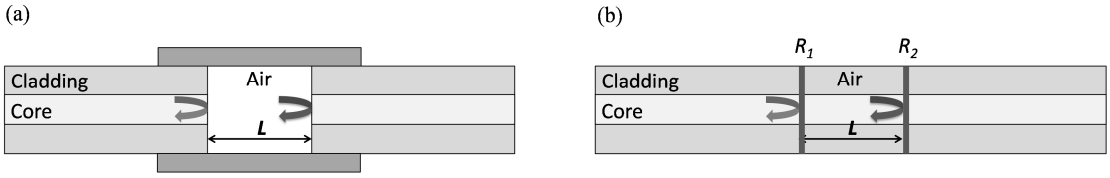

Fig. 1.5. Schematic of an (a) extrinsic and (b) intrinsic Fabry-Pérot interferometer.

- Intrinsic: The cavity in this case is formed in the fiber itself as can be seen in Fig. 1.5(b). There are many solutions that can be used to generate the cavity such as fiber Bragg gratings [26], chemical etching [27], micro machining [28] and thin film deposition [29] among others.

The transfer function of a Fabry-Pérot interferometer is given by [30]:

$$T = \frac{1}{1 + F\sin^2(\phi/2)} \tag{1.7}$$

Where F is the finesse, related with the reflectivity inside the cavity in the following manner:

$$F = \frac{4R}{(1-R)^2} \tag{1.8}$$

And ϕ is the phase difference given by:

$$\phi = \frac{2\pi}{\lambda} 2nL \tag{1.9}$$

Being λ the wavelength of the incident light, n the refractive index in the cavity and L is the length of the cavity. The simulated transfer functions of two FPI interferometers with finesse values of 1 and 100 are displayed in Fig. 1.6. It should be noted that for low finesse values (i.e. low reflectivity inside the cavity) the transfer function can be approximated to a cosine function. In this manner, for a FPI operating in reflection with a low reflectivity (R<5%) the transfer function is very similar to the obtained in two-beam interferometers:

$$T = \left[R + R(1-R)^2 + 2R(1-R)\right]\cos\phi \tag{1.10}$$

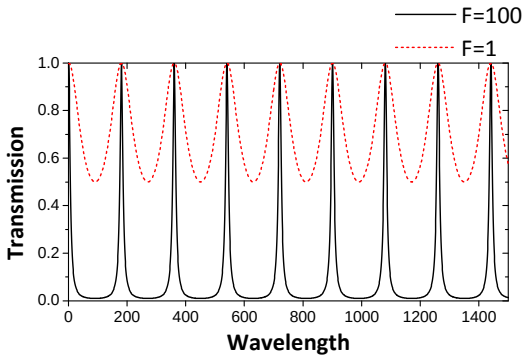

Fig. 1.6. Simulated spectral response of a Fabry-Pérot interferometer with finesse 100 (black) and 1 (red).

Considering (1.9) it is clear that variations in the cavity length or in the refractive index will be reflected in the transfer spectrum of the FPI. Therefore, physical variations that modify one or both parameters can be detected and measured by the system.

Mach-Zehnder interferometer

In a Mach-Zehnder interferometer (MZI) the input light is split and redirected into two arms, one used as reference and the other exposed to the measurand. Another optical coupler is used to recombine the waves and obtain an interference pattern which will reflect the phase difference between the optical paths. Figure 1.7 presents the schematic of a MZI formed by two optical couplers.

The transfer functions obtained at each coupler port supposing ideal 50:50 optical couplers are as follows:

$$T_3 = \frac{1}{2}\left[1-\cos\left(\frac{2\pi}{\lambda}n\Delta L\right)\right]$$
$$T_4 = \frac{1}{2}\left[1+\cos\left(\frac{2\pi}{\lambda}n\Delta L\right)\right] \qquad (1.11)$$

Where ΔL is the path difference between L_1 and L_2. Thus, the transfer function in this case is independent of the length of each branch but only depends on the dissimilarity between the arms. In addition, the signal output at the ports 3 and 4 is in quadrature, effect that has been used to stabilize MZI against environmental phase shifts [31].

Many modifications of the basic setup have been presented for increasing the compactness, the sensitivity or for making the system sensitive to other physical parameters. In this manner, LPGs have been used instead of couplers for combining light propagating by the cladding modes with the light propagating internally [32]. Another approach employs fiber fused with a slight core mismatch so part of the light couples to the cladding [33]. Even though it is arguable that they are strictly MZIs, other tactics used to deflect light into the cladding include collapsing the air-holes of photonic crystal fiber (PCF) [33], inserting sections of multimode fiber [34], using a piece with smaller core [35] or tapering the optical fiber [36].

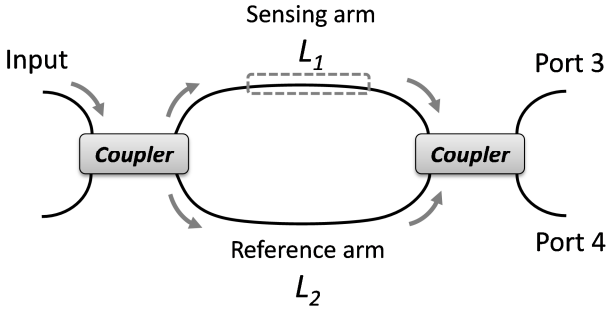

Fig. 1.7. Basic scheme of an all-fiber Mach-Zehnder interferometer.

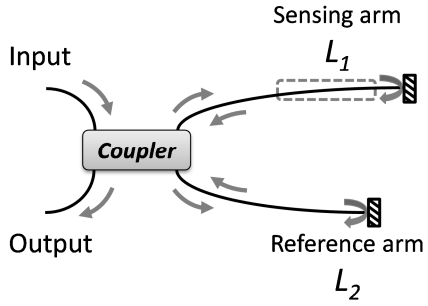

Fig. 1.8. Schematic of an all-fiber Michelson interferometer.

Michelson interferometer

Michelson interferometers (MIs) are very similar to Mach-Zehnder interferometers but instead of recombining the signals in a second optical coupler, they are reflected back using mirrored fiber ends so they interfere at the input coupler. A basic scheme can be seen in Fig. 1.8.

Similarly to MZIs, the transfer function of a Michelson interferometer is given by:

$$T = \frac{1}{2}\left[1 - \cos\left(\frac{2\pi}{\lambda} n 2\Delta L\right)\right] \tag{1.12}$$

However, in this case the period of the interference is given by two times the path difference. The main advantage of MI over MZI is the easier installation in practical applications, especially when the access to the measurand is difficult or dangerous. Additionally, they can also be multiplexed in parallel (unlike MZIs). On the other hand, the mirror used in the optical fiber might suffer degradation decreasing the visibility of the interference. In any case, fabrication techniques and topologies can be extrapolated from MZIs, such as using LPGs for coupling light into the cladding [37].

Ring resonator

Fiber optic ring resonators (FRR) are based on the constructive interference of light at the resonant wavelength (related to the ring's length) during multiple round-trips in the ring. The schematic of a ring resonator using an optical coupler can be seen in Fig. 1.9.

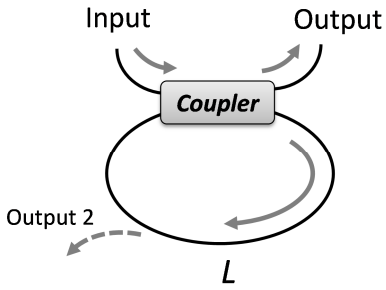

Fig. 1.9. Schematic setup of a ring resonator.

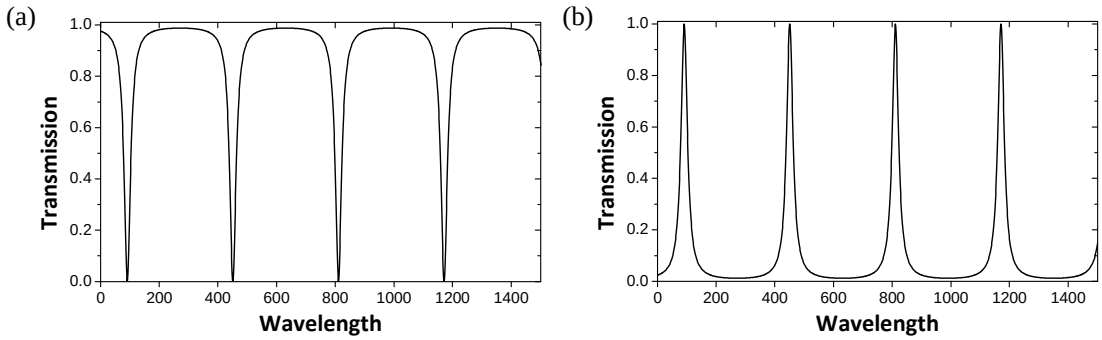

Fig. 1.10. Simulated spectral response of a ring resonator at (a) output 1 and (b) output 2 of Fig. 1.9.

The transfer function at the output port for the resonance condition is described as [38]:

$$T = 1 - \frac{\left(1-k_r\right)^2}{1+k_r^2+2k_r \sin\left(\frac{2\pi}{\lambda} nL\right)} \tag{1.13}$$

Where k_r is the coupling factor of the optical coupler and L is the length of the ring. Note that the response depends on the length of the ring, the refractive index of the fiber. As a result those parameters can be used for sensing applications [39]-[43]. The transfer function is in practice reasonably similar to the obtained for a Fabry-Pérot interferometer. It should be said that another optical coupler can be inserted to extract part of the light from the cavity (output 2 in Fig. 1.9), obtaining the complementary function 1-*T*. Simulation of both outputs are depicted in Fig. 1.10.

Sagnac interferometer

The composition of a Sagnac interferometer is very simple and consists of an optical coupler in which the output ports are connected between them as displayed in Fig. 1.11.

Neglecting birefringence, insertion loss and non-linearities, the transfer function of the device is directly related with the coupling factor *k* of the optical coupler. In addition, there is a function of the reflected light that is complementary to the transfer function. In this manner:

$$\begin{aligned} T &= \left(1-2k\right)^2 \\ R &= 1-T \end{aligned} \tag{1.14}$$

As a result, the system can act as a partial reflector with a reflectivity directly related to the coupling factor of the optical coupler. This simple device is also known as fiber loop mirror or reflector [44]

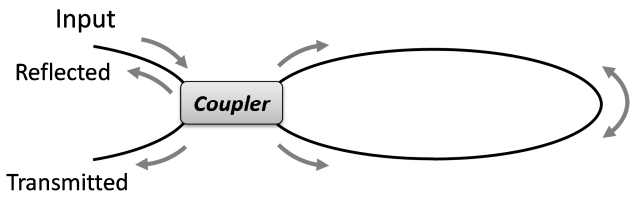

Fig. 1.11. Basic setup of a Sagnac interferometer.

Furthermore, if the interferometer is rotated, a phase shift is generated between the waves propagating in the clockwise and counter-clockwise. This phase shift $\Delta\phi_r$ is related with the time delay induced between the waves and it can be expressed as a function of the fiber length L, the diameter of the loop D (supposing a circular loop), the wavelength of operation λ, the speed of light c and the rotation speed Ω. Thus, the phase shift can be defined as follows:

$$\Delta\phi_r = \frac{2\pi c}{\lambda}\left(\tau_{cw} - \tau_{ccw}\right) = \frac{2\pi LD}{\lambda c}\Omega \tag{1.15}$$

As a consequence, the transfer function obtained including the phase shift between the waves is given by:

$$T = \frac{1}{2}\left(1-2k\right)^2\left(1+\cos\Delta\phi_r\right) = \left(1-2k\right)^2\left(\cos^2\frac{\Delta\phi_r}{2}\right) \tag{1.16}$$

Therefore, the Sagnac interferometer can straightforwardly detect rotation. This effect has been extensively exploited in the development of fiber optic gyroscopes (FOG), which are up to date one of the most successful applications of fiber optic sensors [45]. The sensitivity of a basic Sagnac interferometer to rotation is relatively small but as can be deducted from (1.15) that it can be improved by extending the length and diameter of the loop. Accordingly, FOGs typically use a multiple-loop interferometer. Many other modifications of the initial setup have significantly improved the performance of FOGs [45], also generating new interferometers for measuring many different parameters.

One of the most important types is based on including a section of high birefringence (HiBi) fiber in the loop. It is known as HiBi fiber loop mirror or simply Sagnac interferometer even though the interference is not caused in this case by the phase shift generated during a rotation. The operating principle this time relies on the phase shift induced between the polarization axes of the light traveling at different speeds in the HiBi fiber [44]. Consequently, due to the use of HiBi fiber for generating the interference, the sensing properties of the interferometer are considerably improved. The multiplexing capability of HiBi fiber loop mirrors and its adaptation to all-polarization maintaining fiber is presented in Chapter 2. A more detailed description of HiBi fiber loop mirrors can also be found there.

1.1.4 Microstructured and photonic crystal fiber sensors

In standard fiber optics, the guidance mechanism is based on the total internal reflection induced by the refractive index difference between the fiber core and cladding. Nonetheless, other approaches for confining the light within an optical fiber can additionally be attained. In 1996 the first photonic crystal fibers were presented, with a geometry defined by a periodic arrangement of longitudinal air holes in the optical fiber [46]. These fibers are known as microstructured optical fibers (MOF) while photonic crystal fibers (PCF) refer to microstructured fibers that use the photonic bandgap guidance mechanism [47]. However, there is not a clear distinction in literature, being microstructured fibers commonly named PCFs without considering the underlying guidance mechanism.

The properties and type of guiding principle of MOFs are mainly defined by four parameters: the diameter of the core, the diameter of the air holes, the distance between air-holes and the refractive index chosen for the fiber. Consequently, the election of those parameters will result

in different fiber types. There are two main guiding mechanisms exploited in MOFs: the index-guiding and bandgap-guidance. In general, index-guiding MOFs have a solid core and air holes in the cladding. Those air holes lower the effective refractive index of the fiber surrounding the solid core. In this manner, the light is guided by total internal reflection like in conventional fibers Fig. 1.12(a) [48]. The bandgap-guiding on the other hand confines the light inside a hollow core with a refractive index lower than the presented in the cladding. The bandgap is a consequence of multiple Bragg reflections in the transverse axis of the fiber that lead to the wavelength dependence in the transmitted light [49] as depicted in Fig. 1.12(b) [48]. These two classes can be divided into many subclasses depending on the optical properties and fiber structure [48].

In the case of MOFs, the mode behavior can be described by the V-parameter as in conventional step-index fibers. In a standard fiber, the V-parameter is related to the core radius, the wavelength of operation and the refractive indexes of the core and cladding. In the case of solid-core MOFs the formula is slightly different including the distance between holes instead of the core radius [50]:

$$V(\lambda) = \frac{2\pi}{\lambda}\Lambda\sqrt{n_{core}^2 - n_{clad}^2} \tag{1.17}$$

Where n_{core} and n_{clad} are the effective refractive indexes of the core and the cladding respectively and Λ represents the distance between air-holes. The V-parameter election determines not only the cut-off frequency and multimode/single-mode behavior, but also the confinement distribution in the core. This is of special interest for gas sensing applications, where the interaction between the gas filling the cladding holes is required [51].

It is clear that a MOF presents more parameters than conventional fibers to be considered in the fabrication process. As a result, diverse aspects of the propagation properties of the fiber can be tailored. That is the case of birefringence.

Birefringence can be defined as an optical property of a material that presents different refractive index depending on the transversal axe. Conventional single mode fibers are ideally circular in the traverse plain. Nevertheless, imperfections during the manufacturing process generate slight birefringence changes in the fiber so the polarization states in conventional single mode fiber are mostly unpredictable. To overcome this limitation, optical fibers can be designed to be highly-birefringent. In this manner, linearly polarized light appropriately coupled into the fiber preserve its polarization state along the length of fiber. Those fibers are known as polarization maintaining (PM) or high-birefringence (HiBi) fibers.

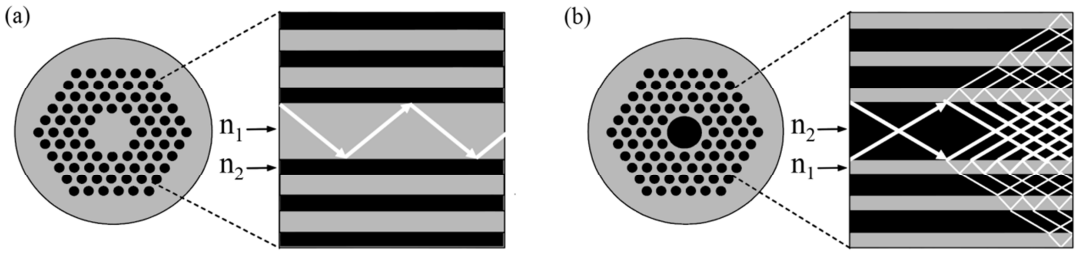

Fig. 1.12. Principle of operation of (a) index-guided and (b) bandgap-guided microstructured optical fiber.

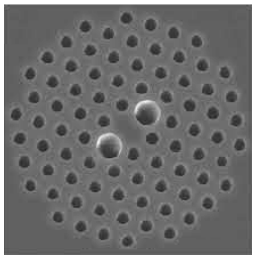

Fig. 1.13. Cross section of a high-birefringence microstructured optical fiber [53].

MOFs can be designed so that the polarization modes corresponding to the fast and slow birefringence axes exhibit high birefringence. It can be quantified using the modal birefringence, which can be expressed as:

$$B = \left| n_x - n_y \right| \tag{1.18}$$

Where n_x and n_y are the refractive indexes of the orthogonal modes. Another way of measuring birefringence is the beat-length that can be defined as the distance by which the polarization rotates 360 degrees: $L_b = \lambda / B$.

There are numerous manners of inducing birefringence in optical fibers, such as using an elliptical core or inserting other material rods for creating stress-induced birefringence (e.g. bow-tie or PANDA fibers). In MOFs, the effective refractive index of the polarization axes can be modified by varying the geometry of the air holes. The first HiBi microstructured fiber was presented in [52], obtaining a beat length of 0.4 mm at 1540 nm. In this Ph.D. work, a commercial HiBi microstructured fiber will be used as sensor device (Fig. 1.13).

Due to the high capabilities of MOFs for sensing, they have opened a wide spectrum of applications for sensing devices based on fiber optics. MOF-based sensors can be made to present negligible temperature sensitivity, which is of crucial importance for avoiding crosstalk in the strain measurements as previously commented. In addition, the air holes of the cladding and core can be filled with gas, modifying the guidance properties and allowing its detection. The fact that they are optical fiber permits their inclusion in all-fiber sensing schemes including fiber lasers of interferometers for enhanced detection/multiplexing. On the other hand, MOF sensors still present some weaknesses such as high losses, difficult handling and fragility. In any case, MOF sensors have been validated for measuring curvature [54], temperature [55], axial strain [56], magnetic field [57], electric field [58], vibration [59], pressure [60], torsion [61], refractive index [62], humidity [63][64], molecules [64], pH [65] and gases [66] among others.

1.2 Fiber optic sensor multiplexing

Multiplexing can be defined as the simultaneous transmission of multiple information channels along a common path [67]. However, in fiber optic sensor multiplexing, sensors can be multiplexed without sharing a common path or sharing just a section of this path. Consequently, a more general definition describe a multiplexed sensing system as a sensor network where the number of sources, channels or detectors is smaller than that which would be required if an equal number of sensing elements were assembled as individual measurement systems [68]. I.e. the key aspect of a multiplexing scheme is sharing elements of the network.

Multiplexing has been deeply developed in optical communications for improving the performance of telecommunication networks but it has also been considered in fiber optic sensing since the very first start. The most evident benefit in sensor multiplexing schemes is the reduction of the cost per sensing element by sharing the light source, the detectors or the fiber (which installation is sometimes the most expensive part of the system). One of the main drawbacks of fiber optic sensors compared with other technologies is typically their higher cost, which even though is decreasing with the development of equipment for optical communications, is still relatively high. Accordingly, sharing the cost per sensing element by means of multiplexing techniques is mandatory for increasing the competitiveness of fiber optic sensing. In this manner, numerous works are focused on this aspect of optical sensing, demonstrating the feasibility of interrogating hundreds or even thousands of sensors in a single network [69].

Another limitation of fiber optic sensors is the crosstalk between measurands. One of the most remarkable examples is the crosstalk between temperature and strain of fiber Bragg gratings. Consequently, instead of using two sensing systems, using multiplexing techniques for reducing as much as possible the number of elements needed for strain/temperature monitoring is highly necessary.

The design of the multiplexing solution strongly relies on the requirements of the network. In this manner, the cost, noise, dynamic range, type of measurand, number and finally, location of the sensors will define the approach used in each multiplexing scheme. For example, if multiple sensors have to monitor a single point, time-division multiplexing techniques, even possible would be initially less adequate. Another possible application might require long-distance monitoring; therefore, reducing the number of fibers installed would significantly decrease the cost.

There are three main aspects of multiplexing to be considered: the network topology, the type of modulation of the sensor and the multiplexing technique itself (i.e. the mechanism used for univocally identifying each sensor). Those three concepts are interrelated so by choosing a multiplexing approach, the type of sensors and topologies might be limited. In the following subsections the main multiplexing techniques will be described.

1.2.1 Wavelength-division multiplexing

In wavelength-division multiplexing (WDM) each sensor is identified by its wavelength location in the optical spectrum. This approach owes much of its success to its intense development in optical communications. Consequently, multiple devices related to WDM networks have become available and reduced their manufacturing costs. In general, WDM do not match the multiplexing capability of other approaches like time-division multiplexing (TDM), but it is a very flexible and simple solution, especially after the emergence of commercial optical fiber Bragg grating interrogators. Furthermore, hybrid WDM/TDM solutions can multiplex a large number of sensors, overpassing the maximum number achievable by other approaches [70]. One of the main advantages of WDM networks is the usually low crosstalk between sensors since their adequate band allocation is fairly simple.

Fiber Bragg gratings are the type of sensors most suitable for WDM schemes. However, since the sensor information is typically encoded in its wavelength, a guard-band between sensors is required. In this manner, high dynamic range of the FBG sensors will imply a wide guard-band to avoid crosstalk, reducing the maximum number of FBGs.

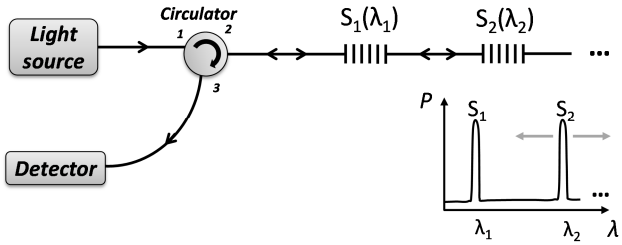

Fig. 1.14. Schematic of a WDM sensor network using FBGs in a serial topology.

A basic WDM network using FBGs is presented in Fig. 1.14. It consists of a usually broadband light source (it can also be a tunable laser) that interrogates an array of FBGs positioned in series. The reflected light is then redirected to a spectrum analyzer by a circulator. A schematic depiction of the obtained spectrum can be seen in the inset of Fig. 1.14, where the wavelength of each FBG encodes the sensing information.

It should be noted that FBGs operate in transmission as well; presenting a deep valley in the spectrum. Accordingly, the detector can be located at the end of the array so the information of the sensors should be retrieved by monitoring the wavelength shift of the valley [71]. The serial configuration is the most basic scheme but WDM can be used with almost any other topology.

On the other hand, other types of sensors can also be monitored in WDM networks. For example, intensity sensors can be interrogated in combination with wavelength-selecting devices such as fiber Bragg gratings or wavelength-division multiplexers. A simple solution is depicted in Fig. 1.15 where fiber Bragg gratings are used this time as wavelength selectors to reflect the intensity-modulated signal of the sensor. In the same manner, wavelength division multiplexers can be employed in combination with simple reflectors instead of FBGs. The main advantage of this approach is that dense wavelength division multiplexing can be employed since almost no guard-band is required. On the downside, it is usually required a reference signal to correct possible power fluctuations in the system.

Equivalently, WDM is able to interrogate interferometric sensors using wavelength-selecting components. However, monitoring the phase shift of the interference provided by an interferometer requires an optical band of several nanometers [72]. As a consequence, wavelength division (WDMs) or optical add and drops multiplexers (OADMs) are preferred. An example can be found in [73], where OADMs were used to interrogate (in amplitude) up to four fiber loop mirrors.

Summarizing, WDM is a simple technique that presents a moderate multiplexing capability that it is frequently used in combination with other approaches. Different types of sensors can be interrogated but it is always needed a wavelength-selective device such as a FBG, WDM or OADM. Multiplexing approaches that combine WDM and TDM have theoretically validated the feasibility of interrogating up to 1000 weak FBGs in a single network [74].

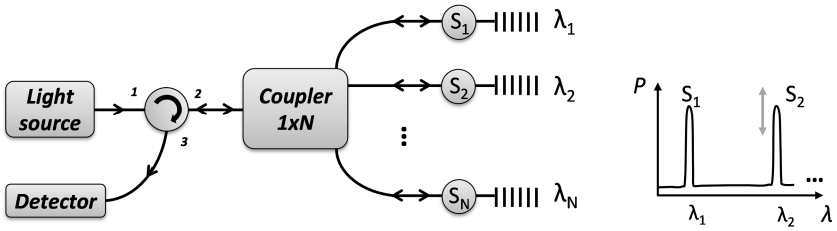

Fig. 1.15. Schematic of a WDM sensor network for interrogating intensity sensors in a parallel topology.

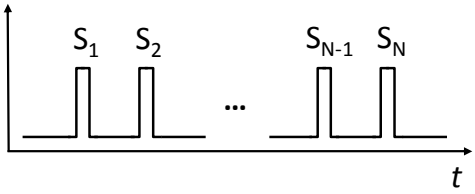

Fig. 1.16. Modulation format of time-division multiplexing.

1.2.2 Time-division multiplexing

Time-division multiplexing (TDM) is based on identifying each individual sensor by the time required for light to travel from the source to the detector across the sensor and the network (Fig. 1.16). This time lapse is known as time of flight (TOF). Depending on the properties of the network, if the sensing elements are located at different positions, the fiber length required might be enough for modifying the TOF between sensors. Otherwise, optical delay elements have to be used.

This is one of the firstly reported multiplexing techniques due to its simplicity, high efficiency and great multiplexing capability. Traditionally, this solution has been employed for monitoring interferometric and intensity-based sensors, but nowadays many other types of sensors can be interrogated by modifying the scheme or by using hybrid techniques. Several TDM approaches can be found such as [68]:

- Optical time-domain reflectometry (OTDR)
- Optical frequency-domain reflectometry (OFDR)
- Optical coherence domain reflectometry (OCDR)

Due to the utilization of OTDR techniques in the research work performed during this thesis, a brief description of its principle of operation is also included.

Optical time-domain reflectometry (OTDR)

The extensive deployment of fiber optic networks for optic communications resulted in the necessity of devices able to diagnose and detect failures or breaks in the fiber. One of these devices was the optical time-domain reflectometer, which can measure the loss and other reflective events of the optical fiber. The first proposal of such system was done by Barnoski and Jensen in 1976 [75].

The principle of operation of OTDRs can be understood as an adaptation of the radar to fiber optics [76]. In this manner, a pulsed optical source is injected in the fiber so the location of an event along the fiber under test is given by the time lapse between the pulse launch and the detection of the reflection. A simple scheme of an OTDR can be seen in Fig. 1.17.

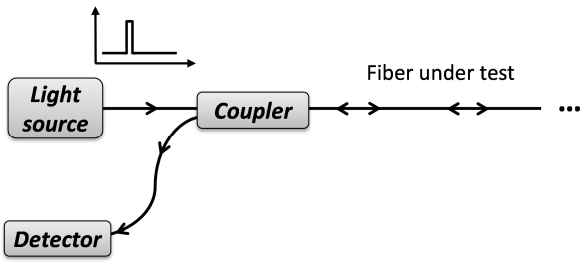

Fig. 1.17. Schematic of a basic OTDR system.

To further explain the operation of OTDRs it must be taken into account that at every point of the fiber, the optical power scattered is given by:

$$P_S(z) = \alpha_s P(z) = \alpha_s P_{in} e^{-z\alpha} \tag{1.19}$$

Where α_s is the scattering coefficient and *P(z)* is the light intensity at the position *z*, which is subsequently related to the input power P_{in} and the total loss α. A small amount of this scattered light, defined by the physical properties (numerical aperture and refractive index) of the fiber, is coupled back into the fiber. Accordingly the total backscattered power at a position *z* can be expressed as:

$$P_{BS}(z) = P_S(z) S = \alpha_S P_{in} e^{-\alpha z} S \tag{1.20}$$

Where $S=(NA/n)^2/4$ (for a step index fiber [77]) quantifies the amount of light coupled back. Finally, the power detected at the photodetector will travel twice the distance to the measured point. As a result, the OTDR detection trace will be defined as [78]:

$$P_{OTDR}(z) = \alpha_S P_{in} S \Delta z e^{-2\alpha z} \tag{1.21}$$

Where Δz is the spatial resolution, defined as:

$$\Delta z = \frac{\Delta t}{2 v_g} \tag{1.22}$$

Being v_g the group velocity and Δt the pulse duration. Consequently, the attenuation profile of the fiber can be measured, but also events like fiber splices, connectors, fiber breaks, etc. can be identified depending on the amount of power reflected and dissipated. For example, fiber connections can be identified by the Fresnel reflection and the fiber end by a high power loss reaching the noise floor (with or without reflection depending on the type of ending: angle cleaved, index matched, mirrored, etc.). An example of a typical OTDR trace is seen in Fig. 1.18.

The performance of an OTDR is mainly defined by two parameters: the dynamic range and the spatial resolution. The dynamic range quantifies the maximum loss that the system can detect; it consequently limits the maximum measurement distance. It is affected by the peak power of the input pulse and by the pulse width so wider pulse implies a higher dynamic range. The spatial resolution is affected by the pulse width and the bandwidth of the photodetector. Commonly the photodetector is chosen to maximize the spatial resolution, being finally the pulse width the most limiting factor. The spatial resolution is directly proportional to the pulse width as defined in (1.22). As a consequence, shorter pulses imply better spatial resolutions but at the cost of lower dynamic range and vice versa.

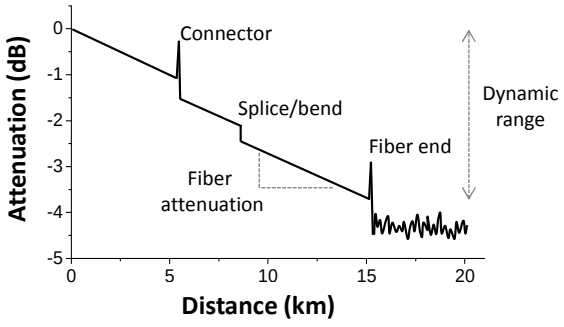

Fig. 1.18. Descriptive example of an OTDR trace.

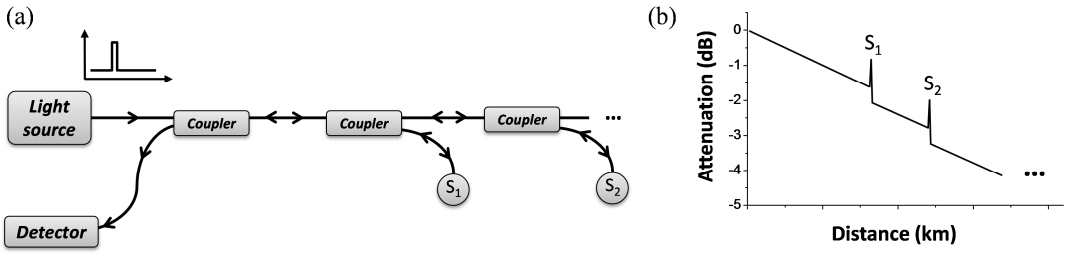

Fig. 1.19. (a) Basic TDM topology used to interrogate optical sensors using OTDR and (b) example of the expected trace.

Besides network diagnosis, a direct application of OTDRs is optical sensing [1], [79]-[82]. Different type of sensors can be monitored, especially those based on amplitude modulation, operated in reflection or using an auxiliary device to reflect the sensor's signal. Therefore, the sensors are identified by their location along the fiber. Accordingly, the topologies that can be used in combination with TDM (OTDR in particular) are not limited, but the number of optical couplers is an important factor to be considered. An example of a sensor network interrogated by an optical OTDR and the expected trace are schematically depicted in Fig. 1.19.

The light source of the OTDR is also a decisive factor in the performance of the system, particularly for sensing applications. It must be noticed that the reflections retrieved in the OTDR trace are wavelength dependent. This has no influence if the reflection is given by a full reflector or a mirror. However, if a FBG is used as sensor or for inducing a reflection, the wavelength and bandwidth of the light source will have a key impact in the results. In this regard, some works have proposed tunable laser sources for retrieving the reflection trace at different wavelengths and detect network failures in dense-WDM systems. In Chapter 4 a tunable random distributed feedback fiber laser will be employed in combination with OTDR techniques for interrogating FBG sensors wavelength multiplexed in an ultra-long range network.

OTDRs have demonstrated their applicability in optical sensing, in particular due to capability of real-time monitor the deformation in large civil structures its suitability for structural health monitoring. In addition, due to the high development of commercial OTDRs, sensors located as far as 253 km can be interrogated without external amplification [1].

1.2.3 Frequency-division multiplexing

In frequency division multiplexing (FDM) each sensor is identified by the frequency of the carrier in which the information is encoded [68]. This technique includes considerably different approaches due to the relatively wide definition.

The most basic approach implies the allocation of the sensor information to a particular frequency band of the electrical domain so the sensor data is encoded in carriers that can be amplitude (AM), frequency (FM) or phase (PM) modulated. In these systems, the sensor signals are electronically distinguished (normally in the radiofrequency spectrum) by frequency selection in the demodulation electronics. The frequency separation between sensors is required to be enough for preventing the FM carrier sidebands from generating crosstalk [83].

Optical frequency-domain reflectometry (OFDR) is sometimes included as a frequency division multiplexing technique. However, the sensor multiplexing itself, even achieved by discriminating the spatial-frequencies of each interference, is reflected in the spatial (i.e. time) domain by

means of the inverse fast Fourier Transform; thus it is mainly considered a TDM solution. In this manner OFDRs compete with OTDRs but reaching higher resolutions at the cost of lower measuring range [68], [70].

Spatial-frequency division multiplexing is also considered by some authors as a particular case of FDM. But without regard to discussions about the classification and considering the important impact of this technique in the Ph.D. work, it is independently considered in the next subsection.

1.2.4 Spatial-frequency division multiplexing

Spatial-frequency division multiplexing (SFDM) can be understood as a multiplexing technique in which each sensor is identified by its particular spatial frequency. In general terms, it can be understood as a WDM in the spatial-frequency domain; that is obtained after applying the fast Fourier transform (FFT) in the optical domain. As a result, the different components that modulate the optical spectrum can be identified.

This technique is of special interest for monitoring interferometric sensors that generate an interference pattern, typically periodic, in the optical spectrum. In the case of a single interferometer, the sensing information is commonly encoded in the period of the interference; however, in some cases the period change so small that it is reflected as a phase change in the optical spectrum. In this respect, the use of the FFT has an important advantage, which is the independence between the FFT phase and amplitude spectrum. Thus, the phase of the interference can be simply monitored independently from the interference magnitude.

Furthermore, when multiple sensors are multiplexed, the optical spectrum is formed by a combination of the sensor interferences as exemplified in Fig. 1.20. In the figure a simple adding combination has been used to illustrate the effect but as it will be explained in Chapter 2, the topology used for multiplexing the sensors will result in a final spectrum formed by different sensor contributions. Nevertheless, it is clear that monitoring the phase shift or period variations of one of the interferometers in the combined spectrum is not straightforward. After performing the FFT to the optical spectrum, the contribution of each interferometer (that must present different interference periods to avoid overlapping) can be identified [Fig. 1.21 (a)]. Afterwards, the sensor information can be retrieved by analyzing the FFT amplitude and/or phase spectrum. Consequently, depending on the sensor type, the information could be recovered from the amplitude, the spatial frequency or the phase shift of the interference.

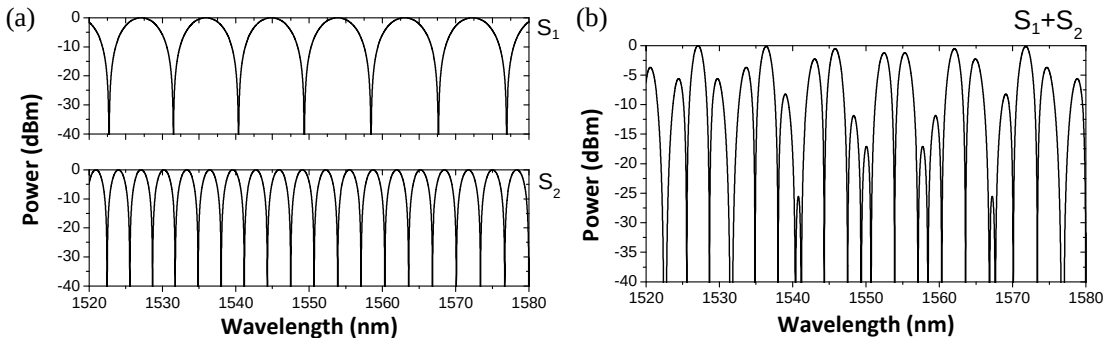

Fig. 1.20. Simulated optical spectra of (a) two interferometric sensors S_1 and S_2 and (b) their combination S_1+S_2.

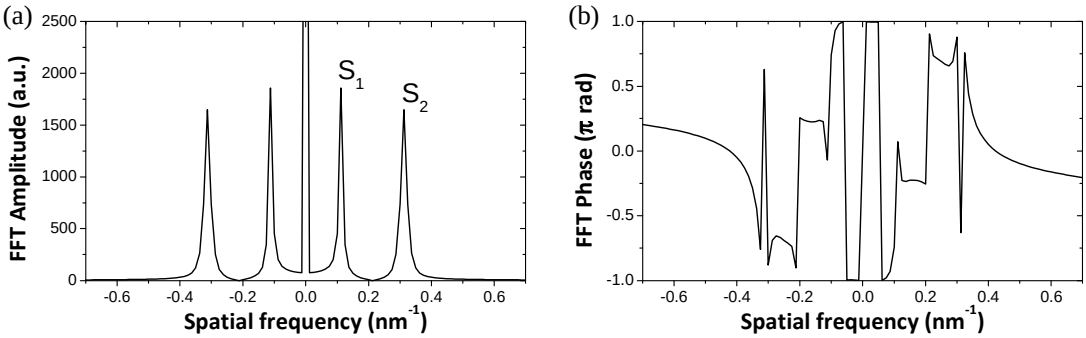

Fig. 1.21. Obtained FFT (a) amplitude and (b) phase spectra of the optical spectrum given by the combination of S_1 and S_2.

Further details about spatial-frequency multiplexing employed for interrogating HiBi fiber-loop mirror interferometers can be found in Chapter 2. Besides fiber loop mirrors, other types of interferometers can be spatial-frequency multiplexed such as single mode-multimode-single mode interferometers [84], graded-index multimode fiber interferometers [85], Fizeau interferometers [86] or Fabry-Pérot sensors using hybrid WDM techniques [87] among others.

1.2.5 Coherence-division multiplexing

In coherence-division multiplexing (CDM), interferometric sensors are interrogated in a single network by exploiting the properties of a short-coherence light source. Together with FDM, this is one of the firstly investigated techniques due to the short coherence length of the early light sources [70]. However, unlike FDM, this approach was not adapted from other technologies since the effect of coherence has a stronger impact in optical devices.

The network design in this multiplexing method relies on the basis that at a certain time, the path difference of a single interferometer is within the coherence length of the light source; ensuring that only this sensor will interfere coherently. Even though this technique cannot compete in general with TDM or WDM, it can be attained without the need of expensive and specialized equipment. However, the adequate design of the network is not simple and the maximum multiplexing capability is moderate with a low signal-to-noise ratio [83].

1.2.6 Spatial-division multiplexing

Spatial division multiplexing (SDM) is the simplest approach for multiplexing a number of sensors in a single network. In this case, as depicted in Fig. 1.22, the sensors are inserted in different fibers so the path itself is different for each sensing device. A common solution is using an optical coupler to illuminate the channels. As a result, using a 1x*N* coupler in a scheme with *N* sensors reduces the number of optical sources from *N* to 1, which implies an important saving in equipment. Additionally, since each sensor is monitored at a time, there is not cross-talk between sensors.

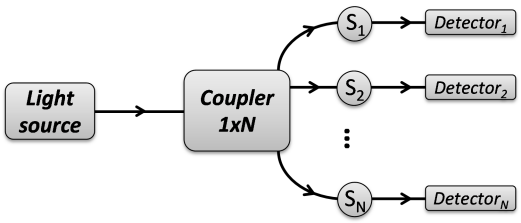

Fig. 1.22. Schematic of a SDM fiber optic sensors network.

FIBER OPTIC SENSORS MULTIPLEXING				
Technique	**Multiplexing capability**	**Sensor type**	**Measurement speed**	**Spatial resolution**
WDM	Medium	A, B, D, E	Very high	-
TDM	High	A, B, D, E	High	10^{-5} m (OFDR)
FDM	Medium	A, B, D	Medium	-
SFDM	Medium	B, C	High	-
CDM	Low	A, B, C	Low	10^{-2} m
SDM	Low	A, B, C, D, E	Very high	-
WDM+TDM	Very high	A, B, D, E	Medium	10^{-2} m
SDM+WDM	Very high	A, B, D, E	Very high	-

Table 1.2. Summary of the properties of the basic multiplexing techniques (A, Intensity; B, Interferometric; C, Polarimetric; D, FBGs; E, Long-period gratings).

This is a flexible solution for undemanding applications and it is commonly used in combination with other multiplexing techniques such as TDM or WDM [88]. One of the main drawbacks is that the power of the optical source is split between the different branches, reducing as a consequence the maximum number of sensors multiplexed.

1.2.7 Comparison of techniques

As it has been shown, there are multiple multiplexing techniques that can be employed in fiber optic sensor networks. The limit between types is sometimes not clearly defined such as between TDM and coherent FDM; but in any case the operating principle is entirely different.

The described types are the most significant but hybrid solutions are indeed those that present the best performance. In order to give a general idea of the relative performance of each multiplexing technique, a brief summary of their main properties can be seen in Table 1.2 [70], [83].

1.3 Optical amplification

In general terms, an optical amplifier can be defined as system that increases the optical power of a signal in the optical domain. These devices have had a great impact in optical communications since the amplification takes place in the optical domain without the need of regenerative repeaters with optoelectronic systems. Nowadays they have been largely developed, being key elements in multiple applications besides communications, such as the design of fiber optic lasers or optical sensor networks [89].

Optical amplification relies on the stimulated emission effect, theoretically proposed by Albert Einstein in the context of the old quantum theory [90]. Stimulated emission is the process by which a photon entering a material can interact with an excited particle (with an energy level E_2), generating an energy drop of the excited particle to a lower energy level E_1. The released energy $\Delta E = E_2 - E_1$ is transferred to a new photon of frequency $\nu = \Delta E/h$ that presents equivalent phase, polarization and direction as the incoming photon (Fig. 1.23). In this manner, light travelling through an excited medium can be amplified keeping its properties, in contrast to spontaneous emission, where some parameters of the emitted light are random.

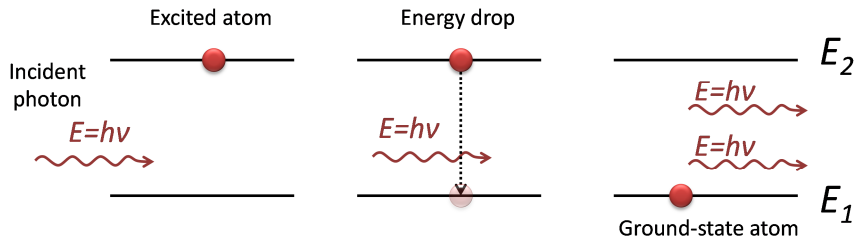

Fig.1.23. Representation of the stimulated emission process.

To achieve net amplification, the rate of stimulated emission must be higher than the absorption at the frequency of the input signal. In order to reach this condition, the number of excited particles should be increased by using another energy source called pump. Accordingly, an optical amplifier basically consists of three elements: an active medium where the amplification occurs; a pump energy source; and an extra device for combining pump and input light in the active medium.

Different amplification techniques can be developed, depending on the active medium and operating mechanism. It must be clarified that even though stimulated emission have to be explained as the most basic mechanism of optical amplification, not all the amplification techniques rely on this effect. For example, approaches based on non-linear scattering effects do not involve the excitation of media to higher energy levels. However, virtual energy levels are often used to describe the process.

An initial classification can be done considering the active media used. As a consequence two main groups can be differentiated: amplifiers using optical fiber or integrated optics waveguides. The last group comprises, among others, semiconductor optical amplifiers (SOAs). This type of amplifier uses semiconductor material as the active medium and presents a structure similar to a Fabry-Pérot laser diode but using anti-reflection coatings. As a result the laser operation is avoided. SOAs present many advantages over other approaches, such as small and compact size and low cost. In addition, the gain spectrum can overpass 100 nm and can be easily flattened. On the other hand, they are not all fiber elements so the coupling with optical fiber generally induces optical losses. The noise level is usually higher than in other techniques and exhibit strong polarization dependence [89].

Regarding the fiber optic-based amplifiers, there are four main classes: using fibers doped with rare earths, stimulated Raman scattering, stimulated Brillouin scattering and parametric amplifiers. In the following sections, the amplifiers based on erbium-doped fiber, Raman and Brillouin scattering will be briefly described due to their importance in the research work presented in Chapters 3 and 4.

1.3.1 Erbium doped fiber amplifiers

Erbium-doped fiber amplifiers (EDFAs) are nowadays the most extended optical amplifiers due to their versatility, appropriate gain bands, high efficiency, low dependence on polarization and low intrinsic noise. Unlike other rare earth-doped amplifiers, EDFAs present a gain spectrum around 1550 nm (in the communications band); being this the reason of its success and large development. The active medium is optical fiber doped with Er^{3+} ions and the emission mechanism relies on stimulated emission [89].

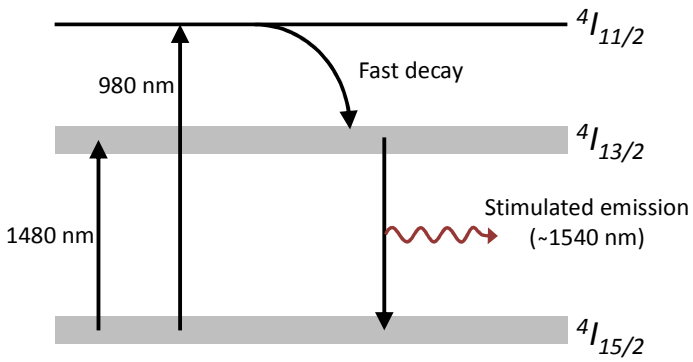

Fig. 1.24. Energy diagram of the radiative emission in Er^{3+} ions.

In this case, the pump energy is typically given by a diode laser at 980 or 1480 nm that stimulates erbium ions to an excited state. In the case of 980nm pump, this is the $^4I_{11/2}$ state from which a rapid non-radiative decay happens to the long-life level $^4I_{13/2}$ (excited state for the 1480 nm pump). Finally, spontaneous or stimulated emission takes place to the $^4I_{15/2}$ energy state. Consequently, if there is an incoming signal in the gain band, it will be amplified [91]. A diagram of the process can be seen in Fig. 1.24.

In the case of spontaneous emission the generated photon will be emitted randomly so it is considered optical noise, which is known as amplified spontaneous emission (ASE). It might also happen that an incoming photon is absorbed by the medium (absorption), reducing the light intensity by inducing a transition to an upper level. In order to achieve amplification, population inversion must occur; i.e. the excited level population must be higher than the population at the lower level [2].

As it is represented in Fig. 1.24, both the ground state and the excited state are not purely discrete but they are a collection of closely spaced energy levels of different energy. Accordingly, the radiative transition is not fixed in energy (and frequency) and comprises an amplified band around 1525 – 1565 nm. Nonetheless, the gain spectrum is not flat and depends on the pump power and also on the input signal amplified. A simplified depiction of the gain profile of an EDFA (ASE spectrum) without input signal can be seen in Fig. 1.25.

An important factor to be considered in amplifiers is the gain efficiency, which quantifies the maximum optical gain achieved per unit of pump power. In the case of EDFAs, the gain efficiencies are around 8-10 dB/mW using 980 nm pumping [77], [92].

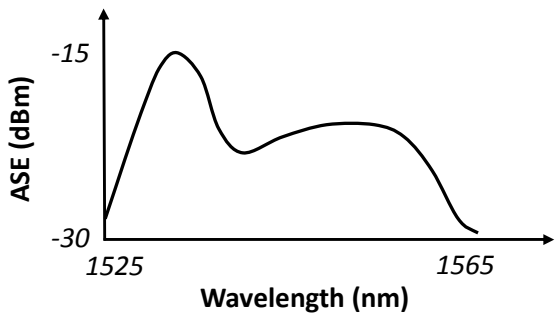

Fig. 1.25. Simplified diagram of the gain spectrum of an EDFA.

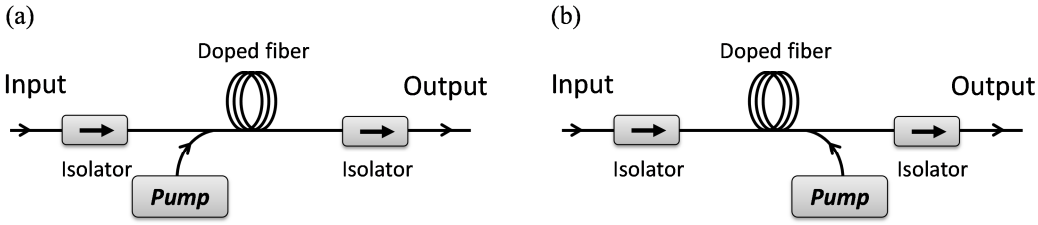

Fig. 1.26. Basic EDFA schemes for (a) co-propagating and (b) counter-propagating amplification.

The basic scheme of an EDFA is formed by at least one pump wave injected by an optical coupler or wavelength-division multiplexer to a few meters of erbium-doped fiber. Depending on the relative direction of the pump wave with respect to the input signal, two main schemes can be considered: co-propagating and counter-propagating amplification. In the first case, depicted in Fig. 1.26(a), the pump wave and the input signal propagate in the same direction while in the counter-propagating [Fig. 1.26(b)] scheme, the signals travel in opposite directions. This option is commonly more efficient; however, the co-propagating approach generates less noise [2]. As a consequence, the most appropriate solution should be chosen for each application, taking into account also the adequate amount of dopant, length of doped-fiber, pump wavelength or pump power. Specific information about the use of EDFA in the design of fiber lasers can be found in this chapter, Section 1.4.

1.3.2 Stimulated Raman scattering amplification

Stimulated Raman scattering (SRS) amplifiers rely on the stimulated emission effect related to the Raman scattering [83], by which part of the incident light (pump) suffers a frequency drop. Pump photons with frequency v_p can excite a molecule up to a virtual energy level (non-resonant state) from which it decays to a lower energy level, emitting a photon with frequency v_s. A schematic of the stimulated emission process can be seen in Fig. 1.27. The frequency difference between the pump and the emitted photon is referred as Stokes shift.

The Raman scattering interactions between the pump and the Stokes waves (in CW operation) can be expressed as [94]:

$$\begin{aligned} \frac{dI_S}{dz} &= g_R I_P I_S - \alpha_S I_S \\ \frac{dI_P}{dz} &= -\frac{\upsilon_P}{\upsilon_P} g_R I_P I_S - \alpha_P I_P \end{aligned} \tag{1.23}$$

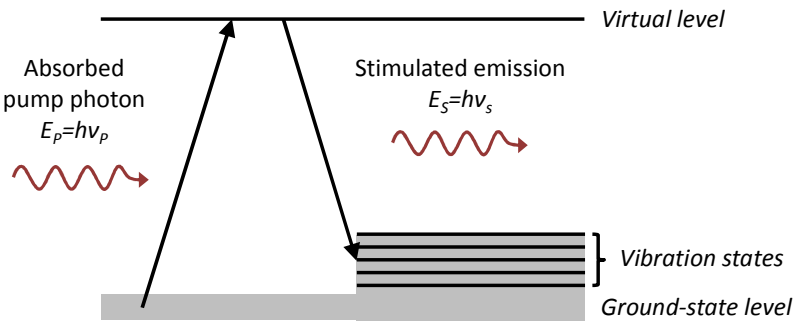

Fig. 1.27. Schematic of the stimulated Raman scattering process.

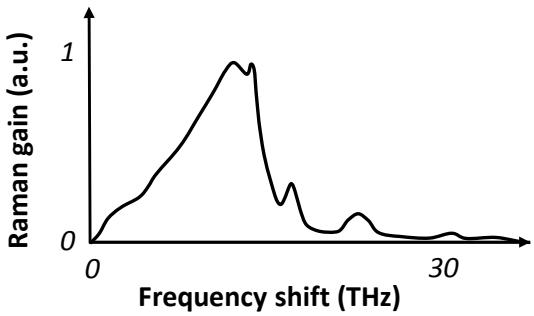

Fig. 1.28. Diagram of the Raman gain spectrum related to the frequency shift between the pump and the Stokes signal.

Where α_P and α_S refer to the attenuation of the pump and Stokes wave, I_P and I_S are the optical intensities of the pump and Stokes wave (in W/m^2) and g_R is the Raman gain coefficient. It is clear from (1.23) that the Stokes wave suffers an amplification directly related to the Raman gain coefficient and the pump wave intensity. On the other hand, the pump wave loses more energy than the transmitted to the Stokes wave. The reason is that in fact a pump photon is converted in a Stokes photon plus a phonon, which energy corresponds to the energy difference between the photons. This energy is mostly dissipated as heat. The vibrational states of the fiber determine the phonon energy and subsequently the Stokes shift. Consequently, the Raman gain spectrum shows the vibration modes of the fiber structure [94], [95]. In the case of pure silica, the peak of the Stokes shift is about 13.2 THz at 1550 nm, as schematically depicted in Fig. 1.28.

It is clear that the Raman gain directly depends on the frequency shift of the signal with respect to the pump and on the pump intensity, which are both related to the vibration states of the fiber. As a result, the Raman gain is strongly determined by the type of fiber, dopants (if any), material, structure, etc. The presence of dopants in the fiber significantly modifies the performance of Raman amplifiers; however, they are not required. In fact, one of the main advantages of Raman amplifiers over EDFAs is that standard silica fiber can be the active medium for the amplification.

Several other fundamental properties have to be taken into account for an adequate design of a Raman amplifier. Some of the most crucial are [89]:

- *Frequency shift between pump and Stokes waves*: The gain band is generated at a frequency relative to the pump wave. That implies that amplification can be generated at almost any spectral band between 0.3 to 2 µm. This is of special interest for developing laser operating at wavelengths which are not covered by other amplifications mechanisms. Additionally, the combination of pumps allows tailoring the gain profile so broad-band Raman amplifiers can be attained.
- *Independence on the relative direction of propagation*: Raman gain amplifies signals co-propagating or counter-propagating with respect to the pump. In the case of co-directional propagation, the noise figure is lower but at the cost of higher non-linearities. On the other hand, counter-directional setups offer reduced non-linear effects. A hybrid solution is the bidirectional pumping, but two pump lasers are required.

- *High polarization dependence:* The polarization dependence should be taken into account in Raman amplifiers since the peak coupling between pump and signal around ten times larger if signal and pump are co-polarized [96].
- *Fiber type:* As it was remarked before, Raman amplification takes also place in standard single-mode fiber; however, the gain factor is relatively low so long fiber lengths (tens of kilometers) are required for an effective amplification. To overcome this limitation other fiber types can be used reducing the fiber length to a few kilometers [97].
- *Distributed gain:* As a consequence of the previous point, the amplification can take place in a distributed manner during tens of kilometers if standard silica fiber is used. This is a useful property especially for long range communication or sensor systems.
- *Noise sources:* Two main types of noise sources should be considered in Raman distributed amplifiers. Firstly, the amplified spontaneous scattering is an unavoidable source of noise which is broad bandwidth, randomly polarized and bidirectional in the fiber. Secondly, Rayleigh backscattering can be added to the signal due to the double-backscattering effect that generates a large number of weak replicas of the signal with random delays and phases but at the same frequency of the signal.

Summarizing, Raman amplification presents some particularities that stand over other approaches such as its operation in standard silica fiber, the arbitrary frequency amplified or the distributed nature of the amplification. However, there are also some factors that have to be carefully taken into consideration. Two of those factors would be avoiding reflections in the amplification cavity and the enhancement of non-linearities under some circumstances. In any case, Raman amplification is increasing its presence due to the aforementioned properties and the availability of new high-power laser sources to be used as pumps. In this manner, they are being intensely researched for the design of fiber lasers, in communications or in sensing applications [98].

1.3.3 Stimulated Brillouin scattering amplification

Spontaneous Brillouin scattering might appear even at low powers due to the coupling of the optical signal (pump) to the acoustic waves due to electrostriction. Accordingly, an incoming photon is converted into a scattered photon of slightly less energy (commonly traveling in the opposite direction) and a phonon. This effect can be stimulated at high optical powers so the pump signal can strongly amplify a weak signal propagating in the opposite direction.

Optical amplification based on stimulated Brillouin scattering (SBS) can be seen, in terms of principle of operation, similar to stimulated Raman scattering amplification. Again this time the effect is caused by nonlinearities in the medium by which an incident wave (pump) induces a Stokes wave at shorter frequencies. Nonetheless, there are a number of important differences in the properties of the amplifiers based on SBS which have resulted in notably dissimilar applications.

A crucial difference between SBS and SRS amplifiers is the amplified bandwidth. As previously stated, the bandwidth of amplification in SRS is of tens of nanometers. On the other hand, the bandwidth of amplification in silica fiber is around 20 MHz (0.16 pm) at 1550 nm and varies with λ^{-2}. This bandwidth can range from tens to hundreds of megahertz depending on the geometry and composition of the fiber.

Furthermore, in contrast to SRS, SBS mostly occurs in counter-propagating topologies due to phase-matching considerations. The Stokes wave induced travels in opposite direction to the pump at a frequency $v = v_{pump} - v_B$; being v_B the frequency shift generated by the SBS, given by:

$$\upsilon_B = \frac{2nV_s}{\lambda} \tag{1.24}$$

Where n is the refractive index of the fiber, V_s is the acoustic velocity in the fiber (typically 5.96 km/s for silica fibers [94]) and λ is the wavelength of operation. A typical frequency shift in silica fiber at the communications window (1550 nm) is around 11 GHz. As a result, SBS only appears in the backward direction and with a frequency shift of ~11GHz in contrast to the ~13 THz shift in SRS between the pump and the amplification band. A direct consequence is that SBS amplifiers are not useful devices for designing fiber lasers at frequency bands which are difficult to achieve, since the pump laser must be closely located. As it can be deducted from 1.1, changes in the refractive index and/or the acoustic velocity of the fiber will modify the Brillouin frequency shift. As a result, this frequency shift can be exploited in sensing applications. The combination of this sensing technique with time-domain analysis gave rise in the late 80s to Brillouin optical time-domain analysis (BOTDA) sensors, which can measure temperature and strain in a distributed manner [99].

Considering the gain coefficient in single mode fiber, SBS overpasses in two orders of magnitude the coefficient of SRS (g_B= 249.5 Km/W against g_R=0.43 Km/W [77]). In accordance, the power threshold of stimulated Brillouin scattering is lower than in SRS. In fact, the threshold for SBS is in the order of tens of miliwatts in contrast to the several hundred of miliwatts required for SRS [77]. Additionally, the gain coefficient will be maximized for highly-coherent laser sources: i.e. narrow-linewidth lasers will generate higher amplification.

To summarize, SBS is a very strong nonlinear process induced at low powers that exhibits high gain in the backward direction, with a frequency shift relatively small. Therefore, this nonlinearity can be extremely detrimental in systems which employ narrow bandwidth lasers with high power [94]. Optical amplifiers based on SBS can be manufactured [100] but their impact up to date is limited beyond the design of fiber lasers (see Section 1.4 in this Chapter).

1.4 Fiber lasers

1.4.1 Background

The first fiber laser was proposed by E. Snitzer in 1961, using a neodymium-doped fiber [1]. A series of works followed this initial demonstration [102]-[104] but it was five years later, in 1966 when the potential applicability of optical fiber was evaluated for telecommunications [105]. In this manner, the first works that used silica-based fiber in the development of lasers were published in 1973 and 1974 by J. Stone and C.A. Burrus [106]-[107]. However, it was not until 1985 that practical rare earth-based fiber amplifiers and lasers were developed [108]. Initially, the main dopant used for the amplification in was neodymium due to its high efficiency, being presented the first erbium-doped fiber laser in 1986 [109]. Since then, fiber lasers based on erbium-doped fiber have been extensively studied. There are of particular interest for telecommunication applications due to the radiative transition of Er^{+3} around 1550 nm, which is the

transmission window that offers minimum loss in silica fiber [110]. Optical amplifiers can also be produced using other rare-earth ions like Ho^{+3}, Tm^{+3}, and Yb^{+3} but up to date, erbium-doped fiber amplifiers (EDFAs) are still dominant.

Nonetheless, rare earth-doped fiber amplifiers are not the only solution for developing fiber lasers. Stimulated scattering Raman can be also used as a mechanism for the amplification in a fiber laser. The first work presenting a Raman laser using an optical fiber as the active medium was demonstrated in 1976 by Ken O. Hill *et al.* [111]. Due to the high power required for the laser generation, the first Raman fiber laser for practical application appeared late in the nineties, when high-power pumps became available. Other effects like stimulated Brillouin scattering of four-wave mixing can be used to provide amplification [112]; however, EDFA and Raman amplification are the most used in fiber lasers.

1.4.2 Principle of operation and main features

Basically, two elements are required to form a fiber laser: a gain medium that generates amplification and a feedback, generally given by a resonator in which the light recirculates. In this manner, the laser emission will initiate when the total gain in the cavity overcomes the total losses. The amplification effect is generally provided by an active medium in which the inversion of population is induced by an external source of energy commonly known as pump. A simple scheme of a fiber laser formed using a linear resonator can be seen in Fig. 1.29, where two reflectors are located at the ends of an optical fiber of length L with an active medium of length l_m. Photons recirculating inside the cavity are successively amplified until the total gain in the resonator reaches the total losses in the cavity.

That limit is defined as lasing threshold, and can be defined as the lowest excitation level at which stimulated emission dominates over spontaneous emission. Supposing the basic scheme presented in Fig. 1.29, the total losses of the resonator in a round trip are induced by the reflectors (R_1 and R_2) and by the attenuation inside the cavity of length L. On the other hand, the total gain of the cavity is defined by the gain coefficient g and the length of the fiber that acts as active medium l_m. Consequently, the lasing threshold in a linear resonator, assuming steady-state operation, can be derived from:

$$R_1 R_2 e^{-2\alpha L} e^{2 g_{th} l_m} = 1 \qquad (1.25)$$

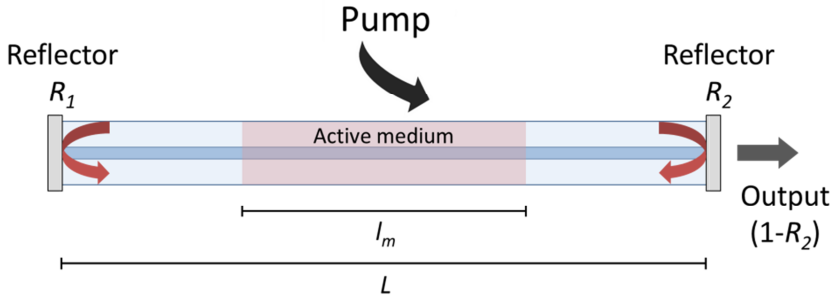

Fig. 1.29. Basic schematic of a linear fiber laser.

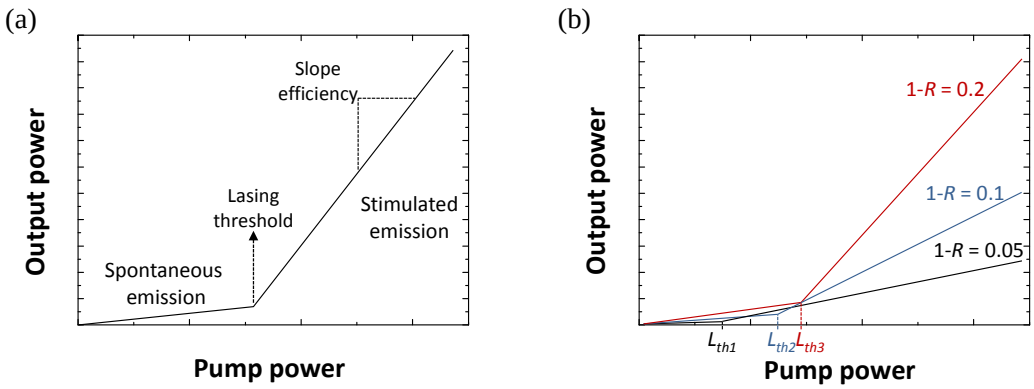

Fig. 1.30. (a) Ideal slope efficiency of a fiber laser. (b) Ideal slope efficiencies for different reflectance values at the output reflector.

Above the lasing threshold, the linewidth and the efficiency slope (pump power vs laser power) of the emitted light become orders of magnitude smaller. If the total losses of the cavity are constant for different pump powers, which is the most usual case, the efficiency slope of a fiber laser is linear as displayed in Fig. 1.30(a). This efficiency is evidently affected by the reflector used for the power extraction. Consequently, an increment of the power ratio extracted from the laser (i.e. decreasing the reflector's reflectivity) increases the laser's output power, but as expressed in (1.25), it also increases the lasing threshold. In this manner, the selection of the output ratio of the laser typically implies a compromise between high slope efficiency and low pump power threshold as schematically depicted in Fig. 1.30(b). As a result, some basic aspects to be taken into account in a laser design are the reflectivity of the mirrors used (in the case of a linear cavity), the attenuation of the fiber, the cavity length and the properties of the amplification process.

Normally, the power efficiency of fiber lasers ranges between 30-70%, using other laser sources as pumping (laser diodes in particular). The wavelength of operation of fiber lasers depends in general on the amplification medium, but includes infrared, mid-infrared, visible and ultraviolet bands. Filtering elements, such as fiber Bragg gratings, can be included in the laser design to force the laser emission at a given wavelength. In this manner, wavelength tuning is possible over tens of nanometers. This range is usually related to the amplification bandwidth given by the gain medium [113]. Other properties of fiber lasers include, for example, the capability of being mode-locked to generate ultra-short (femtoseconds) optical pulses [114]. In this Ph.D. work, all the lasers designed/used operate in continuous wave (CW) except in [PAPER J], where the laser is internally modulated.

Comparing fiber lasers with other laser types such as solid-state or diode lasers is not straightforward. In general terms, in contrast with solid-state lasers, fiber lasers are simpler, more compact, reliable and can be pumped using laser diodes (which in fact implies that fiber lasers can be considered as wavelength converters). Additionally, compared with laser diodes, fiber lasers present a cleaner optical spectrum and better capabilities when modulated (less distortion and less chirp). Furthermore, due to the fiber design, fiber lasers offer ideal compatibility with optical communication systems. In addition, fiber lasers present some important features over other types of lasers [83], [115]-[116]:

- *High pump intensity:* Due to the small core diameter of optical fibers, the mode field diameter of the pump wave guided through an optical fiber yields higher pump intensity in a fiber laser that in bulk devices. This is reflected in a reduced lasing threshold.
- *Signal and pump light wave-guiding:* Improved efficiency operation is attained due to the excellent mode overlapping between the signal and pump light and the guaranteed parallelism between the two light beams.
- *Independence of pump spot size and active medium length:* Due to the independence between the pump and the active medium length, the density of the dopant can be kept low enough to avoid undesired ion-ion effects like cooperative up-conversion. In this manner, weak pump absorption lines can be utilized to excite the laser transition. This can result of practical importance for exploiting weak radiative transitions, as in L-band erbium doped fiber amplifiers.
- *Compactness*: Depending on the amplification type, the active medium can be arbitrarily long, and it can also be compact. Some silica-based fibers can be coiled and packaged with a bend radius smaller than 1 cm.
- *Heat dissipation*: The small diameter of the optical fiber implies good heat dissipation. Consequently, heat-related unwanted effects have a limited impact in fiber lasers.
- *Beam quality*: Even at high output powers, fiber lasers in single-mode optical fiber provide diffraction-limited beams.
- *Robustness:* All-fiber lasers are in general more robust and reliable under mechanical perturbations than free-space lasers. Thanks to the guiding provided by the optical fiber, there is no need of alignment.
- *Flexible design:* Many different laser cavities, configurations and variations can be implemented. Setups can be easily assembled using fiber connectors or splices without the need of optical alignment. Consequently, fiber lasers are less cumbersome and more stable than free-space lasers.

These merits, plus the potential low cost [113], make fiber lasers a promising technology in applications like material processing, telecommunications, optical metrology, surgery and optical sensing. However, there are also some aspects of fiber lasers that limit their performance and need to be addressed. Some examples are that fiber can be damaged at high powers; the pump wave absorbed per length unit is limited; and finally, nonlinear effects can impose a limitation in the laser operation. In this regard, numerous works have been published handling these limitations and have proposed different types of fiber lasers for each specific application. As a result, there are different aspects that should be taken into account to define each fiber laser: the type of amplification, the topology, the longitudinal mode distribution or the number of emission lines. In the next subsections these main classifications will be briefly considered to give a better overview of the technology that will be developed in Chapters 3 and 4.

1.4.3 Fiber laser types: Considering amplification

The type of amplification employed in the laser generation is a crucial aspect that has an important impact in the final performance of the laser. There are many amplification approaches (and hybrid combinations) that can be used for designing a laser. As a consequence, a classification of fiber lasers can be done depending on the amplification type. In this subsection the

most important are briefly explained, emphasizing on the erbium-doped fiber and Raman-based solutions since they will be utilized in the research works presented in Chapter 3 and 4.

Erbium-doped fiber lasers

Nowadays, fiber lasers based on erbium-doped fiber amplification are present in numerous applications such as dense wavelength-division multiplexing, optical signal processing, sensor multiplexing, optical spectroscopy and soliton sources among others [117]-[121]. Despite the fact that erbium-doped fiber lasers (EDFLs) can be designed to operate at different frequency bands, the most important development has been done in the C-band (1530-1565 nm). The main reason of this evolution is the application for optical communications, since the silica-based optical fibers present minimum loss at those wavelengths.

In order to appropriately design an EDFL that fulfils the requirements of each application, different parameters have to be considered. First of all, the length of doped fiber used in the setup is a crucial factor. Long fiber lengths increase the absorbed pump power, accordingly increasing the output power. However, if the doped fiber section is too long, the un-pumped fiber will induce a strong attenuation in the cavity, which will consequently increase the lasing threshold. On the other hand, if the doped fiber length is short, part of the pump wave might not be absorbed, limiting the maximum output power. Thus, there is a trade-off between these effects, so the length of doped fiber has to be appropriately chosen to obtain the adequate output power, lasing threshold and slope efficiency.

Another important element that has to be taken into account is the erbium concentration in the doped fiber. Experimental data indicates that high erbium concentrations imply also high lasing thresholds and low slope efficiencies. Nevertheless, high dopant concentrations allow reducing the length of the cavity required in the laser, which can be exploited in the development of single-longitudinal mode fiber lasers [116].

The pump laser used in the amplification process is a key factor to be considered. Many pump wavelengths are obtainable through semiconductor diode lasers: 670, 800, 980, 1480 and 1530nm [122]-[127]. But two pumping approaches are the most extended up to date: at 980 nm and 1480 nm. The election of one of the choices is not easy since each option has its own advantages. High-power diode lasers are available at 1480 nm which also offers higher slope efficiency. On the other hand, pumping at 980 nm pump presents the highest gain efficiency [128]. In any case, both solutions have been successfully used in numerous works [129]-[133]. Typically, a combination of 980 nm and 1480 nm pumps is used in commercial erbium doped fiber amplifiers.

The properties of the EDFL strongly depend on the spectral filters used in the wavelength selection. The emission line will initiate at the optical wavelength with a highest relationship between gain/loss in the cavity. Consequently, including optical devices in the laser that modify the losses in the cavity at certain wavelengths can result in *forcing* the laser emission at some frequencies. Many different optical filters have been used for the wavelength selection, among others, the most frequent are Mach-Zehnder filters [110], arrayed waveguide gratings (AWG) [121], Fabry-Pérot filter (FPF) [134], fiber loop mirrors (FLM) [44], high-birefringence fiber filter [133] and FBGs [135]-[136]. Every option presents its specific upsides and downsides, being preferred in this work the FBG approach due to the narrow linewidth, temperature/strain

sensing capability and individual wavelength tuning control which is especially interesting for multi-wavelength systems.

Regarding the amplification process, those are the main aspects to be considered in the design of an EDFL. However, many other parameters should be taken into account like the spectral bandwidth of amplification, which is a key aspect in the development of widely tunable lasers and EDFLs used in wavelength division multiplexing applications [131]-[137].

Raman fiber lasers

The amplification induced by the stimulated Raman scattering can be also used to develop fiber lasers. These lasers are known as Raman fiber lasers (RFL) and have been subject of intense research since the first published work in 1976 [111]. As previously shown in Section 3 of Chapter 1, Raman amplification takes advantage of the inelastic interaction between photon and molecules. This interaction can lead to a drop in the energy of the photon which is consequently translated in a frequency drop. In this manner, if a Raman pump is launched into a cavity, a Stokes wave will be generated at a frequency ~13 THz lower than the pump power. If there is another signal located at these frequencies, it will be amplified. In the same manner, part of the Stokes light can be *trapped* in the cavity using reflectors (like FBGs) and successively amplified until the lasing threshold is reached, obtaining a Raman fiber laser [138].

As in any other fiber laser, also in this case the pump laser used for the gain generation is a key element in the laser's design. In contrast to erbium-doped fiber lasers, the wavelength operation of the pump laser is necessarily fixed ~13 THz above the gain band. It is preferred as well to use an unpolarized laser source due to the strong polarization dependence of the Raman gain. In addition, the power of the pump source should be high (hundreds of miliwatts) due to the small Raman gain coefficient. Finally, relatively broad pump sources are desired to avoid the generation of Brillouin scattering [139]. An important advantage of Raman-based amplifiers is that multiple pump sources can be combined to tailor the shape of the optical gain spectrum due to the fixed frequency shift between the pump and the Stokes wave [140]. This also implies that Raman amplification can be used to produce fiber lasers at almost any frequency, in particular when combined with *cascade* operation. In the cascading technique, the 1st Stokes wave is confined and amplified to generate a laser, so a 2nd Stokes wave is induced and so on [141]. This process can be repeated to obtain amplification (or lasers) at higher wavelengths. This effect has been successfully used in the fabrication of fiber lasers at 1480 nm to be used as erbium-doped fiber amplifiers pump.

Concerning the gain medium, Raman fiber lasers also differ from EDFL. In this case, since the gain process is based on the interaction between photons and particles, Raman scattering occurs in germanosilicate glass, which is commonly used in the core of standard single-mode fibers. Therefore, the fiber used in the laser's cavity acts as the active medium for the amplification as well. Nevertheless, the Raman gain coefficient can be enhanced if different fiber types are used. For example, dispersion compensation fiber (DCF) and nonzero dispersion fiber (NZDF) present gain coefficients much higher than the standard single-mode fiber (SMF), being this especially useful in the development of more compact Raman fiber lasers. Thus, the type and quantity of dopant used in the fiber used as active medium have an important impact in the laser's performance [142]. For example, Raman fiber lasers with cavity lengths as long as 270 km [143] and as short as 2.4 km [144] can be attained using SMF or DCF fiber respectively.

In the same manner as in EDFL, the optical devices used for the wavelength selection and the feedback source strongly define the properties of the Raman laser. Accordingly, numerous approaches have been proposed, selecting the wavelength of operation of the laser by means of Fabry-Pérot filters [145], FBGs [146] and high-birefringence fiber loop mirrors [147]-[148] among others. Regarding the topology used, ring and linear cavities have been validated; additionally, distributed cavities based on the feedback provided by the Rayleigh scattering have been proposed [149]. It is worth also noting that an important advantage of RFLs is the inhomogeneous broadening gain provided by the stimulated Raman scattering. This effect is of particular interest in multi-wavelength lasers since the gain competition between lines is reduced [150].

Due to the abovementioned properties, Raman fiber lasers have been proposed as a good solution in a number of applications such as long-distance remote sensing [151]-[153], optical tomography or super continuum generation among others [138]. In addition, RFLs have shown to be especially useful for soliton-based systems and in applications for quasi-lossless optical communications [154].

Brillouin fiber lasers

Similarly to Raman fiber lasers, Brillouin fiber lasers exploit the amplification generated by stimulated Brillouin scattering (SBS), which is also an inelastic non-linear optical effect. In this case, a pump wave propagating induces a Stokes wave in the direction opposite to the pumping. For liquids and gases, the Stokes frequency shift is typically of the order of 1–10 GHz. In the case of standard SMF, this value is around 10-11 GHz for the C-band.

In this manner, as in Raman-based approaches, the gain provided can be used to generate a laser emission as demonstrated in a pioneer work published also in 1976 and by the same research group as the first Raman fiber laser [155].The gain bandwidth induced by Brillouin scattering has much narrower bandwidth than Raman-based lasers but it requires lower pump powers. In this case, the pump laser should have a narrow linewidth since SBS is favored by highly coherent pumps. The type and length of fiber in the amplification is also a decisive factor in a Brillouin laser, because each class of fiber can present different SBS parameters (like Stokes frequency).

Cascaded operation is a key parameter in Brillouin fiber lasers as well, due to the low pump power required and the narrow bandwidth of the gain [156]. But it has to be taken into account that in the case of using ring instead of Fabry-Pérot topologies, the frequency separation of the cascade effect will be double in each direction of propagation. Many fiber laser schemes have been presented up to date exploiting stimulated Brillouin scattering; however, most of them include a second amplification technique like erbium [156]-[158] or Raman [159].

Other rare-earth doped fibers

Besides erbium ions, other rare-earth dopants can be used in the gain generation of a fiber laser. As mentioned above, the first fiber laser used Neodymium as dopant in the active fiber [106]-[107]. Other rare-earths employed are for example Praseodymium ions (Pr^{3+}), which have been used to fabricate fiber lasers operating at 1310 nm [160]. Pr-doped fiber lasers have also demonstrated capability to operate at 1050 nm using a dye laser as pumping at 592 nm [161]. Thulium-based fiber lasers attracted significant attention due to their potential applications, such as optical-based hydrocarbon sensing [162].On the other hand, Holmium-doped fiber la-

sers have been considered due to their capability to operate around 2000 nm, which is of special interest in medical and other eye-safe applications. In [163] a Ho-doped fiber laser pumped at 800 nm generated an output power of 10 mW and a wavelength tunable between 2037 – 2096 nm. Finally, Ytterbium-doped fibers have been used to generate amplification in fiber lasers operating around 1010 nm with a tunable wavelength range of 60 nm [164]. Additionally, more than 200 mW of output power with a quantum efficiency of 80% was attained using a silica-based Yb-doped fiber laser pumped at 869 nm [165].

1.4.4 Fiber laser types: Considering cavity

First of all, it is worth clarifying that the use of *cavity* is a misnomer (that is related to a closed cavity employed at microwave frequencies). Instead of *cavity* it would be more appropriate the use of *optical resonator*. However, the term cavity is broadly extended in the literature and it seems to be largely accepted so in this work both terms are used without distinction. In either case, they refer to the space in which the light is confined in a closed path during the laser generation. In this manner, the optical cavity/resonator provides the feedback required for the laser emission. The type of cavity used in the design of the laser has an important role in the final performance. Most practical schemes take use of hybrid approaches, but it can be considered that the basic topologies are the ring and the linear (or Fabry-Pérot) cavities. It will also be described in this section a third topology that might not strictly be a different type by itself. Nevertheless, due to the special importance in this work and completely different properties, the random distributed feedback cavity will also be illustrated.

Linear/Fabry-Pérot resonator

The linear cavity, also known as Fabry-Pérot cavity consists of an optical fiber section between two reflectors in which the light travels back and forth as depicted in Fig.1.31. The main difference between linear and ring resonators is that in linear resonators the light necessarily propagates simultaneously in both directions. This implies that light reaches every component placed within the cavity two times per round-trip, except in the case of the reflectors. As a consequence, undesired effects like spatial hole-burning can arise.

Spatial hole-burning can be defined as a modification of the gain shape in a laser medium caused by saturation effects of a standing wave. If two waves travel in different directions simultaneously in a resonator, interference between these waves will produce a so-called standing-wave, with a period equal to half the wavelength. This interference effect in turn might produce changes in the amount of saturation in the active medium. As a consequence, it can result in the deformation of the spectral shape of the gain.

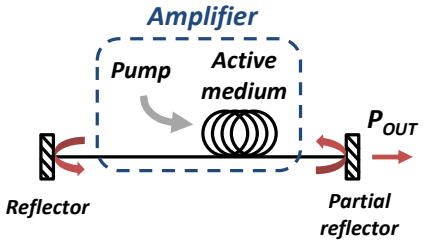

Fig. 1.31. Schematic of a simple linear cavity-based fiber laser.

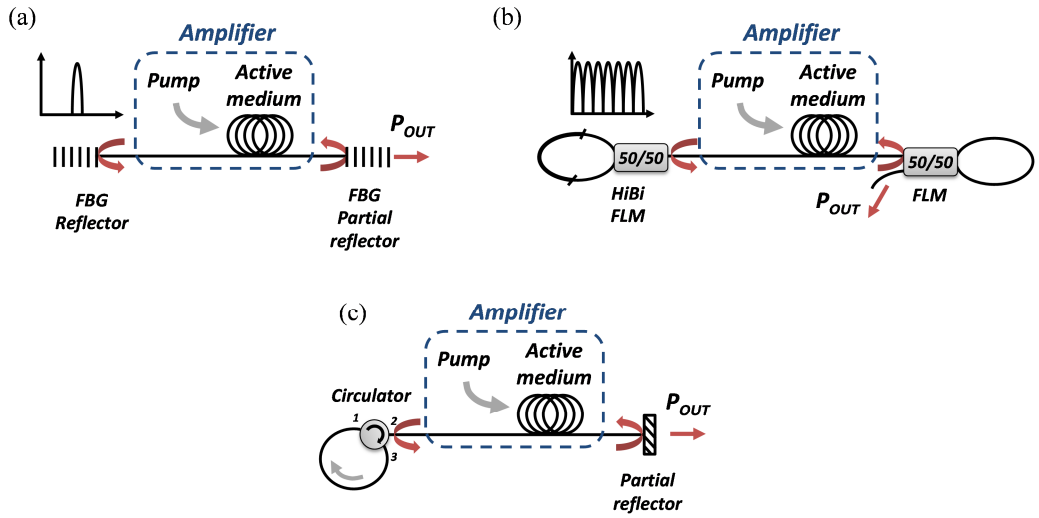

Fig. 1.32. Fiber lasers based on linear cavities using different reflectors: (a) FBGs (b) HiBi FLM + FLM (c) circulator connected as a mirror.

Other drawbacks of basic linear resonators are lower efficiency and broader emission lines than the obtained using ring cavities [115]. On the other hand, they are very simple topologies that allow the design of very short cavities, which can be exploited for developing single-longitudinal mode fiber lasers [166]. In order to decrease the total loss in the cavity, the pump wave is typically inserted in the cavity through a wavelength-division multiplexer (WDM) instead of an optical coupler [167]. Regarding the type of reflectors used, a widespread solution uses FBGs as wavelength-selecting mirrors in one or both ends of the fiber cavity as depicted in Fig. 1.32(a) [168]. In the same manner, other filtering devices like fiber loop mirrors can be used; both as wavelength-selectors (by inserting a section of Hi-Bi fiber in the loop) or as simple mirror devices as in Fig. 1.32(b) [44]. Other approach used to attain simple all-fiber reflectors is to enhance the Fresnel reflection of the fiber end by a highly reflective coating, such as silver or gold-based solutions. Finally, a flexible solution is to use a circulator connected as a reflector like displayed in Fig. 1.32(c). The main advantage of this solution is that optical devices can be placed in the single-direction loop formed in the circulator, like filters operating in transmission or couplers used in the power extraction. On the downside, the total length of the cavity is extended. It should be also said that this solution can be considered in fact as a hybrid topology between linear and ring cavity. In any case, using a circulator to create a loop reflector is used in several works presented in Chapter 3 and 4.

Ring resonator

The second simplest topology to be presented is the ring cavity. In this case there is no need of reflectors since the light path is closed by connecting/fusing the optical fiber in a closed loop. The main advantages of ring resonators over linear cavities are the more efficient use of the optical gain and the double free spectral range (FSR) obtained for an equal cavity length [110]. In addition, ring-based fiber lasers can operate in unidirectional regime if an optical isolator/circulator is placed in the cavity; avoiding detrimental effects such as hole burning. A basic scheme of a unidirectional linear fiber laser is presented in Fig. 1.33(a), where the pump power can be inserted in the cavity using for example a WDM or an optical coupler. A polarization controller should be also included in the loop if conventional doped-fibers are used for the amplification. Nevertheless, it has been demonstrated that that the polarization control has little influence on multiwavelength-fiber lasers [169].

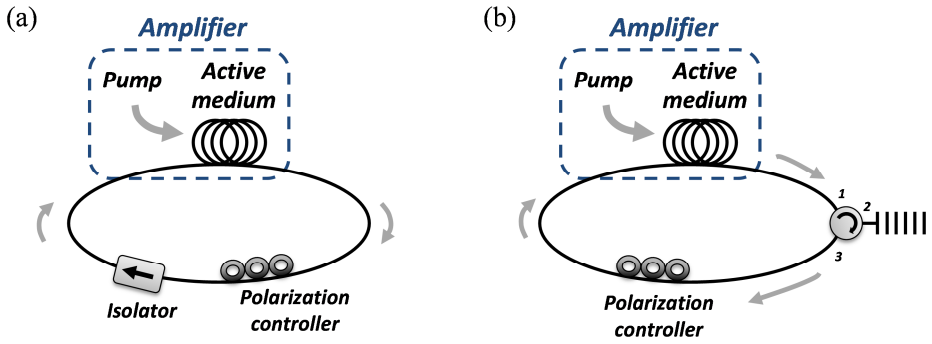

Fig. 1.33. Basic schemes of ring fiber lasers using (a) an isolator and (b) an optical circulator to ensure the unidirectional operation.

One of the main drawbacks of ring resonators is that the cavity length is typically much longer than in linear topologies. This can be an issue if short cavities are desired for achieving single-longitudinal mode operation. Additionally, ring topologies are commonly more susceptible to power fluctuations [170].

In the case of unidirectional operation, filtering devices operating in transmission can be placed inside the resonator, which is not possible using a basic linear cavity. However, in the same manner as in linear topologies, the contribution of another device like an optical coupler or circulator is needed to insert in the cavity filters that operate in reflection. A common solution is presented in Fig. 1.33(b) that uses an optical circulator both as an isolator and to redirect the power into an optical filter in reflection such as a FBG [171]. Again this time, this could be considered a hybrid solution since the light's path includes both linear and ring sections.

Random distributed feedback cavity

Finally, it is worth mentioning a different type of topology that even though it might not strictly be a different type by itself, it is also described due to its particularities and importance in the design of random distributed feedback fiber lasers [172]. The random distributed feedback-cavity is sometimes also referred as random cavity or open cavity. This scheme consists of a single linear cavity of optical fiber in which at least in one of the ends the light is not mirrored by a point reflector. In this manner, the feedback required for the laser generation is provided (from at least one of the cavity sides) by the Rayleigh scattering (RS) effect. An example of this setup can be seen in Fig. 1.34 in where single mode fiber is used to generate RS feedback in a double-arm topology. It should be noted that the optical fiber can act as both, gain medium for the amplification and RS generator. In the case of using Raman amplification (the most common), tens of kilometers of SMF are typically used as active medium and distributed reflector simultaneously [149].

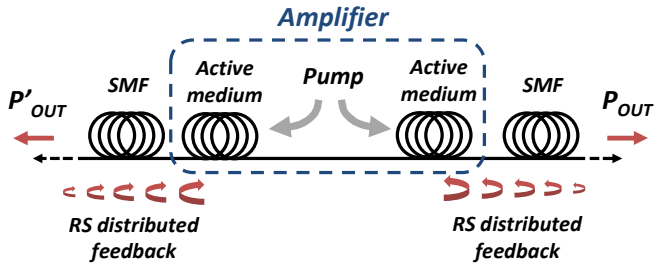

Fig. 1.34. Basic scheme of a random distributed feedback fiber laser.

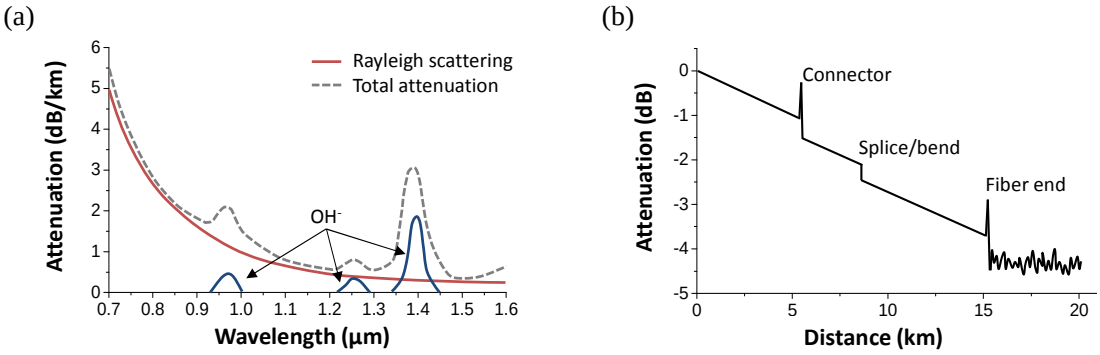

Fig. 1.35. (a) Typical attenuation profile of a standard single mode fiber. (b) Schematic of an OTDR trace.

The Rayleigh scattering in optical fibers is an elastic scattering of light due to its interaction with particles much smaller than the wavelength of the radiation. It is a linear effect by which the incoming light interacts with the random density fluctuations created in the fiber during the manufacturing process. This interaction results in some of the incoming radiation emitted out of the fiber, being RS the most important cause of attenuation in standard optical fibers at 1550 nm [Fig. 1.35(a)]. Operating at higher wavelengths benefits from less Rayleigh scattering since it is inversely proportional to the fourth power of the wavelength, being expressed as [173]:

$$\alpha = \frac{8\pi^3}{3\lambda^4} n^8 p^2 \beta_c K T_F (1+\cos\theta) \qquad (1.26)$$

Where λ is the wavelength of the light, n is the fiber refractive index, p is the average photo-elastic coefficient, T_F is the fictive temperature (approximately the temperature of fabrication), K is the Boltzmann's constant, β_c is the isothermal compressibility at T_F and θ is the scattering angle. Most of the radiation is coupled out of the fiber; however, a small amount of the light (about~1/1000) is coupled back into the fiber, being this quantity related to the numerical aperture and geometrical dimensions of the fiber [174].

As a result, Rayleigh scattering provides an optical feedback that even weak, has been used since the 1970s to monitor the loss of optical fiber using optical time-domain reflectometry (OTDR) [175]. An example of the trace obtained using OTDR can be seen in Fig. 1.35(b), where the reflected light due to Rayleigh scattering can be seen together with other local effects in the optical fiber. Under some circumstances, the feedback provided by RS can be enough to stimulate the laser generation. In 2009, it was demonstrated that the feedback provided by a FBG in an ultra-long (270 km) linear cavity was lower than the given by RS [143]. Few years ago, the demonstration of a fiber laser solely based on the feedback provided by RS was presented [149]. Since then a lot of attention has been paid to this new type of fiber lasers, known as random distributed feedback fiber lasers (RDFLs) [172],[176].

In this manner, a random distributed feedback cavity can be considered as a combination of a vast number of linear cavities with different fiber lengths and extremely weak reflectors. As it will be later explained, that implies that no longitudinal modes are present in the cavity, which is the main difference with linear and ring topologies. As in linear cavities, the light propagates in both directions simultaneously so complementary optical devices can be also included in the cavity to allow the integration of filters operating in transmission. In the first demonstration of a RDFL, a single fiber cavity without any reflector was used. However, a single-arm version with one reflector and an open cavity can also attain similar results (using a half of the pump power) [172]. Typically, Raman amplification is used with this topology due to the distributed

nature and high gain attained in long cavities; nevertheless, also Brillouin or EDFA can be utilized [177].

As it will be further explained in Chapter 4, RDFLs have some important differences over conventional fiber laser, being those singularities mainly related to the use of RS as the feedback source. During this Ph.D. work, research has been carried out exploring the capabilities of such RDFLs for sensing applications.

1.4.5 Fiber laser types: Considering longitudinal mode operation

As it has been mentioned previously, the laser cavity is in fact a resonator, in which the physical features of the guiding medium (length, refractive index, etc.) define the resonance modes. The cross-section properties of the fiber, like cladding/core refractive index difference and fiber radius determine the transverse modes. In the case of single-mode fibers, only the fundamental mode is supported, mostly presenting a Gaussian profile.

The resonance modes in the axial direction of the cavity are known as longitudinal-modes and are defined by the length of the resonator and the refractive index of the core. The longitudinal modes (frequencies) that are allowed to propagate inside a resonator must fulfil the following condition:

$$d = N \cdot \lambda \tag{1.27}$$

Where d is the total distance in a round-trip, N is an integer and λ is the resonant wavelength. In this manner, only certain frequencies can circulate in the cavity with a frequency distance between them dependent on the length of the cavity. During the laser generation, if the total gain overcomes the total losses in the cavity for a number of longitudinal modes, they will start lasing. The number of longitudinal modes lasing will be determined by the correlation between the cavity length and the gain bandwidth. As a consequence, only one (single-longitudinal mode fiber laser), or multiple longitudinal modes can emit simultaneously (multi-longitudinal mode fiber laser). Additionally, it is also considered in this section a particular case (*modeless* operation) in which no longitudinal modes can be identified in the fiber laser.

Multi-longitudinal mode operation

Typically, the amplification inside a fiber laser's cavity has a gain bandwidth that is wider than the intermodal distance. In this manner, many longitudinal modes can be sufficiently amplified to overcome the total losses of the cavity and start lasing. This effect can be seen in Fig. 1.36, where multiple longitudinal modes fall within the gain bandwidth and emit simultaneously.

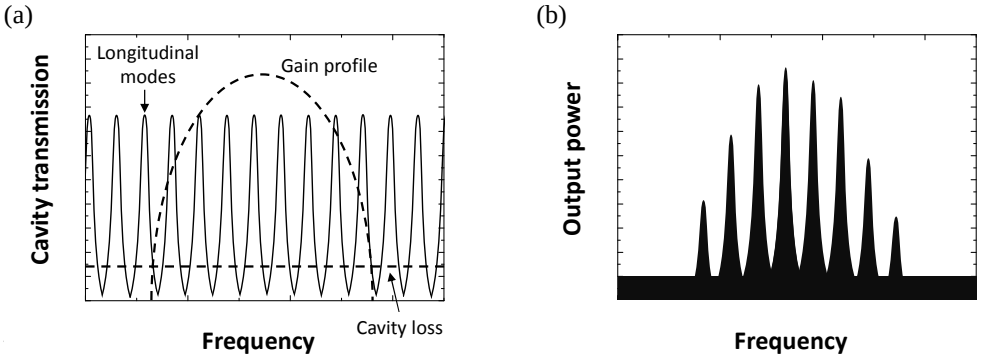

Fig. 1.36. (a) Cavity transmission response and (b) output spectrum of a multimode fiber laser.

In this manner, if multiple longitudinal modes reach the lasing threshold, the laser emission is considered as a multi-longitudinal mode laser which free spectral range (FSR) in the case of a single-material cavity can be derived from:

$$\Delta \upsilon = \frac{c}{n \cdot d} \tag{1.28}$$

Where c is the speed of light in vacuum, n represents the refractive index of the fiber and d is the round-trip distance of the resonator. It must be noted that in Fabry-Pérot cavities, this distance is related with two times the cavity length while in ring resonators d is defined by the length of the ring. However, not only the gain bandwidth and the intermodal distance define the number of emitting longitudinal modes, also the laser bandwidth and type of broadening present (homogeneous or inhomogeneous) have to be taken into account. In addition, the formula (1.28) has to be modified if multiple materials are present in the cavity:

$$\Delta \upsilon = \frac{c}{n_1 \cdot d_1 + n_2 \cdot d_2 + ... + n_k \cdot d_k} = \frac{c}{\sum_{i=1}^{k} n_i \cdot d_i} \tag{1.29}$$

Where n_k refers to the refractive index of the k-th material and d_k refers to its effective length (double in the case of a linear cavity).

Multi-longitudinal mode laser emission is the most common since typically the free spectral range Δv for a fiber laser with a cavity length between 10-100 m is around 1-10 MHz. Accordingly, it is extremely difficult to achieve single-longitudinal mode (SLM) operation without complementary techniques. Thus, the bandwidth of a multi-longitudinal mode fiber laser is a multiple of the mode spacing. Nevertheless, some applications require narrow laser emissions so reliable single-longitudinal mode fiber lasers designs are also of interest.

Single-longitudinal mode operation

As explained in the previous subsection, the number of longitudinal modes that can be excited in a laser emission depends on the relationship between the cavity length and the gain bandwidth. As a consequence, a single longitudinal mode laser emission (also known as single-frequency fiber lasers) can be attained by increasing the free spectral range, reducing the gain bandwidth, or generally, a combination thereof (Fig. 1.37).

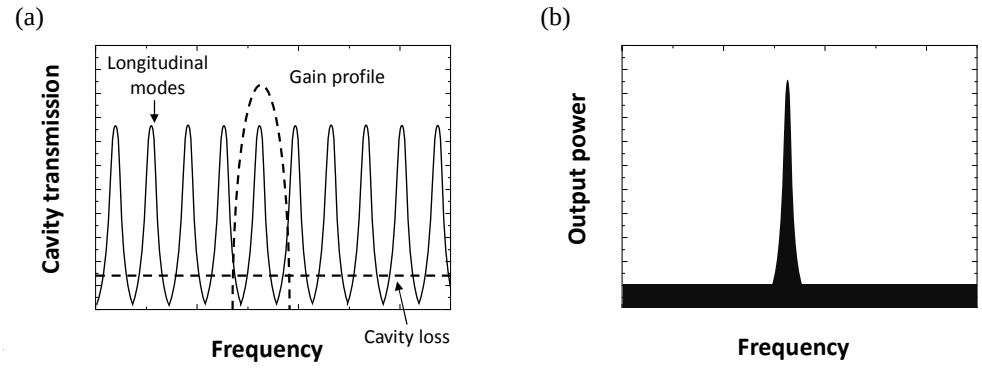

Fig. 1.37. (a) Cavity transmission response and (b) output spectrum of a single-longitudinal mode fiber laser.

In order to increase the free spectral range, short cavity lasers have been designed [166]. In those setups, highly-doped fiber is mainly used due to the high gain provided in a very short linear cavity. As a result, linear cavities with about 5 cm of doped fiber have been presented, corresponding with a free spectral in the order of gigahertz. This high FSR together with narrow filter devices allowed achieving single-longitudinal mode fiber lasers using a linear cavity. In addition, other resonator types, such as Fox-Smith interferometers, can be used to increase the FSR of the system [178]. Moreover, compound laser cavities can be formed so the allowed longitudinal modes have to satisfy the conditions imposed by multiple resonators [179].

Apart from simple FBGs, other optical devices and combinations of filters can be used to limit the gain bandwidth of the fiber laser. Phase shifted Bragg gratings present a transmission line that in general is narrower (~10 times) than the given by regular FBGs, so combining PS-FBGs in transmission with additional filtering elements can be used for achieving SLM operation [180]. A different approach for reducing the gain bandwidth in the resonator consists of using saturable absorbers for both reducing the gain bandwidth and enhancing the laser stability. For example, a section of doped fiber can be inserted in the resonator to induce some losses in the cavity, which are lower for high optical intensities [181].

In the case of single-longitudinal mode fiber lasers, the behavior of the system is significantly affected by the profile of the longitudinal modes. An example of the shape of the longitudinal mode distribution in a linear cavity can be seen in Fig. 1.38. It is worth noticing that the full width at half maximum (FWHM) of the longitudinal modes depends on the reflectivity of the cavity mirrors so a narrower linewidth is obtained if high-reflectivity mirrors are used in the laser setup.

However, even though the linewidth of SLM fiber lasers can be of a few kilohertz, the laser is affected by wavelength-instabilities that can reach hundreds of megahertz or even some gigahertz. The most important effect is called mode hopping, and refers to the *jump* of the emission line from a valid mode to another (not necessarily adjacent). This effect might be induced by different causes, like temperature variations in the filtering device or gain medium, external random noise, mirror vibrations or changes in the pump power. In any case, reducing mode hopping is a crucial factor in SLM fiber lasers. As a consequence, besides of reducing the external sources of instability, increasing the FSR and reducing the gain bandwidth as much as possible definitely reduce mode hopping.

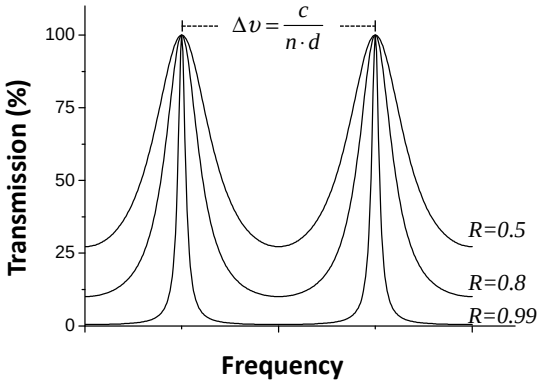

Fig. 1.38. Longitudinal mode distribution in a linear cavity for equal mirrors of reflectivity *R*.

Other interesting effect that can be used in favor of SLM operation is mode competition. In the case of homogeneous broadening, optical waves from different longitudinal modes that share a gain medium compete for the energy provided by the amplifier. This leads to cross-saturation effects, where stimulated emission by one mode causes gain saturation not only for itself (self-saturation), but also for other longitudinal modes. Therefore, in a situation with strong mode competition, the mode with the highest gain can saturate the gain so it equals its losses; accordingly any other longitudinal mode would then experience a negative net gain, which would prevent it from lasing.

Modeless operation

Finally, a last type of longitudinal-mode behavior should be considered: the *modeless* operation. This case takes place in fiber lasers with random distributed feedback cavities where at least one of the reflectors of a linear resonator is replaced by a distributed mirror like depicted in Fig. 1.34.

The reflection is typically provided by Rayleigh scattering in the optical fiber, without the need of point reflectors in at least one of the laser arms. That is a distributed weak reflection along the fiber but under certain circumstances (high gain) the system can initiate the laser emission. In this scheme, the laser resonator can be understood as the combination of numerous broad low-Q longitudinal modes, in contrast to the narrow high-Q modes induced in a Fabry-Pérot resonator [172]. As a consequence, the cavity does not impose any spectral selectivity, being the feedback frequency-independent [Fig 1.39(a)].

If the total gain inside the cavity overcomes the high losses of the cavity, the system will start lasing at a frequency given by the maximum of the gain profile like represented in Fig. 1.39(b). When the lasing threshold is reached, a continuous collective mode formation is generated, presenting a linewidth which is typically a few nanometers wide in a system without wavelength-selective elements. In contraposition to single-longitudinal mode fiber lasers, the linewidth of the emission line is not mainly defined by the shape of the longitudinal modes but by the response of the filtering elements used, if any. Otherwise, the laser form will be mainly characterized by the gain profile.

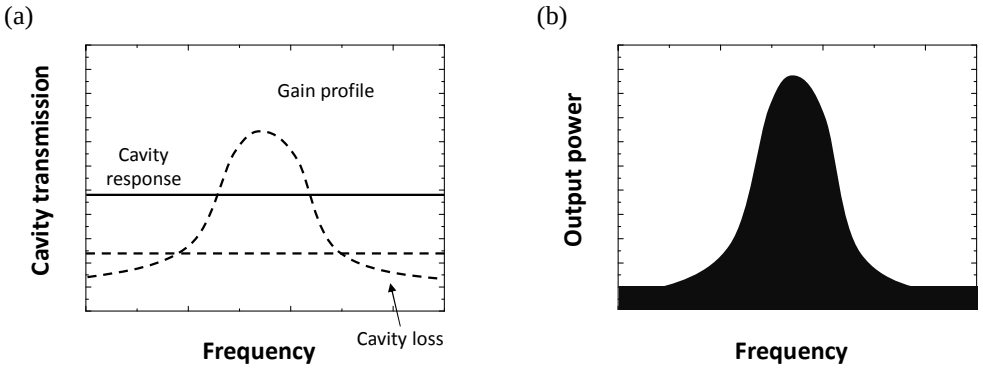

Fig. 1.39. (a) Spectral longitudinal-mode distribution and (b) *modeless* emission of an open-cavity RDFL.

This *modeless* behavior has some important implications in the laser properties, which are in some aspects completely different from the presented by conventional lasers. As a result, some applications can benefit from these particularities. Random distributed feedback fiber lasers are analyzed in detail in Chapter 4, studying their capabilities in particular for sensing applications.

1.4.6 Fiber laser types: Considering number of emission lines

The number of emission lines is also an important parameter to define fiber lasers. Thus, two main groups of fiber lasers can be conceived: single-emission and multiwavelength fiber lasers. In the previous sections single-emission lines were mainly considered; however, modifications can be included in the fiber laser scheme to emit multiple emission lines simultaneously. Those lasers are known as multiwavelength fiber lasers.

Multiwavelength laser sources have attracted special interest in applications like optical communications, instrument testing, optical processing and optical sensing mainly due to their advantages over single-emission fiber lasers, such as reduced cost, high power and low insertion loss among others [146]. Dense wavelength division multiplexing (DWDM) in particular has powered the development of multiwavelength laser sources for high-capacity communication systems due to its cost-effectiveness. In general, the desired properties of multiwavelength lasers include: high number of laser lines over a broad bandwidth, moderate output powers (~100 µW per channel), high OSNR, precise and stable wavelength spacing and small power fluctuations among others. In addition, it is also advisable the single-longitudinal mode operation, the wavelength tunability of each emission line and the independent power equalization of each channel [145]. Nevertheless, fulfil all those requirements simultaneously is very challenging since satisfying some properties prevent others to be attained. As a consequence, numerous approaches have been presented up to date using different amplification processes, topologies, wavelength selectors, etc.

Schemes based on semiconductor optical amplifiers (SOAs) present stable operation at room temperature but on the other hand they are not all-fiber structures. As a result, they suffer from relatively high insertion losses, large polarization dependence and high sensitivity to temperature changes [182].

Other approaches use stimulated Raman scattering amplification for the laser generation, appearing as a successful solution to avoid some of the disadvantages given by other amplification media. Multiwavelength Raman fiber lasers have been deeply analyzed due to the inhomogeneous broadening behavior, which significantly improves the wavelength stability by reducing the gain competition between lines. That also implies that depending on the configuration, independent control of the power of each emission like can be attained. Other advantages of such lasers are the high extinction ratio and wide wavelength flexibility. It should be noticed that the wavelength region amplified by stimulated Raman scattering is located at a frequency 13 THz lower than the pump wave. In this manner, wide amplification ranges can be obtained by combining pump lasers at different frequencies. Accordingly, multiwavelength Raman fiber lasers are appropriate for DWDM applications. However, as mentioned previously, each laser line bandwidth is commonly broader than the achieved using erbium doped fiber amplification. Regarding the devices employed for the wavelength selection, multiple methods have been reported such as Hi-Bi fiber loop mirrors [146], fiber Bragg gratings [152], long period gratings [183] or photonic crystal fibers [144].

Finally, the third main amplification technique used is based on erbium doped fiber. In this case, multiwavelength schemes present high power conversion efficiency and low threshold. In addition, as presented in this Ph.D. work, single-longitudinal mode operation of erbium-based multiwavelength fiber lasers is also feasible. Even though equalizing and maintaining the simultaneous emission of multiple lines is difficult due to the cross-gain saturation in the homogeneous gain broadening, some techniques can improve the stability of the system enough to remain in stable multiwavelength SLM operation. For example, previous publications have demonstrated that SLM operation can be reached by avoiding the mode competition when two emission lines are generated with similar power levels, due to the interaction of the seed light produced from one channel to the other and vice versa [171]. Other techniques exploit effects such as Four Wave Mixing (FWM) [184], polarization hole burning [185] or the cooling of the doped fiber in liquid-nitrogen [186].

Considering the topologies used in the design of multiwavelength fiber lasers, there are three main approaches. Initially, the simplest solution is to use different active medium and cavity for each emission line and to multiplex the obtained laser lines. In this case, each laser emission can be considered independent from the others; however, this approach presents high cost, complexity and low flexibility [187]. Another technique achieves the multiwavelength operation sharing a single amplification medium and the whole cavity, selecting the emission lines by the insertion of optical filters like HiBi fiber loop mirrors or comb filters. Numerous emission lines can be obtained using this solution, but the power stability deteriorates if using EDF amplification due to its homogeneous gain broadening effect [186]. The last practical method used in multiwavelength fiber lasers is to share part of the cavity using different active media (easier power equalization) [188] or a single one [171]. In addition, as in the first solution, easy wavelength tunability can be obtained if independent optical filters such as FBGs are used for the wavelength selection.

1.5 References

[1] Bravo, M., Baptista, J. M., Santos, J. L., Lopez-Amo, M., & Frazão, O. (2011). Ultralong 250 km remote sensor system based on a fiber loop mirror interrogated by an optical time-domain reflectometer. *Optics letters*, *36*(20), 4059-4061.

[2] Lopez-Higuera, J. M. (2002). Introduction to fibre optic sensing technology. *Handbook of Optical Fibre Sensing Technology*, 1-22.

[3] Li, H. N., Li, D. S., & Song, G. B. (2004). Recent applications of fiber optic sensors to health monitoring in civil engineering. *Engineering structures*, *26*(11), 1647-1657.

[4] Culshaw, B. (2004). Optical fiber sensor technologies: opportunities and-perhaps-pitfalls. *Journal of lightwave technology*, *22*(1), 39.

[5] Rao, Y. J., Huang, S. (2008). *Fiber Optic Sensors, Chapter 10, Applications of Fiber Optic Sensors.* Ed. by S. Yin, P. B. Ruffin, F. T. S. Yu.

[6] Lee, B. (2003). Review of the present status of optical fiber sensors. *Optical fiber technology*, *9*(2), 57-79.

[7] Kashyap, R. (1999). *Fiber bragg gratings*. Academic press.

[8] Selleri, S., & Poli, F. (2008, June). Doped fiber lasers: From telecom to industrial applications. In *2008 10th Anniversary International Conference on Transparent Optical Networks*.

[9] Hill, K. O., & Meltz, G. (1997). Fiber Bragg grating technology fundamentals and overview. *Journal of lightwave technology*, *15*(8), 1263-1276.

[10] Dong, B., Hao, J., Liaw, C. Y., Lin, B., & Tjin, S. C. (2010). Simultaneous strain and temperature measurement using a compact photonic crystal fiber inter-modal interferometer and a fiber Bragg grating. *Applied optics*, *49*(32), 6232-6235.

[11] Li, T., Dong, X., Chan, C. C., Hu, L., & Qian, W. (2012). Simultaneous strain and temperature measurement based on a photonic crystal fiber modal-interference interacting with a long period fiber grating. *Optics Communications*, *285*(24), 4874-4877.

[12] Zhou, D. P., Wei, L., Liu, W. K., & Lit, J. W. (2009). Simultaneous strain and temperature measurement with fiber Bragg grating and multimode fibers using an intensity-based interrogation method. *Photonics Technology Letters, IEEE*, *21*(7), 468-470.

[13] Guan, B. O., Tam, H. Y., Tao, X. M., & Dong, X. Y. (2000). Simultaneous strain and temperature measurement using a superstructure fiber Bragg grating. *Photonics Technology Letters, IEEE*, *12*(6), 675-677.

[14] Haus, H. A., & Shank, C. V. (1976). Antisymmetric taper of distributed feedback lasers. *Quantum Electronics, IEEE Journal of*, *12*(9), 532-539.

[15] Agrawal, G. P., & Radic, S. (1994). Phase-shifted fiber Bragg gratings and their application for wavelength demultiplexing. *Photonics Technology Letters, IEEE*, *6*(8), 995-997.

[16] James, S. W., & Tatam, R. P. (2003). Optical fibre long-period grating sensors: characteristics and application. *Measurement science and technology*, *14*(5), R49.

[17] Bhatia V, Campbell D K, Sherr D, D'Alberto T G, Zabar onick N A, Ten Eyck G A, Murphy K A and Claus R O 1997 Temperature-insensitive and strain insensitive long-period grating sensors for smart structures Opt. Eng. 36 1872–6

[18] Dobb, H., Kalli, K., & Webb, D. J. (2004, November). Temperature insensitive long-period grating sensors in photonic crystal fiber. In *Photonics North* (pp. 66-79). International Society for Optics and Photonics.

[19] Shu, X., Allsop, T., Gwandu, B., Zhang, L., & Bennion, I. (2001). High-temperature sensitivity of long-period gratings in B-Ge codoped fiber. *Photonics Technology Letters, IEEE*, *13*(8), 818-820.

[20] Grattan, K. T. V., & Sun, T. (2000). Fiber optic sensor technology: an overview. *Sensors and Actuators A: Physical*, *82*(1), 40-61.

[21] Grattan, K. T., & Meggitt, B. T. (Eds.). (1995). *Optical fiber sensor technology* (Vol. 1). London: Chapman & Hall.

[22] Lee, B. H., Kim, Y. H., Park, K. S., Eom, J. B., Kim, M. J., Rho, B. S., & Choi, H. Y. (2012). Interferometric fiber optic sensors. *Sensors*, *12*(3), 2467-2486.

[23] Rao, Y. J. (2006). Recent progress in fiber-optic extrinsic Fabry–Perot interferometric sensors. *Optical Fiber Technology*, *12*(3), 227-237.

[24] Hunger, D., Steinmetz, T., Colombe, Y., Deutsch, C., Hänsch, T. W., & Reichel, J. (2010). A fiber Fabry–Perot cavity with high finesse. *New Journal of Physics*, *12*(6), 065038.

[25] Putman, M. A., Berkoff, T. A., Kersey, A. D., Sirkis, J. S., Brennan, D. D., & Friebele, E. J. (1993). In-line fiber etalon for strain measurement. *Optics letters*, *18*(22), 1973-1975.

[26] Wang, Z., Shen, F., Song, L., Wang, X., & Wang, A. (2007). Multiplexed fiber Fabry–Perot interferometer sensors based on ultrashort Bragg gratings. *Photonics Technology Letters, IEEE*, *19*(8), 622-624.
[27] Machavaram, V. R., Badcock, R. A., & Fernando, G. F. (2007). Fabrication of intrinsic fibre Fabry–Perot sensors in silica fibres using hydrofluoric acid etching. *Sensors and Actuators A: Physical*, *138*(1), 248-260.
[28] Ran, Z. L., Rao, Y. J., Liu, W. J., Liao, X., & Chiang, K. S. (2008). Laser-micromachined Fabry-Perot optical fiber tip sensor for high-resolution temperature-independent measurement of refractive index. *Optics express*, *16*(3), 2252-2263.
[29] Zhao, J. R., Huang, X. G., He, W. X., & Chen, J. H. (2010). High-resolution and temperature-insensitive fiber optic refractive index sensor based on fresnel reflection modulated by Fabry–Perot interference. *Journal of Lightwave Technology*, *28*(19), 2799-2803.
[30] Born, M., & Wolf, E. (2000). *Principles of optics: electromagnetic theory of propagation, interference and diffraction of light*. CUP Archive.
[31] Jackson, D. A., Priest, R., Dandridge, A., & Tveten, A. B. (1980). Elimination of drift in a single-mode optical fiber interferometer using a piezoelectrically stretched coiled fiber. *Applied Optics*, *19*(17), 2926-2929.
[32] Kim, Y. J., Paek, U. C., & Lee, B. H. (2002). Measurement of refractive-index variation with temperature by use of long-period fiber gratings. *Optics letters*, *27*(15), 1297-1299.
[33] Choi, H. Y., Kim, M. J., & Lee, B. H. (2007). All-fiber Mach-Zehnder type interferometers formed in photonic crystal fiber. *Optics Express*, *15*(9), 5711-5720.
[34] Nguyen, L. V., Hwang, D., Moon, S., Moon, D. S., & Chung, Y. (2008). High temperature fiber sensor with high sensitivity based on core diameter mismatch. *Optics express*, *16*(15), 11369-11375.
[35] Zhu, J. J., Zhang, A. P., Xia, T. H., He, S., & Xue, W. (2010). Fiber-optic high-temperature sensor based on thin-core fiber modal interferometer. *Sensors Journal, IEEE*, *10*(9), 1415-1418.
[36] Tian, Z., Yam, S. S. H., Barnes, J., Bock, W., Greig, P., Fraser, J. M., ... & Oleschuk, R. D. (2008). Refractive index sensing with Mach–Zehnder interferometer based on concatenating two single-mode fiber tapers. *Photonics Technology Letters, IEEE*, *20*(8), 626-628.
[37] Kim, D. W., Zhang, Y., Cooper, K. L., & Wang, A. (2005). In-fiber reflection mode interferometer based on a long-period grating for external refractive-index measurement. *Applied optics*, *44*(26), 5368-5373.
[38] Stokes, L. F., Chodorow, M., & Shaw, H. J. (1982). All-single-mode fiber resonator. *Optics Letters*, *7*(6), 288-290.
[39] Yu, C., Zhang, Y., Zhang, X., Wang, K., Yao, C., Yuan, P., & Guan, Y. (2012). Nested fiber ring resonator enhanced Mach–Zehnder interferometer for temperature sensing. *Applied optics*, *51*(36), 8873-8876.
[40] Zhang, L., Lu, P., Chen, L., Huang, C., Liu, D., & Jiang, S. (2012). Optical fiber strain sensor using fiber resonator based on frequency comb Vernier spectroscopy. *Optics letters*, *37*(13), 2622-2624.
[41] Guo, Y., & Fan, X. (2012, February). Optofluidics in bio-chemical analysis. In *SPIE BiOS* (pp. 82120C-82120C). International Society for Optics and Photonics.
[42] Bravo, M., Angulo-Vinuesa, X., Martin-Lopez, S., López-Amo, M., & González-Herráez, M. (2013). Slow-light and enhanced sensitivity in a displacement sensor using a lossy fiber-based ring resonator. *Journal of Lightwave Technology*, *31*(23), 3752-3757.
[43] Rota-Rodrigo, S., González-Herráez, M., & López-Amo, M. (2015). Compound Lasing Fiber Optic Ring Resonators for Sensor Sensitivity Enhancement. *Journal of Lightwave Technology*, *33*(12), 2690-2696.
[44] Mortimore, D. B. (1988). Fiber loop reflectors. *Lightwave Technology, Journal of*, *6*(7), 1217-1224.
[45] Culshaw, B. (2005). The optical fibre Sagnac interferometer: an overview of its principles and applications. *Measurement Science and Technology*, *17*(1), R1.
[46] Knight, J. C., Birks, T. A., Russell, P. S. J., & Atkin, D. M. (1996). All-silica single-mode optical fiber with photonic crystal cladding. *Optics letters*, *21*(19), 1547-1549.
[47] Russell, P. S. J. (2006). Photonic-crystal fibers. *Journal of lightwave technology*, *24*(12), 4729-4749.
[48] Ritari, T. (2006). *Novel sensor and telecommunication applications of photonic crystal fibers*. (Doctoral dissertation, Helsinki University of Technology).

[49] Cregan, R. F., Mangan, B. J., Knight, J. C., & Birks, T. A. (1999). Single-mode photonic band gap guidance of light in air. *science*, *285*(5433), 1537.
[50] Mortensen, N. A., Folkenberg, J. R., Nielsen, M. D., & Hansen, K. P. (2003). Modal cutoff and the V parameter in photonic crystal fibers. *Optics letters*, *28*(20), 1879-1881.
[51] Rota Rodrigo, S. (2015). *Development of advanced structures for optical fiber lasers and sensors*. (Doctoral dissertation, Universidad Publica de Navarra).
[52] Ortigosa-Blanch, A., Knight, J. C., Wadsworth, W. J., Arriaga, J., Mangan, B. J., Birks, T. A., & Russell, P. S. J. (2000). Highly birefringent photonic crystal fibers. *Optics letters*, *25*(18), 1325-1327.
[53] http://www.nktphotonics.com/files/files/PM-1550-01.pdf
[54] Liu, S., Liu, N., Hou, M., Guo, J., Li, Z., & Lu, P. (2013). Direction-independent fiber inclinometer based on simplified hollow core photonic crystal fiber. *Optics letters*, *38*(4), 449-451.
[55] Wang, R., Yao, J., Miao, Y., Lu, Y., Xu, D., Luan, N., ... & Hao, C. (2013). A reflective photonic crystal fiber temperature sensor probe based on infiltration with liquid mixtures. *Sensors*, *13*(6), 7916-7925.
[56] Qureshi, K. K., Liu, Z., Tam, H. Y., & Zia, M. F. (2013). A strain sensor based on in-line fiber Mach–Zehnder interferometer in twin-core photonic crystal fiber. *Optics Communications*, *309*, 68-70.
[57] Thakur, H. V., Nalawade, S. M., Gupta, S., Kitture, R., & Kale, S. N. (2011). Photonic crystal fiber injected with Fe3O4 nanofluid for magnetic field detection. *Applied Physics Letters*, *99*(16), 161101.
[58] Mathews, S., Farrell, G., & Semenova, Y. (2011). Directional electric field sensitivity of a liquid crystal infiltrated photonic crystal fiber. *Photonics Technology Letters, IEEE*, *23*(7), 408-410.
[59] Thakur, H. V., Nalawade, S. M., Saxena, Y., & Grattan, K. T. V. (2011). All-fiber embedded PM-PCF vibration sensor for Structural Health Monitoring of composite. *Sensors and Actuators A: Physical*, *167*(2), 204-212.
[60] Fu, H. Y., Wu, C., Tse, M. L. V., Zhang, L., Cheng, K. C. D., Tam, H. Y., ... & Lu, C. (2010). High pressure sensor based on photonic crystal fiber for downhole application. *Applied optics*, *49*(14), 2639-2643.
[61] Ceballos-Herrera, D. E., Torres-Gómez, I., Martinez-Rios, A., García, L., & Sanchez-Mondragon, J. J. (2010). Torsion sensing characteristics of mechanically induced long-period holey fiber gratings. *Sensors Journal, IEEE*, *10*(7), 1200-1205.
[62] Smietana, M., Brabant, D., Bock, W. J., Mikulic, P., & Eftimov, T. (2011, May). Inline core-cladding intermodal interferometer based on nano-coated photonic crystal fiber for refractive-index sensing. In *21st International Conference on Optical Fibre Sensors (OFS21)* (pp. 77531R-77531R). International Society for Optics and Photonics.
[63] Li, T., Dong, X., Chan, C. C., Ni, K., Zhang, S., & Shum, P. P. (2013). Humidity sensor with a PVA-coated photonic crystal fiber interferometer. *Sensors Journal, IEEE*, *13*(6), 2214-2216.
[64] Myaing, M. T., Ye, J. Y., Norris, T. B., Thomas, T., Baker Jr, J. R., Wadsworth, W. J., ... & Russell, P. S. J. (2003). Enhanced two-photon biosensing with double-clad photonic crystal fibers. *Optics Letters*, *28*(14), 1224-1226.
[65] Yang, X. H., & Wang, L. L. (2007). Fluorescence pH probe based on microstructured polymer optical fiber. *Optics express*, *15*(25), 16478-16483.
[66] Yan, G., Zhang, A. P., Ma, G., Wang, B., Kim, B., Im, J., ... & Chung, Y. (2011). Fiber-optic acetylene gas sensor based on microstructured optical fiber Bragg gratings. *Photonics Technology Letters, IEEE*, *23*(21), 1588-1590.
[67] Lopez-Amo, M., and Lopez-Higuera, J. M. (2011). *Fiber Bragg Gratings Sensors: Research Advancements, Industrial Applications and Market Exploitation, Chapter 6, Multiplexing Techniques for FBG Sensors*, Ed. by Bentham Science Publishers Ltd.
[68] Jones, J.D.C. and McBride, R. (1998). *Optical Fiber Sensor Technology, Chapter 4, Multiplexing optical fiber sensors*. Ed. by Chapman and Hall.
[69] Liao, Y., Austin, E., Nash, P. J., Kingsley, S. A., & Richardson, D. J. (2013). Highly scalable amplified hybrid TDM/DWDM array architecture for interferometric fiber-optic sensor systems. *Lightwave Technology, Journal of*, *31*(6), 882-888.
[70] Cranch, J. (2014). *Handbook of Optical Sensors, Chapter 15, Fiber-optic sensor multiplexing principles*. Crc Press.
[71] Rao, Y. J. (1997). In-fibre Bragg grating sensors. *Measurement science and technology*, *8*(4), 355.

[72] Fu, H. Y., Wong, A. C. L., Childs, P. A., Tam, H. Y., Liao, Y. B., Lu, C., & Wai, P. K. A. (2009). Multiplexing of polarization-maintaining photonic crystal fiber based Sagnac interferometric sensors. *Optics express*, *17*(21), 18501-18512.
[73] Bravo, M., Candiani, A., Cucinotta, A., Selleri, S., Lopez-Amo, M., Kobelke, J., & Schuster, K. (2014). Remote PCF-based sensors multiplexing by using optical add–drop multiplexers. *Optics & Laser Technology*, *57*, 9-11.
[74] Zhang, M., Sun, Q., Wang, Z., Li, X., Liu, H., & Liu, D. (2012). A large capacity sensing network with identical weak fiber Bragg gratings multiplexing. *Optics Communications*, *285*(13), 3082-3087.
[75] Barnoski, M. K., & Jensen, S. M. (1976). Fiber waveguides: a novel technique for investigating attenuation characteristics. *Applied Optics*, *15*(9), 2112-2115.
[76] Davies, D. E. N. (1984, November). Signal processing for distributed optical fibre sensors. In *2nd International Conference on Optical Fiber Sensors* (pp. 285-296). International Society for Optics and Photonics.
[77] Maughan, S. M. (2002). *Distributed fibre sensing using microwave heterodyne detection of spontaneous Brillouin backscatter* (Doctoral dissertation, University of Southampton).
[78] Brinkmeyer, E. (1980). Analysis of the backscattering method for single-mode optical fibers. *JOSA*, *70*(8), 1010-1012.
[79] Pinto, N. M. P., Frazao, O., Baptista, J. M., & Santos, J. L. (2006). Quasi-distributed displacement sensor for structural monitoring using a commercial OTDR. *Optics and lasers in Engineering*, *44*(8), 771-778.
[80] Luo, F., Liu, J., Ma, N., & Morse, T. F. (1999). A fiber optic microbend sensor for distributed sensing application in the structural strain monitoring. *Sensors and Actuators A: Physical*, *75*(1), 41-44.
[81] Binu, S., Pillai, V. M., & Chandrasekaran, N. (2006). OTDR based fiber optic microbend sensor for distributed sensing applications in structural pressure monitoring. *Journal of Optics*, *35*(1), 36-44.
[82] Guangping, X., Keey, S. L., & Asundi, A. (1999). Optical time-domain reflectometry for distributed sensing of the structural strain and deformation. *Optics and Lasers in Engineering*, *32*(5), 437-447.
[83] Fernandez Vallejo, M. (2012). *Contribution to the development of optical networks for fiber optic sensors using fiber lasers*. (Doctoral. Dissertation. Universidad Publica de Navarra).
[84] Barrera, D., Villatoro, J., Finazzi, V. P., Cárdenas-Sevilla, G. A., Minkovich, V. P., Sales, S., & Pruneri, V. (2010). Low-loss photonic crystal fiber interferometers for sensor networks. *Lightwave Technology, Journal of*, *28*(24), 3542-3547.
[85] Liu, L., Gong, Y., Wu, Y., Zhao, T., Wu, H. J., & Rao, Y. J. (2012). Spatial frequency multiplexing of fiber-optic interferometric refractive index sensors based on graded-index multimode fibers. *Sensors*, *12*(9), 12377-12385.
[86] Rao, Y. J., Jiang, J., & Zhou, C. X. (2005). Spatial-frequency multiplexed fiber-optic Fizeau strain sensor system with optical amplification. *Sensors and Actuators A: Physical*, *120*(2), 354-359.
[87] Rao, Y. J., Ran, Z. L., & Zhou, C. X. (2006). Fiber-optic Fabry-Perot sensors based on a combination of spatial-frequency division multiplexing and wavelength division multiplexing formed by chirped fiber Bragg grating pairs. *Applied optics*, *45*(23), 5815-5818.
[88] Jiang, Y., Tang, C., & Zhang, F. (2009). WDM/SDM of intensity-type fiber-optic sensors. *Microwave and Optical Technology Letters*, *51*(2), 432-435.
[89] Urquhart, P., López, O. G., Boyen, G., & Bruckmann, A. (2007). Optical amplifiers for telecommunications. In *2007 IEEE International Symposium on Intelligent Signal Processing*.
[90] Einstein, A. (1917). Zur quantentheorie der strahlung. *Physikalische Zeitschrift*, *18*.
[91] Harrington, J. A. (2003, December). Infrared fibers and their applications. SPIE-International Society for Optical Engineering.
[92] Zervas, M. N., Laming, R. I., Townsend, J. E., & Payne, D. N. (1992). Design and fabrication of high gain-efficiency erbium-doped fiber amplifiers. *Photonics Technology Letters, IEEE*, *4*(12), 1342-1344.
[93] Raman, C. V., & Krishnan, K. S. (1928). A new type of secondary radiation. *Nature*, *121*, 501-502.
[94] Agrawal, G. P. (2007). *Nonlinear fiber optics*. Academic press.
[95] R. H. Stolen (2003) *Raman Amplifiers for Telecommunication 1, Physical Principle, Chapter 2, Fundamentals of Raman Amplification in Fibers*, Ed. by M. N. Islam.
[96] Islam, M. N. (Ed.). (2003). *Raman Amplifiers for Telecommunication 1, Physical Principle, Chapter 1 Raman Amplification in Telecommunications*.

[97] Agrawal, G. P. (2011). *Chapter 7, Loss management in Fiber-Optic Communication Systems: Fourth Edition*, John Wiley & Sons.
[98] Namiki, S., & Emori, Y. (2001). Ultrabroad-band Raman amplifiers pumped and gain-equalized by wavelength-division-multiplexed high-power laser diodes. *Selected Topics in Quantum Electronics, IEEE Journal of*, *7*(1), 3-16.
[99] Horiguchi, T., & Tateda, M. (1989). Optical-fiber-attenuation investigation using stimulated Brillouin scattering between a pulse and a continuous wave. *Optics Letters*, *14*(8), 408-410.
[100] Tkach, R. W., & Chraplyvy, A. R. (1989). Fibre Brillouin amplifiers. *Optical and quantum electronics*, *21*(1), S105-S112.
[101] Snitzer, E. (1961). Optical maser action of Nd+ 3 in a barium crown glass. *Physical Review Letters*, *7*(12), 444.
[102] Prokhorov, A. M. (1963). Amplification properties of a dielectric filament. *Optics and Spectroscopy*, *14*, 38.
[103] Wolff, N. E., & Pressley, R. J. (1963). Optical maser action in an Eu+ 3-containing organic matrix. *Applied Physics Letters*, *2*(8), 152-154.
[104] Koester, C. J., & Snitzer, E. (1964). Amplification in a fiber laser. *Applied Optics*, *3*(10), 1182-1186.
[105] Kao, K. C., & Hockham, G. A. (1966). Dielectric-fibre surface waveguides for optical frequencies. *Electrical Engineers, Proceedings of the Institution of*, *113*(7), 1151-1158.
[106] Stone, J., & Burrus, C. (1973). Neodymium-doped silica lasers in end-pumped fiber geometry. *Applied Physics Letters*, *23*(7), 388-389.
[107] Stone, J., & Burrus, C. A. (1974). Neodymium-doped fiber lasers: room temperature cw operation with an injection laser pump. *Applied optics*, *13*(6), 1256-1258.
[108] Mears, R. J., Reekie, L., Poole, S. B., & Payne, D. N. (1985). Neodymium-doped silica single-mode fibre lasers. *Electronics Letters*, *21*(17), 738-740.
[109] Mears, R. J., Reekie, L., Poole, S. B., & Payne, D. N. (1986). Low-threshold tunable CW and Q-switched fibre laser operating at 1.55 μm. *Electronics Letters*, *22*(3), 159-160.
[110] Bellemare, A. (2003). Continuous-wave silica-based erbium-doped fibre lasers. *Progress in Quantum Electronics*, *27*(4), 211-266.
[111] Hill, K. O., Kawasaki, B. S., & Johnson, D. C. (1976). Low-threshold cw Raman laser. *Applied Physics Letters*, *29*(3), 181-183.
[112] Smith, S. P., Zarinetchi, F., & Ezekiel, S. (1991). Narrow-linewidth stimulated Brillouin fiber laser and applications. *Optics letters*, *16*(6), 393-395.
[113] Paschotta, R. (2008). *Field Guide to Lasers* (Vol. 12). SPIE press.
[114] Nelson, L. E., Jones, D. J., Tamura, K., Haus, H. A., & Ippen, E. P. (1997). Ultrashort-pulse fiber ring lasers. *Applied Physics B: Lasers and Optics*, *65*(2), 277-294.
[115] Urquhart, P. (1988, December). Review of rare earth doped fibre lasers and amplifiers. In *Optoelectronics, IEE Proceedings J* (Vol. 135, No. 6, pp. 385-407). IET.
[116] Digonnet, M. J. (Ed.). (2001). *Rare-earth-doped fiber lasers and amplifiers, revised and expanded*. CRC press.
[117] Bellemare, A., Rochette, M., & LaRochelle, S. (2000). Room temperature multifrequency erbium-doped fiber lasers anchored on the ITU frequency grid. *journal of lightwave technology*, *18*(6), 825.
[118] Park, N., & Wysocki, P. F. (1996). 24-line multiwavelength operation of erbium-doped fiber-ring laser. *Photonics Technology Letters, IEEE*, *8*(11), 1459-1461.
[119] Talaverano, L., Abad, S., Jarabo, S., & Lopez-Amo, M. (2001). Multiwavelength fiber laser sources with Bragg-grating sensor multiplexing capability. *Journal of lightwave technology*, *19*(4), 553.
[120] Han, Y. G., Kim, G., Lee, J. H., Kim, S. H., & Lee, S. B. (2005). Lasing wavelength and spacing switchable multiwavelength fiber laser from 1510 to 1620 nm. *Photonics Technology Letters, IEEE*, *17*(5), 989-991.
[121] Han, Y. G., Tran, T. V. A., & Lee, S. B. (2006). Wavelength-spacing tunable multiwavelength erbium-doped fiber laser based on four-wave mixing of dispersion-shifted fiber. *Optics letters*, *31*(6), 697-699.
[122] Horiguchi, M., Yoshino, K., Shimizu, M., & Yamada, M. (1993). 670 nm semiconductor laser diode pumped erbium-doped fibre amplifiers. *Electronics Letters*, *29*(7), 593-595.
[123] Whitley, T. J. (1988). Laser diode pumped operation of Er3+-doped fibre amplifier. *Electronics Letters*, *24*(25), 1537-1539.

[124] Horiguchi, M., Shimizu, M., Yamada, M., Yoshino, K., & Hanafusa, H. (1990). Highly efficient optical fibre amplifier pumped by a 0.8 μm band laser diode. *Electronics Letters*, *26*(21), 1758-1759.

[125] Yamada, M., Shimizu, M., Takeshita, T., Okayasu, M., Horiguchi, M., Uehara, S., & Sugita, E. (1989). Er/sup 3+/-doped fiber amplifier pumped by 0.98 mu m laser diodes. *Photonics Technology Letters, IEEE*, *1*(12), 422-424.

[126] Suyama, M., Nakamura, K., Kashiwa, S., & Kuwahara, H. (1989, February). 14.4-dB Gain of Erbium-Doped Fiber Amplifier Pumped by 1.49-μm Laser Diode. In *Optical Fiber Communication Conference* (p. PD6). Optical Society of America.

[127] Nakamura, H., Fujisaka, A., & Ogoshi, H. (1996, February). Gain and noise characteristics of erbium-doped fiber amplifier pumped at 1530 nm. In *Optical Fiber Communications, 1996. OFC'96* (pp. 158-159). IEEE.

[128] Al-Alimi, A. W., Al-Mansoori, M. H., Abas, A. F., Mahdi, M. A., & Ajiya, M. (2009). Optimization of tunable dual wavelength erbium-doped fiber laser. *Laser Physics Letters*, *6*(10), 727-731.

[129] Humphrey, P. D., & Bowers, J. E. (1993). Fiber-birefringence tuning technique for an erbium-doped fiber ring laser. *Photonics Technology Letters, IEEE*, *5*(1), 32-34.

[130] Parvizi, R., Harun, S. W., Shahabuddin, N. S., Yusoff, Z., & Ahmad, H. (2010). Multi-wavelength bismuth-based erbium-doped fiber laser based on four-wave mixing effect in photonic crystal fiber. *Optics & Laser Technology*, *42*(8), 1250-1252.

[131] Bellemare, A., Karbsek, M., Riviere, C., Babin, F., He, G., Roy, V., & Schinn, G. W. (2001). A broadly tunable erbium-doped fiber ring laser: experimentation and modeling. *Selected Topics in Quantum Electronics, IEEE Journal of*, *7*(1), 22-29.

[132] Pan, S., & Lou, C. (2006). Stable multiwavelength erbium-doped fiber laser at room temperature with tunable wavelength, wavelength spacing, and channel number. *Optical Engineering*, *45*(11), 114203-114203.

[133] Lin, H. (2010). Waveband-tunable multiwavelength erbium-doped fiber laser. *Applied Optics*, *49*(14), 2653-2657.

[134] Park, N., Dawson, J. W., Vahala, K. J., & Miller, C. (1991). All fiber, low threshold, widely tunable single-frequency, erbium-doped fiber ring laser with a tandem fiber Fabry–Perot filter. *Applied physics letters*, *59*(19), 2369-2371.

[135] Achaerandio, E., Jarabo, S., Abad, S., & López-Amo, M. (1999). New WDM amplified network for optical sensor multiplexing. *Photonics Technology Letters, IEEE*, *11*(12), 1644-1646.

[136] Kersey, A. D., & Morey, W. W. (1993). Multi-element Bragg-grating based fibre-laser strain sensor. *Electronics Letters*, *29*(11), 964-966.

[137] Fu, Z., Yang, D., Ye, W., Kong, J., & Shen, Y. (2009). Widely tunable compact erbium-doped fiber ring laser for fiber-optic sensing applications. *Optics & Laser Technology*, *41*(4), 392-396.

[138] Karalekas, V., Ania-Casta, J. D., Harper, P., Babin, S. A., Podivilov, E. V., & Turitsyn, S. K. (2007). Impact of nonlinear spectral broadening in ultra-long Raman fibre lasers. *Optics express*, *15*(25), 16690-16695.

[139] Rottwitt, K. (2005). *Raman Amplification in Fiber Optical Communication Systems, Chapter 3, Distributed Raman Amplifiers*. Ed. by C. Headley and G. P. Agrawal.

[140] Agrawal, G. P. (2005). *Raman Amplification in Fiber Optical Communication Systems, Chapter 2, Theory of Raman Amplifiers.* Ed. by C. Headley and G. P. Agrawal, 2005.

[141] Grubb, S. G., Erdogan, T., Mizrahi, V., Strasser, T., Cheung, W. Y., Reed, W. A., ... & Becker, P. C. (1994, August). 1.3 μm cascaded Raman amplifier in germanosilicate fibers. In *Optical Amplifiers and Their Applications* (p. PD3). Optical Society of America.

[142] Headly, C., Mermelstein, M., & Bouteiller, J.C. (2003). *Raman Amplifiers for Telecommunication 2, Sub-Systems and Systems, Chapter 11, Raman Fiber Lasers.* Ed. by M. N. Islam.

[143] Turitsyn, S. K., Ania-Castañón, J. D., Babin, S. A., Karalekas, V., Harper, P., Churkin, D., ... & Mezentsev, V. K. (2009). 270-km ultralong Raman fiber laser. *Physical review letters*, *103*(13), 133901.

[144] Pinto, A. M. R., Frazão, O., Santos, J. L., & Lopez-Amo, M. (2011). Multiwavelength Raman fiber lasers using Hi-Bi photonic crystal fiber loop mirrors combined with random cavities. *Journal of Lightwave Technology*, *29*(10), 1482-1488.

[145] Kim, N. S., Zou, X., & Lewis, K. (2002, March). CW depolarized multiwavelength Raman fiber ring laser with over 58 channels and 50 GHz channel spacing. In *Optical Fiber Communication Conference and Exhibit, 2002. OFC 2002* (pp. 640-642). IEEE.

[146] Wang, Z., Cui, Y., Yun, B., & Lu, C. (2005). Multiwavelength generation in a Raman fiber laser with sampled Bragg grating. *Photonics Technology Letters, IEEE*, *17*(10), 2044-2046.
[147] Kim, C. S., Sova, R. M., & Kang, J. U. (2003). Tunable multi-wavelength all-fiber Raman source using fiber Sagnac loop filter. *Optics communications*, *218*(4), 291-295.
[148] Dong, X., Shum, P., Ngo, N. Q., & Chan, C. C. (2006). Multiwavelength Raman fiber laser with a continuously-tunable spacing. *Optics express*, *14*(8), 3288-3293.
[149] Turitsyn, S. K., Babin, S. A., El-Taher, A. E., Harper, P., Churkin, D. V., Kablukov, S. I., ... & Podivilov, E. V. (2010). Random distributed feedback fibre laser. *Nature Photonics*, *4*(4), 231-235.
[150] De Matos, C. J. S., Chestnut, D. A., Reeves-Hall, P. C., Koch, F., & Taylor, J. R. (2001). Multi-wavelength, continuous wave fibre Raman ring laser operating at 1.55 [mu] m. *Electronics Letters*, *37*(13), 1.
[151] Lee, J., Kim, J., Han, Y. G., Kim, S. H., & Lee, S. (2004). Investigation of Raman fiber laser temperature probe based on fiber Bragg gratings for long-distance remote sensing applications. *Optics express*, *12*(8), 1747-1752.
[152] Peng, P. C., Tseng, H. Y., & Chi, S. (2004). Long-distance FBG sensor system using a linear-cavity fiber Raman laser scheme. *Photonics Technology Letters, IEEE*, *16*(2), 575-577.
[153] Han, Y. G., Tran, T. V. A., Kim, S. H., & Lee, S. B. (2005). Multiwavelength Raman-fiber-laser-based long-distance remote sensor for simultaneous measurement of strain and temperature. *Optics letters*, *30*(11), 1282-1284.
[154] Ania-Castañón, J. D. (2004). Quasi-lossless transmission using second-order Raman amplification and fibre Bragg gratings. *Optics express*, *12*(19), 4372-4377.
[155] Hill, K. O., Kawasaki, B. S., & Johnson, D. C. (1976). CW Brillouin laser. *Applied Physics Letters*, *28*(10), 608-609.
[156] Cowle, G. J., & Stepanov, D. Y. (1996). Multiple wavelength generation with Brillouin/erbium fiber lasers. *Photonics Technology Letters, IEEE*, *8*(11), 1465-1467.
[157] Stepanov, D. Y., & Cowle, G. J. (1997). Properties of Brillouin/erbium fiber lasers. *Selected Topics in Quantum Electronics, IEEE Journal of*, *3*(4), 1049-1057.
[158] Shee, Y. G., Al-Mansoori, M. H., Ismail, A., Hitam, S., & Mahdi, M. A. (2011). Multiwavelength Brillouin-erbium fiber laser with double-Brillouin-frequency spacing. *Optics express*, *19*(3), 1699-1706.
[159] Zamzuri, A. K., Ali, M. M., Ahmad, A., Mohamad, R., & Mahdi, M. A. (2006). Brillouin-Raman comb fiber laser with cooperative Rayleigh scattering in a linear cavity. *Optics letters*, *31*(7), 918-920.
[160] Carter, S. F., Szebesta, D., Davey, S. T., Wyatt, R., Brierley, M. C., & France, P. W. (1991). Amplification at 1.3 μm in a Pr3+-doped single-mode fluorozirconate fibre. *Electronics letters*, *27*(8), 628-629.
[161] Shi, Y., Poulsen, C. V., Sejka, M., Ibsen, M., & Poulsen, O. (1993). Tunable Pr3+-doped silica-based fibre laser. *Electronics Letters*, *29*(16), 1426-1427.
[162] McAleavey, F. J., Gorman, J. O., Donegan, J. F., MacCraith, B. D., Hegarty, J., & Mazé, G. (1997). Narrow linewidth, tunable Tm 3+-doped fluoride fiber laser for optical-based hydrocarbon gas sensing. *Selected Topics in Quantum Electronics, IEEE Journal of*, *3*(4), 1103-1111.
[163] Oh, K., Morse, T. F., Weber, P. M., Kilian, A., & Reinhart, L. (1994). Continuous-wave oscillation of thulium-sensitized holmium-doped silica fiber laser. *Optics letters*, *19*(4), 278-280.
[164] Hanna, D. C., Percival, R. M., Perry, I. R., Smart, R. G., Suni, P. J. M., Townsend, J. E., & Tropper, A. C. (1988, June). Continuous-wave oscillation of a monomode ytterbium-doped fibre laser. In *All-Fibre Devices, IEE Colloquium on* (pp. 14-1). IET.
[165] Allain, J. Y., Bayon, J. F., Monerie, M., Bernage, P., & Niay, P. (1993). Ytterbium-doped silica fibre laser with intracore Bragg gratings operating at 1.02 μm. *Electronics Letters*, *29*(3), 309-310.
[166] Perez-Herrera, R. A., Chen, S., Zhao, W., Sun, T., Grattan, K. T. V., & Lopez-Amo, M. (2010). Stability performance of short cavity Er-doped fiber lasers. *Optics Communications*, *283*(6), 1067-1070.
[167] Fernández-Vallejo, M., Diaz, S., Perez-Herrera, R. A., Unzu, R., Quintela, M. A., López-Higuera, J. M., & López-Amo, M. (2009). Comparison of the stability of ring resonator structures for multiwavelength fiber lasers using Raman or Er-doped fiber amplification. *IEEE Journal of Quantum electronics*, *45*(11-12), 1551-1557.
[168] Kashyap, R., Armitage, J. R., Wyatt, R., Davey, S. T., & Williams, D. L. (1990). All-fibre narrowband reflection gratings at 1500 nm. *Electronics Letters*, *26*(11), 730-732.

[169] A. Gusarov and F. Liegeois, "Experimental study of a tunable fiber ring laser stability," *Opt. Commun.*, vol. 234, pp. 391-397, 2004.
[170] Perez-Herrera, R. A., & Sainz, M. L. A. (2010, November). Fiber lasers for optical sensing applications. In *Proceedings of the 3rd WSEAS international conference on Advances in sensors, signals and materials* (pp. 125-129). World Scientific and Engineering Academy and Society (WSEAS).
[171] Quintela, M., Perez-Herrera, R. A., Canales, I., Fernandez-Vallejo, M., Lopez-Amo, M., & López-Higuera, J. M. (2010). Stabilization of dual-wavelength erbium-doped fiber ring lasers by single-mode operation. *Photonics Technology Letters, IEEE, 22*(6), 368-370.
[172] Turitsyn, S. K., Babin, S. A., Churkin, D. V., Vatnik, I. D., Nikulin, M., & Podivilov, E. V. (2014). Random distributed feedback fibre lasers. *Physics reports*, *542*(2), 133-193.
[173] Senior, J. M., & Jamro, M. Y. (2009). *Optical fiber communications: principles and practice*. Pearson Education.
[174] Nakazawa, M. (1983). Rayleigh backscattering theory for single-mode optical fibers. *JOSA*, *73*(9), 1175-1180.
[175] Barnoski, M., Rourke, M., Jensen, S. M., & Melville, R. T. (1977). Optical time domain reflectometer. *Applied optics*, *16*(9), 2375-2379.
[176] Churkin, D. V., Sugavanam, S., Vatnik, I. D., Wang, Z., Podivilov, E. V., Babin, S. A., ... & Turitsyn, S. K. (2015). Recent advances in fundamentals and applications of random fiber lasers. *Advances in Optics and Photonics*, *7*(3), 516-569.
[177] Huang, C., Dong, X., Zhang, N., Zhang, S., & Shum, P. P. (2014). Multiwavelength Brillouin-erbium random fiber laser incorporating a chirped fiber Bragg grating. *Selected Topics in Quantum Electronics, IEEE Journal of*, *20*(5), 294-298.
[178] Barnsley, P., Urquhart, P., Millar, C., & Brierley, M. (1988). Fiber Fox–Smith resonators: application to single-longitudinal-mode operation of fiber lasers. *JOSA A*, *5*(8), 1339-1346.
[179] Pan, S., Zhao, X., & Lou, C. (2008). Switchable single-longitudinal-mode dual-wavelength erbium-doped fiber ring laser incorporating a semiconductor optical amplifier. *Optics letters*, *33*(8), 764-766.
[180] Rota-Rodrigo, S., Rodriguez-Cobo, L., Angeles Quintela, M., Lopez-Higuera, J. M., & Lopez-Amo, M. (2014). Dual-wavelength single-longitudinal mode fiber laser using phase-shift Bragg gratings. *Selected Topics in Quantum Electronics, IEEE Journal of*, *20*(5), 161-165.
[181] Yang, X. X., Zhan, L., Shen, Q. S., & Xia, Y. X. (2008). High-power single-longitudinal-mode fiber laser with a ring Fabry–Perot resonator and a saturable absorber. *Photonics Technology Letters, IEEE*, *20*(11), 879-881.
[182] Qin, S., Chen, D., Tang, Y., & He, S. (2006). Stable and uniform multi-wavelength fiber laser based on hybrid Raman and Erbium-doped fiber gains. *Optics express*, *14*(22), 10522-10527.
[183] Han, Y. G., Kim, C. S., Kang, J. U., Paek, U. C., & Chung, Y. (2003). Multiwavelength Raman fiber-ring laser based on tunable cascaded long-period fiber gratings. *Photonics Technology Letters, IEEE*, *15*(3), 383-385.
[184] Liu, X. (2009). Stability function of lightwaves based on the cascade of multiple four-wave mixing processes and its application to multi-wavelength erbium lasers. *Journal of Modern Optics*, *56*(7), 903-909.
[185] Sun, J., Qiu, J., & Huang, D. (2000). Multiwavelength erbium-doped fiber lasers exploiting polarization hole burning. *Optics communications*, *182*(1), 193-197.
[186] Yamashita, S., & Hotate, K. (1996). Multiwavelength erbium-doped fibre laser using intracavity etalon and cooled by liquid nitrogen. *Electronics Letters*, *32*(14), 1298-1299.
[187] Lei, D., Gui-Yun, K., Yan-Jun, X., Bai-Ou, G., Shu-Zhong, Y., Xiao-Yi, D., & Chun-Feng, G. (2001). A four-wavelength all-fibre laser for wavelength division multiplexing system. *Chinese Physics Letters*, *18*(3), 376.
[188] Mao, Q., & Lit, J. W. (2003). Multiwavelength erbium-doped fiber lasers with active overlapping linear cavities. *Journal of lightwave technology*, *21*(1), 160.

Chapter 2

High-Birefringence fiber sensor multiplexing in fiber loop mirror structures

In this chapter, the multiplexing capability of high-birefringence fiber loop mirrors and their adaptation to full polarization-maintaining schemes are studied. The use of a fast Fourier trans-form-based monitoring technique, together with the direct splicing between fibers and an adequate interpretation of the theory allowed the design and validation of several new fiber loop mirror-based topologies.

2.1. Introduction to high-birefringence fiber loop mirrors

2.1.1. Background

Since the first demonstration by Georges Sagnac in 1913 [1], numerous works have been published exploiting and analyzing the capabilities of Sagnac interferometers. The basic principle is simple: light is injected through a beam splitter, so it travels around a loop in two opposite directions [Fig. 2.1(a)]. If the loop is rotated, the light travelling in the direction of the rotation will reach the beam splitter at a later time than the light travelling counter-directionally to the rotation. As a consequence, that phase shift induced by the rotation can be detected using optical interferometry.

The adaptation of this system to fiber optic was performed in 1976 [2]. The main advantage of this scheme is the sensitivity increment by using a multiple turn loop instead of the single loop used in the original Sagnac experiment [Fig 2.1(b)]. This initial fiber optic gyroscope (FOG) was followed by numerous works analyzing the performance of the system. After an intense development, FOGs are up to date one of the most successful fiber optic sensors. As a result of the exploration of the Sagnac interferometer properties, different solutions/devices have been created, such as optical fiber Sagnac current sensors [3], Sagnac interferometer-based hydrophones and geophones [4], and fiber loop mirrors among others.

Fiber loop mirrors (FLM) are simple all-fiber optical interferometers in which the ports of an optical coupler are spliced together so a variable amount of incoming light is redirected to the output port or it is otherwise reflected to the input channel. In this case, the length of the loop is very short compared to FOGs, being minimal its sensitivity as rotation-detector.

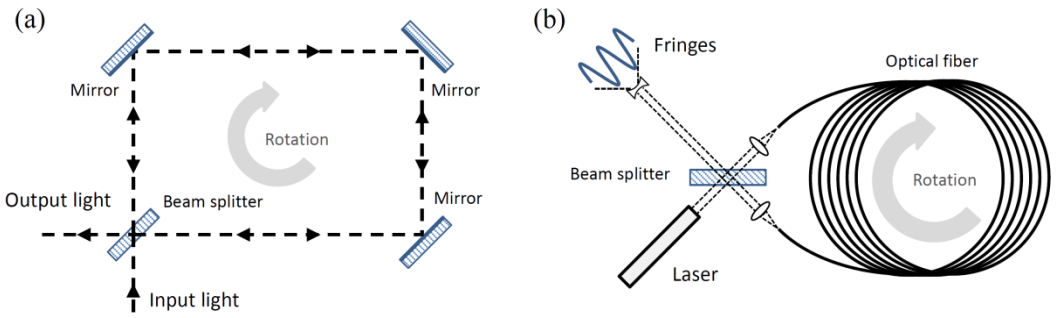

Fig. 2.1. (a) Schematic of a Sagnac interferometer and (b) its fiber optic version.

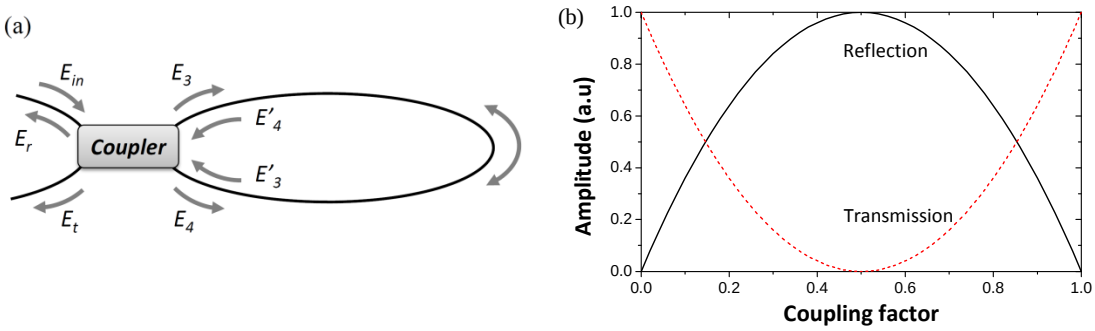

Fig. 2.2. (a) Schematic illustration of a fiber loop mirror. (b) Relationship between coupling factor and transmitted/reflected power in a simple FLM.

Taking into account the schematic shown in Fig. 2.2(a) and the transfer matrix of an optical coupler, ideally (neglecting birefringence, etc.) the transfer function of a fiber loop mirror can be derived as follows:

$$E_r = \sqrt{1-\gamma}\sqrt{k}\ E'_4 + i\sqrt{1-\gamma}\sqrt{1-k}\ E'_3$$
$$E_t = i\sqrt{1-\gamma}\sqrt{1-k}\ E'_4 + \sqrt{1-\gamma}\sqrt{k}\ E'_3 \qquad (2.1)$$

Where:

$$E'_3 = E_3 e^{i\beta L} = \sqrt{1-\gamma}\sqrt{k}\ E_{in} e^{i\beta L}$$
$$E'_4 = E_4 e^{i\beta L} = i\sqrt{1-\gamma}\sqrt{1-k}\ E_{in} e^{i\beta L} \qquad (2.2)$$

Accordingly:

$$E_r = 2i(1-\gamma)\sqrt{k}\sqrt{1-k}\ E_{in} e^{j\beta L}$$
$$E_t = (1-\gamma)(1-2k)\ E_{in} e^{j\beta L} \qquad (2.3)$$

Therefore, the transfer functions can be derived:

$$T = \frac{I_t}{I_{in}} = (1-\gamma)^2 (1-2k)^2$$
$$R = \frac{I_r}{I_{in}} = 4(1-\gamma)^2 k(1-k) \tag{2.4}$$

Where k is the coupling factor and γ represents the insertion loss of the optical coupler. Neglecting the constant factor related with the insertion loss of the coupler, it is clear that the transmitted and reflected power of the device depend entirely on the coupling factor of the optical coupler as depicted in Fig. 2.2(b). This simplified study offers an overall idea of the system's performance; however, additional factors also influence the response of the FLM and can be consequently used to create different optical devices. For example, very fast optical switching can be attained by means of the cross-phase modulation generated by the Kerr effect, which can induce a differential delay in the counter propagating waves [5]. Moreover, small birefringence changes can generate a phase shift between the polarization states in the fiber loop, altering the operation of the FLM. David B. Mortimore thoroughly studied this topology and the birefringence repercussion to be used in the development of fiber lasers [6]. The effect of birefringence can be enhanced, being of special interest the case that arises when a section of high-birefringence optical fiber is inserted into the fiber loop mirror. This topology is known as highly-birefringence fiber loop mirror (HiBi FLM) and has been subject of a deep study during the past years due to its interesting properties.

2.1.2. Principle of operation

Figure 2.3(a) presents the schematic depiction of a high-birefringence fiber loop mirror that comprises a fused taper optical coupler which output ports (made of single-mode fiber) are fused to a HiBi fiber section. In this case, the strong birefringence in the loop generates a phase shift between the fast and slow polarization axes of the light, generating an interference pattern at the optical coupler.

To simplify the analysis of the structure, the loss in the fiber and the insertion loss of the coupler are neglected, neglecting also birefringence in the single-mode fiber. However, it is taken into account birefringence in the HiBi fiber and the relative rotation angles between the polarization axes of the input field and its alignment with the HiBi fiber.

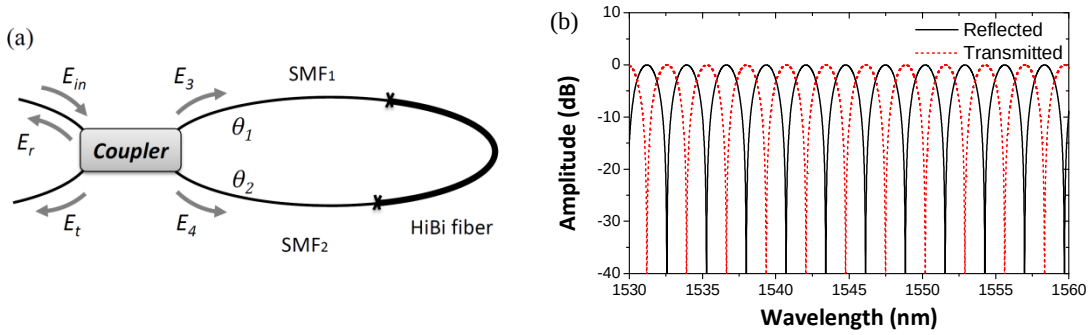

Fig. 2.3. (a) Schematic illustration of a HiBi fiber loop mirror. (b) Transfer functions (transmitted/reflected power) in a simple HiBi FLM.

Accordingly, the output fields would be as follow:

$$\begin{aligned} E_3 &= \sqrt{k}E_{in} \\ E_4 &= i\sqrt{1-k}E_{in} \\ E_r &= i\sqrt{1-k}M_c E_3 + \sqrt{k}M_a E_4 \\ E_t &= \sqrt{k}M_c E_3 + i\sqrt{1-k}M_a E_4 \end{aligned} \tag{2.5}$$

Where k is the coupling factor of the coupler, $E_{in}=[E_{xin}, E_{yin}]$ is the input field and M_c and M_a represent the transfer matrices of the clockwise and anticlockwise turn:

$$\begin{aligned} M_c &= R_2 T_1 R_1 \\ M_a &= R_1^{-1} T_1 R_2^{-1} \end{aligned} \tag{2.6}$$

Being R_n the rotation matrix of the polarization state induced by the rotation angle θ_n:

$$R_n = \begin{pmatrix} \cos\theta_n & -\sin\theta_n \\ \sin\theta_n & \cos\theta_n \end{pmatrix} \tag{2.7}$$

And T_n the phase delay matrix induced by the HiBi fiber section n with length l_n, wavelength λ and refractive indices n_o and n_e.

$$T_n = e^{-i\frac{2\pi n_e l_n}{\lambda}} \begin{pmatrix} 1 & 0 \\ 0 & e^{-i\frac{2\pi(n_o-n_e)l_n}{\lambda}} \end{pmatrix} \tag{2.8}$$

Consequently, after evaluation of the equations, the obtained transfer functions are:

$$\begin{aligned} T &= \frac{I_t}{I_{in}} = (1-2k)^2 \left[\sin^2(\theta_1+\theta_2)\cos^2\left(\frac{\pi(n_e-n_o)l_n}{\lambda}\right)\right] \\ R &= \frac{I_r}{I_{in}} = 4k(1-k)\left[\sin^2(\theta_1+\theta_2)\cos^2\left(\frac{\pi(n_e-n_o)l_n}{\lambda}\right)\right] = 1-T \end{aligned} \tag{2.9}$$

Therefore, in a HiBi FLM, the rotation angles θ_n between the ports of the coupler and the HiBi fiber section modulate the amount of power reflected/transmitted. The angle relationship is typically controlled by a polarization controller placed in one of the SMF fiber sections. However, the most important conclusion is that the length and birefringence (given by $b=|n_e - n_o|$ of the HiBi fiber section generates a sinusoid modulation of the transfer function as depicted in Fig. 2.3(b). Moreover, in contrast to conventional Sagnac interferometers, the generated interference depends on the length of HiBi fiber instead on the total length of the loop. In addition, the interference pattern does not depend on the polarization state of the input light. FLMs were initially presented as a new approach to the design of wavelength-division multiplexers [7], but many other applications have been also proposed. Other uses have been found, such as flattening the response of an erbium doped-fiber amplifier [8], eliminating the polarization dependence of acousto-optic filters [9] or as dispersion-compensation filters [10]. Fiber lasers have also benefited from HiBi FLMs, being of special interest the use as a filter for multiwavelength laser generation with doped-fiber lasers [11] and semiconductor amplifiers [12] but also with

Raman amplification, even in combination with random cavities [13]. Tunability and switching capability are also achieved using PM fiber in a fiber loop mirror [14]. Furthermore, it is of particular significance the potential of HiBi FLMs to be used in the optical sensing field.

2.1.3. HiBi Fiber loop mirrors for sensing applications

As stated before, the original aim of Sagnac interferometers was to detect and measure rotation. However, the loop distance in HiBi fiber loop mirrors is typically not enough to detect rotation, being the cause of the interference in this case the phase shift induced by the high-birefringence fiber. As a consequence, changes in the phase shift between the counter-propagating fields generated by the HiBi fiber can be detected and measured. Considering that a 50/50 optical coupler is used in the setup, the transfer function of a one-section HiBi FLM is the following:

$$T(\lambda)=\sin^2(\theta_1+\theta_2)\cos^2\left(\frac{\pi bl}{\lambda}\right) \tag{2.10}$$

Thus, variations in the birefringence b or in the length l of the HiBi fiber cause a variation in the interference. Those changes can be induced by different physical parameters as temperature or strain among others. Typically, a change in the physical parameter produces a simultaneous variation in both birefringence and length of the fiber. In this manner:

$$\begin{aligned} T(\lambda)&=\sin^2(\theta_1+\theta_2)\cos^2\left(\frac{\pi(b+\Delta b)(l+\Delta l)}{\lambda}\right)\\ &=\sin^2(\theta_1+\theta_2)\cos^2\left(\frac{\pi bl}{\lambda}+\Delta\phi\right)\end{aligned} \tag{2.11}$$

Where:

$$\Delta\phi(\lambda)=\frac{\pi}{\lambda}(b\Delta l+l\Delta b+\Delta l\Delta b)\approx\frac{\pi}{\lambda}(b\Delta l+l\Delta b) \tag{2.12}$$

Thus, a variation in the birefringence and/or fiber length can be understood as a phase change in the transfer function of the HiBi fiber loop mirror. Different physical parameters can induce birefringence or fiber length variations, as a consequence, the appropriate type of HiBi fibers have to be selected depending on the application. For example, conventional PM optical fibers (e.g. PANDA fibers) contain two materials with different thermal (thermal expansion coefficient) and mechanical properties (Young's modulus and Poisson's ratio), which generate high thermal stress-strain with temperature variations, so they are highly sensitive to temperature [15]. In addition, fiber can be doped to induce higher birefringence variations and increase the sensitivity [16]. On the other hand, microstructured HiBi fibers made of a single material present a negligible strain-induced birefringence change [17], so the sensitivity to temperature is very limited, up to 55 times smaller than a common PANDA fiber [18]. That is the reason why single-material microstructured fibers are preferred for axial-strain sensing applications, especially taking into account that the temperature-insensitivity can be increased by striping the PCF fiber [19]. Besides strain and temperature, numerous physical parameters can be also interrogated by means of HiBi FLMs, such as torsion [20], pressure [21], liquid level [22], bending [23] refractive index [24] or humidity [25]. Additionally, chemical sensors can also be attained by employing different fiber types [26]. Finally, several parameters can be simultaneously monitored by combining FLMs with other sensing techniques like a hybrid FLM-MZI (Mach

Zehnder interferometer) [27] or a combination of a FLM with a long-period grating pair for measuring temperature and strain simultaneously [28].

Interrogation techniques

Several interrogation techniques can be employed to measure the phase shift in the transfer function of a HiBi FLM. In this section, the most basic ones are described and compared, particularly focusing on the method used in the experimental work of this thesis, which is based on the fast Fourier transform. In order to compare the performance of each technique, a series of simulations has been performed considering a FLM with a HiBi fiber length of 30 cm and a beat-length of 1.75 mm. To illustrate the phase change induced by a temperature or strain shift, it is considered a simple case where the HiBi fiber is subject exclusively to temperature variations between 0 and 20°C with a sensitivity of 0.16 rad/°C.

As it has been previously shown, when birefringence/fiber length variations occur in a HiBi FLM, the period of its transfer function is modified. In this manner, the first and most evident interrogation technique is to monitor the period of the transfer function and evaluate its variation with the physical parameter under study. However, the period change is minor in practice, being generally under the resolution achieved by the optical devices used to retrieve the optical spectrum. To illustrate this effect, it is depicted in Fig. 2.4(a) the simulated transfer functions of a HiBi FLM subject to temperature changes. Figure 2.4(b) shows the results measuring the distance between peaks (period) using an optical spectrum analyzer with a resolution of 5 pm. It is evident observing the picture that even using that high optical resolution, the results are not accurate. The results can be improved by measuring the wavelength distance between a number of periods but in any case, the resolution achieved is relatively low. As a conclusion, this technique provides low resolution, requiring two maxima/minima to be monitored simultaneously.

It can be inferred for Fig. 2.4(a) that such a slight period variation generates in practice a phase shift of the transfer function. As a consequence, the fiber loop mirror can be interrogated just by tracking the wavelength of a peak or a valley in the optical spectrum. As it can be seen in Fig. 2.5, the results show in this case a good linear fitting. It must also be taken into account that the uncertainty of the period and the peak/valley tracking would be higher in experimental applications due to the difficulty of precisely retrieve the peak/valley value in practice. An example of this effect will be shown in [PAPER B] where the resolution obtained using the peak/valley tracking technique is significantly lower than the theoretically expected. In any case, this technique is up to date the most extended due to its simplicity and reasonably accurate results; however, it still requires the detection and tracking in the optical spectrum of a peak or a valley.

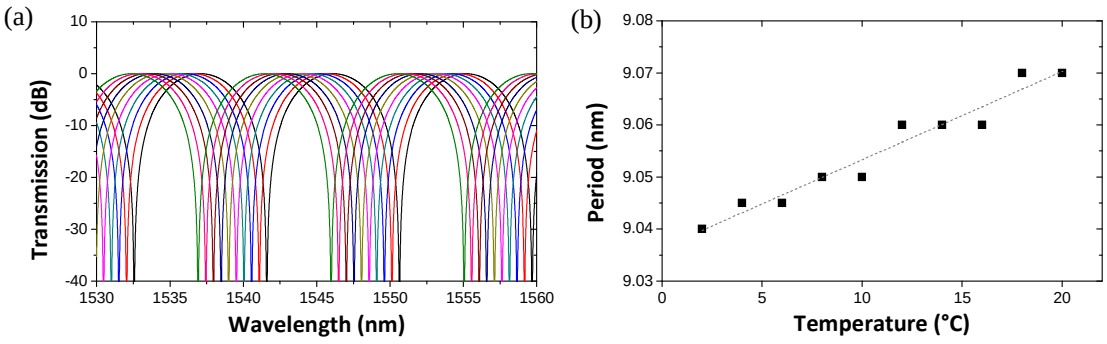

Fig. 2.4. (a) Simulated optical spectra of a HiBi FLM under temperature variations and its period variation.

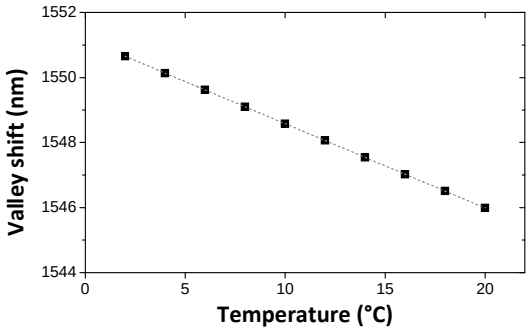

Fig. 2.5. Wavelength shift of the valley located at 1551 nm under temperature variations.

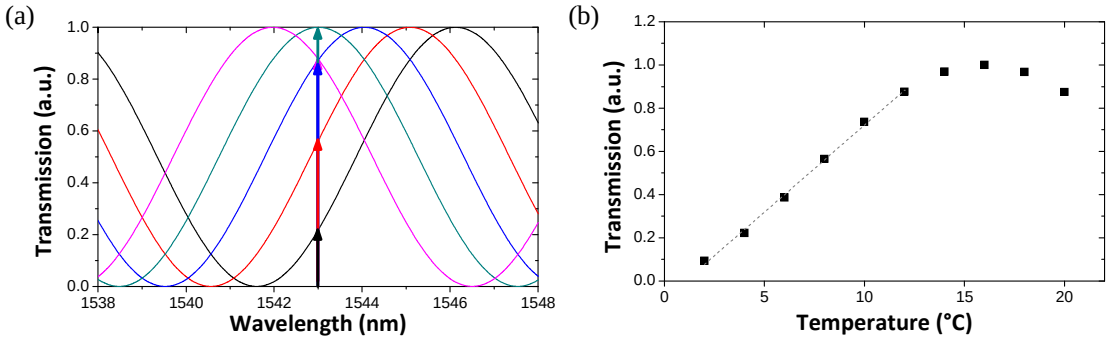

Fig. 2.6. (a) Schematic depiction of the amplitude-based interrogation technique and (b) the results obtained for a fixed wavelength (1542.5 nm).

To simplify the equipment required in the interrogation, other basic approach can be conducted needing just a DFB laser and a power-meter. It is based on monitoring the transmission loss in the fiber loop mirror for a given wavelength. To achieve this, a DFB laser source is located at a fixed wavelength in the linear slope of the transfer function. In this manner, the reading of the sensor is obtained by detecting the received power at the output port. Figure 2.6(a) illustrates this process, in which the DFB laser (arrow) experiences different attenuation depending on the phase shift of the interference. It should be noted that the simulation data is in every case equivalent to the used in the previous interrogation techniques [Fig. 2.4(a)]. The reading of the transmitted power at 1542.5 nm is depicted in Fig. 2.6(b). It can be clearly seen that the main drawback of the system is the limited linear region in which the DFB has to be located. This significantly restricts the range of the physical parameter to be measured. On the other hand, this technique is not limited by the wavelength resolution like the previously presented. Furthermore, it provides the easiest measuring process requiring just a reading of the power value. In theory, the resolution attained by this approach can clearly overcome the previous techniques (in practice it will depend on the DFB stability and the detector's accuracy). Additionally, in order to compensate possible power variations in the fiber, a reference line is typically employed.

Nevertheless, these techniques present a major issue that is the limited capability to interrogate interferometric sensors in multiplexing networks. The main difficulty that arises when HiBi FLMs (interferometric sensors in general) are multiplexed is that the total transfer function of the system is given by a combination of the interferometric sensors multiplexed. In this manner, the interrogation techniques previously presented cannot be used straightforwardly. To over-

come this limitation, a technique based on the fast Fourier transform (FFT) can be used. The FFT is a mathematical tool that decomposes a signal into the frequencies that compose it. Therefore, in the case of a HiBi FLM, the Fourier transform of the transfer function has an amplitude spectrum with a peak placed at a spatial frequency related with the period of the transfer function. In addition, the phase spectrum of the fast Fourier transform encodes the phase information of the FLM-related sinusoid. Taking into account that the sensing information can be related to a phase variation in the optical spectrum (as in the peak/valley tracking technique); the sensing information of a FLM can be retrieved from the FFT phase spectrum.

To exemplify the process, Fig. 2.7(a) displays the transmission of two HiBi FLMs with different fiber lengths and equal birefringence and Fig. 2.7(b) represents the combination of those transfer functions. The FFT of the combined transfer function can be represented in the spatial frequency domain by two spectra: One corresponding to the FFT amplitude and other corresponding to the phase as depicted in Fig. 2.8. The two main contributions can be seen in the amplitude spectrum at the spatial frequencies given by the relationship $Sf(l_n)=l_n/(\lambda_0 L_b)$ between the HiBi fiber length l_n, the central wavelength λ and the beat-length of the fiber L_b. It should be noticed that the beat-length is related with the birefringence as follows: $L_b= \lambda_0/b$. To perform the simulations, the optical spectrum is based on the specifications of a commercial fiber Bragg grating interrogator (like in the previous interrogation techniques) with a resolution of 5 pm and a wavelength range between 1510 and 1590 nm (that corresponds to a 16001 pts FFT).

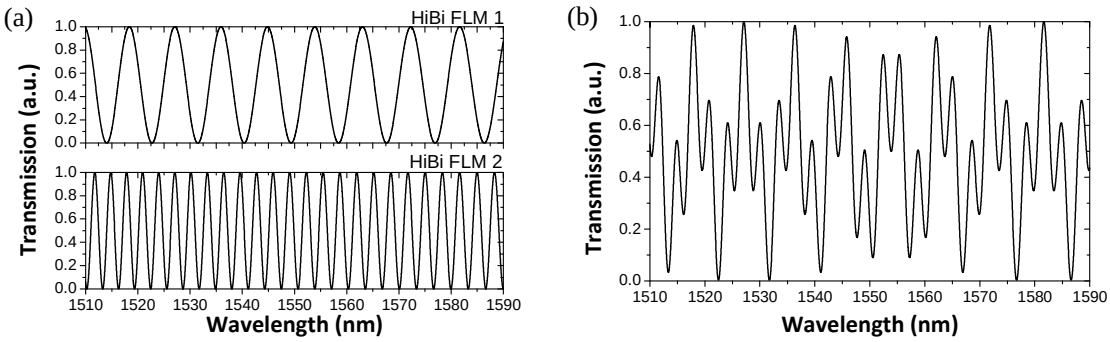

Fig. 2.7. (a) Simulated transfer functions of two HiBi FLMs with different fiber lengths and (b) its combination.

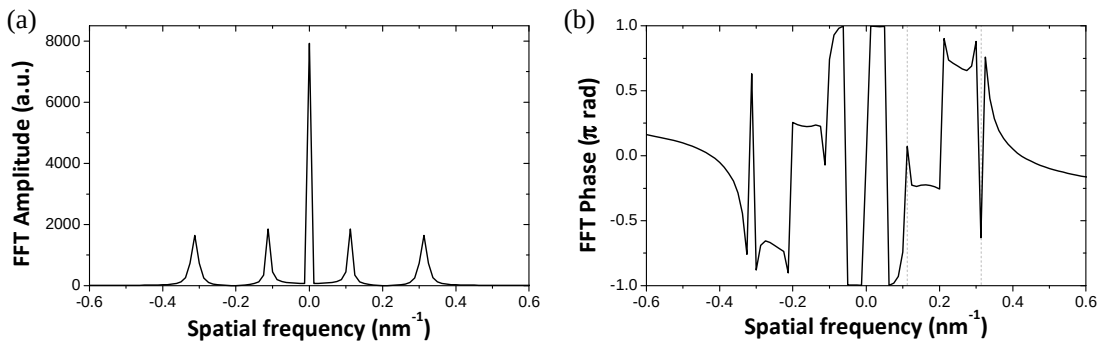

Fig. 2.8. (a) FFT amplitude and (b) phase spectra of the combination of two HiBi FLMs.

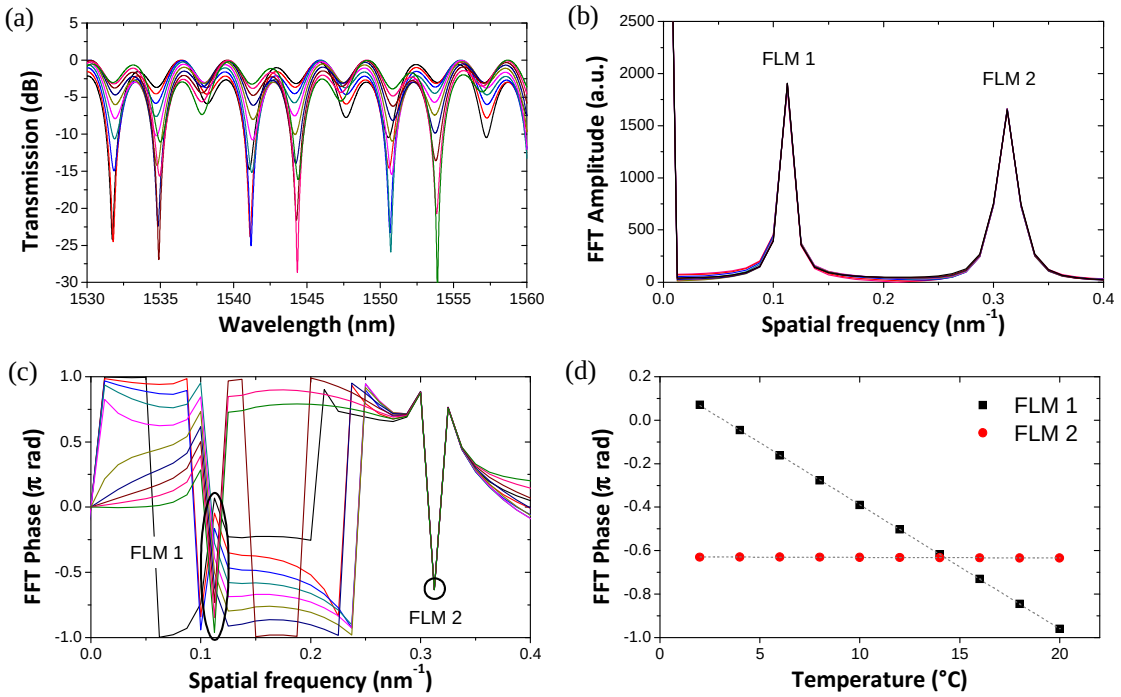

Fig. 2.9. (a) Simulated optical spectra of the combination of two HiBi FLMs where FLM_1 is subject to temperature variations while FLM_2 remains unchanged and (b) its FFT amplitude and (c) phase. (d) FFT phase at the spatial frequencies 0.1125 and 0.3125 nm^{-1} under temperature variations applied to FLM_1.

To show the measurement procedure of this technique, the combination of the transfer function of the two HiBi FLMs [Fig. 2.7(a)] has been used, where HiBi FLM_1 is equivalent to the example used in the previous techniques. Supposing that physical variations are applied only to the HiBi FLM_1, the transmission of the system would vary as represented in Fig. 2.9(a). It is evident that in this case the previous techniques cannot be directly used due to the influence of the second FLM interference. As expected, Fig. 2.9 (b) shows that the FFT amplitude spectrum remains unchanged since the period variation in the transfer function is almost negligible. On the other hand, the FFT phase spectrum [Fig. 2.9(c)] presents important variations that might appear random. However, if the spatial frequencies that correspond to the FLM contributions ($Sf(FLM_1)$=0.1125 nm^{-1} and $Sf(FLM_2)$=0.3125 nm^{-1} in the example) are monitored as depicted in Fig. 2.9(d), it is clear that the phase variation at those points comprises the sensing information of each HiBi FLM.

As a conclusion, the FFT-based interrogation technique presents important advantages with respect to the period and peak/valley tracking and to the amplitude-based technique; being the most important feature its capability to interrogate multiplexing schemes. Furthermore, the spatial-frequency analysis allows discerning between the different contributions in multimodal interferometers [29]. The measuring process is very simple, like in the amplitude-based technique, being only needed the evaluation of a single point (one per sensor) in the FFT phase spectrum. The robustness of the FFT-based technique is also superior to the amplitude-based due to the immunity of the FFT phase to amplitude variations in the spectrum. Referring to the measurement range, it is confined between $\pm\pi$ radians but this limit can be easily handled by software [30]. As an advantage, the amplitude-related approach offers the simplest setup which is more cost-efficient than the other techniques where optical spectrum analyzers are required.

On the other hand, the wavelength-based techniques offer less resolution than the FFT technique, but they are more intuitive and relatively simpler.

The evaluated techniques can be considered the most common and simplest, but numerous variations, combinations and other complex techniques can be utilized. For example, by combining the period and the peak tracking techniques, absolute temperature measurements can be attained using a HiBi FLM [31]. Other approaches take advantage of lasing architectures in combination with amplitude measurements for a fixed wavelength [32]. In the works reported in this chapter, the FFT-based interrogation technique is mainly used due to its high resolution, easy measuring process when implemented in a commercial interrogator and its capability to interrogate multiplexing networks.

2.2. [PAPER A] Real-Time FFT analysis for interferometric sensors multiplexing

Due to the aforementioned properties, numerous works based on HiBi FLMs have been published during the last years. The input polarization independence, the high sensitivity and the dependence of the transmitted spectrum with the length of the HiBi fiber instead of the total length of the loop are the main advantages of HiBi FLMs over regular FLMs. Those features are of special importance in optical sensing, where different physical parameters can be monitored, like rotation, axial strain, temperature, liquid level or curvature. However, compared to other technologies like fiber Bragg gratings, HiBi FLMs have important downsides. The most important is the limited multiplexing capability. Typically, a valley or a peak of the optical spectrum is tracked to interrogate a FLM. However, this is not possible when multiple interferometric devices are multiplexed, since the resulting optical spectrum is the combination of the transfer functions of the interferometers. Another advantage of FBGs over FLMs is that many commercial devices have been designed to interrogate FBG networks in real time.

Taking all this into consideration, the motivation of this work was to present the spatial-frequency multiplexing by means of the fast Fourier transform as an interrogation technique that offers a high multiplexing capability for FLMs, without deteriorating (actually improving) the results. In addition, this study was also aimed to show that a commercial FBG interrogator can be easily adapted by software to monitor multiple interferometric sensors, considerably enhancing the capabilities of the interrogator. In accordance, the main contributions of this work are:

- *Superior interrogation technique:* The FFT-based interrogation technique is presented as a better solution for interferometric sensor multiplexing. In addition to be used for interrogating multiplexing schemes, this technique offers better resolution, easier measuring procedure and less dependence on the amplitude of the interference.
- *FBG technology adaptation:* Commercial FBG interrogators are shown to be able to real-time interrogate interferometric sensor networks after simple software processing.
- *New interferometric sensor networks*: Based on FLM structures, new multiplexing setups are validated experimentally and confirmed by means of simulations.
    - Star topology: Up to four HiBi sensing fibers are monitored simultaneously in a multiple-loop FLM using a 2x8 optical coupler.
    - Two-section HiBi FLM: Two HiBi sensing fibers are placed in series and independently measured in a single FLM.
- *Sensor validation:* Both structures are validated as sensor multiplexing networks by applying axial strain to each sensing element. The sensor's reading is extracted from the FFT phase, obtaining linear results without crosstalk between sensors.
- *Further work:* As a result of this work, the study in depth of the multi-section HiBi FLM structure allowed the design of new systems such as the all-PM HiBi FLMs presented in [PAPER B].

PAPER A

Journal of Lightwave Technology ***33****(2), 354 (2015)*

http://dx.doi.org/10.1109/JLT.2014.2388134

Real-Time FFT Analysis for Interferometric Sensors Multiplexing

Daniel Leandro, Mikel Bravo, Amaia Ortigosa,

and Manuel López-Amo

2.3. [PAPER B] High resolution polarization-independent high-birefringence fiber loop mirror sensor

There is an important factor to be taken into account in every HiBi FLM which, although critical, is barely mentioned in the literature: that is the polarization control inside the cavity. In every HiBi FLM structure, at least one polarization controller (PC) is required to set the angle difference of the polarization states of the light entering to the ports of the optical coupler. However, in research works about HiBi FLMs, it is usually obviated that the polarization states of the light propagating through a single-mode fiber gradually vary in a random an uncontrolled manner. This is due to the fact that single-mode fiber is not purely symmetric; presenting certain degree of birefringence that depends on many factors like bending or temperature changes. In practice, that implies that once the PC of the cavity is set, the single mode fiber sections of the loop must remain steady. Even then, the PC has to be periodically adjusted, being this effect a serious constraint in practical applications.

Using polarization-maintaining (PM) fiber in the whole setup can be considered a direct solution, but the ports of a PM coupler are made of HiBi fiber as well. As a consequence, in the simplest case, the loop of a full-PM FLM is formed by two HiBi fiber sections. Accordingly, the two-section FLM analysis validated in [PAPER A] is required for an adequate design of the structure. The aim of this work was to design all-PM versions of the classical HiBi FLMs without the need of polarization control inside the loop, expecting a significant increase in the system's performance. As a result, the main findings of this study are:

- *Easier operation, increased performance:* All-PM HiBi FLM schemes present superior performance with respect to their classical counterparts (using SMF optical couplers). No polarization control is needed in the loop, being this of special importance in long-term measurements where all-PM FLMs present more accurate results. That increase in performance and reliability makes the system a better candidate for practical applications.
- *FFT-related resolution increase:* The FFT-based monitoring technique offers a resolution more than 100 times higher than the conventional method (monitoring the wavelength of a peak or a valley in the optical spectrum).
- *High-resolution:* Temperature measurements (under 0.001 °C) can be attained by combining the FFT-based technique with the all-PM FLMs schemes. Higher resolutions could be straightforwardly obtained by increasing the length of sensing fiber.
- *Tailored transfer function:* An appropriate control of the rotation angles between fibers allows tailoring the total transfer function of the FLM. For instance, two fiber sections located at different positions can act as a single fiber piece (with a length given by the length difference between the two fibers) if a rotation angle of 90° is set between them.

PAPER B

Optics Express ***23****(24), 30985 (2015)*

http://dx.doi.org/10.1364/OE.23.030985

High Resolution Polarization-Independent High-Birefringence Fiber Loop Mirror Sensor

Daniel Leandro, Mikel Bravo, and Manuel López-Amo

2.4. [PAPER C] Monitoring Multiple HiBi Sensing Fibers in a Single Fiber Loop Mirror

If more than two sections of HiBi fiber are multiplexed in a single fiber loop mirror, the behavior of the system becomes significantly more complex. The transfer function of a single-section FLM has just a main contribution; modulated by a polarization controller. On the other hand, the transfer function of the two-section FLM presented in [PAPER A] presents two main and two secondary contributions, requiring in this case two polarization controllers to be appropriately set. As a consequence, due to the fast increase in the possible combinations, a large number of secondary contributions are expected if more sensing fibers are multiplexed in the loop. This implies that the length of the fiber sections must be precisely chosen to avoid overlapping between the main and the secondary contributions, which would lead to crosstalk in the measurements. In addition, more polarization controllers have to be operated (one per sensing fiber), significantly complicating the operation of the system.

Considering all these aspects, the main motivation of this work was to explore the experimental functionality (for sensing purposes) of fiber loop mirror schemes that multiplex more than two sensing fibers. Again this time, the FFT-based monitoring technique is used to interrogate the spatial-frequency multiplexed sensing elements; real-time monitoring the system using a commercial FBG sensor interrogator as in [PAPER A] and [PAPER B]. It is worth saying that this work is an extended version of the oral contribution presented in the *24th Optical Fiber Sensors (OFS 24)* conference that took place in Curitiba (Brazil) in October 2015 [CONF 2]. [PAPER C] includes some of the preliminary results which were expanded for the full-paper version with a complete theoretical study and a new full-polarization maintaining scheme. As a result, the main contributions of this paper are:

- *Two new multiplexing schemes:* The theoretical and experimental studies of two new HiBi FLM interferometers for sensing applications are presented. The first one is a three-section HiBi FLM and the second is the modification of the setup to all-polarization maintaining fiber.
- *Saving polarization controllers:* Instead of placing a polarization controller to select the rotation angle between fibers, the HiBi fibers were fused together with an angle offset between them*. That greatly simplifies the operation of the system and reduces the loss inside the loop. As a consequence, the number of required PCs is reduced from 3 to 1 in the first scheme. No PCs are needed in the all-PM version.
- *Maximizing main contributions:* A theoretical study of the two setups under the three and four-section FLM theory allowed the main contributions (with the sensing information) to be maximized by finding the optimal rotation angles of the polarization states along the loop.
- *Last stage*: In theory, a higher number of HiBi fibers can be included in the FLM to be used as sensing elements. However, the large number of secondary contributions would imply a complex and precise selection of the fiber lengths, limiting the practical applicability of the system.

* The timeline of the papers presented in this chapter would be the following: [PAPER A], [CONF 2], [PAPER B] and [PAPER C]. That is the reason why the use of splices with a fixed rotation angle to avoid using polarization controllers is claimed as a contribution of this work instead of [PAPER B].

PAPER C

Journal of Lightwave Technology

(In press: available online)

DOI: 10.1109/JLT.2016.2523880

http://dx.doi.org/10.1109/JLT.2016.2523880

Monitoring Multiple Hibi Sensing Fibers in a Single Fiber Loop Mirror

Daniel Leandro, Aitor López, Mikel Bravo
and Manuel López-Amo

2.5. References

[1] Sagnac, G. (1913). L'éther lumineux démontré par l'effet du vent relatif d'éther dans un interféromètre en rotation uniforme. *CR Acad. Sci.*, *157*, 708-710.

[2] Vali, V., & Shorthill, R. W. (1976). Fiber ring interferometer. *Appl. Opt*, *15*(5), 1099-1100.

[3] Blake, J., Tantaswadi, P., & De Carvalho, R. T. (1996). In-line Sagnac interferometer current sensor. *IEEE Transactions on Power Delivery*, *11*(1), 116-121.

[4] Knudsen, S., & Bløtekjær, K. (1994). An ultrasonic fiber-optic hydrophone incorporating a push-pull transducer in a Sagnac interferometer. *Lightwave Technology, Journal of*, *12*(9), 1696-1700.

[5] Jinno, M., & Matsumoto, T. (1992). Nonlinear Sagnac interferometer switch and its applications. *Quantum Electronics, IEEE Journal of*, *28*(4), 875-882.

[6] Mortimore, D. B. (1988). Fiber loop reflectors. *Lightwave Technology, Journal of*, *6*(7), 1217-1224.

[7] Fang, X., & Claus, R. O. (1995). Polarization-independent all-fiber wavelength-division multiplexer based on a Sagnac interferometer. *Optics letters*, *20*(20), 2146-2148.

[8] Li, S., Chiang, K. S., & Gambling, W. A. (2001). Gain flattening of an erbium-doped fiber amplifier using a high-birefringence fiber loop mirror. *Photonics Technology Letters, IEEE*, *13*(9), 942-944.

[9] Zhao, C. L., Jin, W., Ju, J., Dong, X., Kang, J., Zhang, Z., & Jin, S. (2010, December). Polarization independent acousto-optic filter based on photonic crystal fibers by using a fiber loop mirror. In *Asia Communications and Photonics Conference and Exhibition* (79860N). Optical Society of America.

[10] Chung, S., Yu, B. A., & Lee, B. (2003). Phase response design of a polarization-maintaining fiber loop mirror for dispersion compensation. *Photonics Technology Letters, IEEE*, *15*(5), 715-717.

[11] Hu, S., Zhan, L., Song, Y. J., Li, W., Luo, S. Y., & Xia, Y. X. (2005). Switchable multiwavelength erbium-doped fiber ring laser with a multisection high-birefringence fiber loop mirror. *Photonics Technology Letters, IEEE*, *17*(7), 1387-1389.

[12] Im, J. E., Kim, B. K., & Chung, Y. (2010). Stable SOA-based multi-wavelength fiber ring laser using Sagnac loop mirror incorporating a high-birefringence photonic crystal fiber. *Laser physics*, *20*(10), 1918-1922.

[13] Pinto, A. M. R., Frazão, O., Santos, J. L., & Lopez-Amo, M. (2011). Multiwavelength Raman fiber lasers using Hi-Bi photonic crystal fiber loop mirrors combined with random cavities. *Journal of Lightwave Technology*, *29*(10), 1482-1488.

[14] Ma, X., Luo, S., & Chen, D. (2014). Switchable and tunable thulium-doped fiber laser incorporating a Sagnac loop mirror. *Applied optics*, *53*(20), 4382-4385.

[15] Kim, D. H., & Kang, J. U. (2007). Analysis of temperature-dependent birefringence of a polarization-maintaining photonic crystal fiber. *Optical Engineering*, *46*(7), 075003-075003.

[16] Moon, D. S., Kim, B. H., Lin, A., Sun, G., Han, Y. G., Han, W. T., & Chung, Y. (2007). The temperature sensitivity of Sagnac loop interferometer based on polarization maintaining side-hole fiber. *Optics express*, *15*(13), 7962-7967.

[17] Kotynski, R., Nasilowski, T., Antkowiak, M., Berghmansa, F., & Thienpont, H. (2003, July). Sensitivity of holey fiber based sensors. In *Transparent Optical Networks, 2003. Proceedings of 2003 5th International Conference on* (Vol. 1, pp. 340-343). IEEE.

[18] Zhao, C. L., Yang, X., Lu, C., Jin, W., & Demokan, M. S. (2004). Temperature-insensitive interferometer using a highly birefringent photonic crystal fiber loop mirror. *Photonics Technology Letters, IEEE*, *16*(11), 2535-2537.

[19] Frazao, O., Baptista, J. M., & Santos, J. L. (2007). Temperature-independent strain sensor based on a Hi-Bi photonic crystal fiber loop mirror. *IEEE Sensors Journal*, *7*(9/10), 1453.

[20] Kim, H. M., Kim, T. H., Kim, B., & Chung, Y. (2010). Temperature-insensitive torsion sensor with enhanced sensitivity by use of a highly birefringent photonic crystal fiber. *Photonics Technology Letters, IEEE*, *22*(20), 1539-1541.

[21] Fu, H. Y., Tam, H. Y., Shao, L. Y., Dong, X., Wai, P. K. A., Lu, C., & Khijwania, S. K. (2008). Pressure sensor realized with polarization-maintaining photonic crystal fiber-based Sagnac interferometer. *Applied optics*, *47*(15), 2835-2839.

[22] Bo, D., Qida, Z., Feng, L., Tuan, G., Lifang, X., Shuhong, L., & Hong, G. (2006). Liquid-level sensor with a high-birefringence-fiber loop mirror. *Applied Optics*, *45*(30), 7767-7771.

[23] Frazão, O., Baptista, J. M., Santos, J. L., & Roy, P. (2008). Curvature sensor using a highly birefringent photonic crystal fiber with two asymmetric hole regions in a Sagnac interferometer. *Applied optics*, *47*(13), 2520-2523.

[24] Zhong, C., Shen, C., You, Y., Chu, J., Zou, X., Dong, X., ... & Wang, J. (2012). A polarization-maintaining fiber loop mirror based sensor for liquid refractive index absolute measurement. *Sensors and Actuators B: Chemical*, *168*, 360-364.
[25] Liang, H., Jin, Y., Wang, J., & Zhao, Y. (2012, May). Temperature-independent humidity sensor based on polarization maintaining fiber loop mirror. In *Photonics and Optoelectronics (SOPO), 2012 Symposium on* (pp. 1-3). IEEE.
[26] Pinto, A. M., & Lopez-Amo, M. (2012). Photonic crystal fibers for sensing applications. *Journal of Sensors*, *2012*.
[27] Kim, H. M., Nam, H., Moon, D. S., Kim, Y. H., Lee, B. H., & Chung, Y. (2009). Simultaneous measurement of strain and temperature with high sensing accuracy. In *2009 14th OptoElectronics and Communications Conference*.
[28] Frazão, O., Marques, L. M., Santos, S., Baptista, J. M., & Santos, J. L. (2006). Simultaneous measurement for strain and temperature based on a long-period grating combined with a high-birefringence fiber loop mirror. *Photonics Technology Letters, IEEE*, *18*(22), 2407-2409.
[29] Rota-Rodrigo, S., López-Amo, M., Kobelke, J., Schuster, K., Santos, J. L., & Frazao, O. (2015). Multimodal interferometer based on a suspended core fiber for simultaneous measurement of physical parameters. *Journal of Lightwave Technology*, *33*(12), 2468-2473.
[30] Chen, Y., Yang, Y., Liu, S., Yang, M., & Jin, W. (2015, September). Fourier transform-based absolute phase interrogation algorithm for Sagnac Interferometer-based PMF Sensors. In *International Conference on Optical Fibre Sensors (OFS24)* (pp. 96343A-96343A). International Society for Optics and Photonics.
[31] De la Rosa, E., Zenteno, L. A., Starodumov, A. N., & Monzon, D. (1997). All-fiber absolute temperature sensor using an unbalanced high-birefringence Sagnac loop. *Optics letters*, *22*(7), 481-483.
[32] Bravo, M., Fernández-Vallejo, M., Echapare, M., López-Amo, M., Kobelke, J., & Schuster, K. (2013). Multiplexing of six micro-displacement suspended-core Sagnac interferometer sensors with a Raman-Erbium fiber laser. *Optics express*, *21*(3), 2971-2977.

Chapter 3

Sensor schemes based on fiber lasers

In this chapter, fiber lasers are presented as suitable systems for optical sensing due mainly to their high flexibility. Different types of fiber lasers are developed: from single-longitudinal mode fiber lasers using short cavities to fiber lasers for remote interrogation of sensors located 100 or 155 km away. Multiple topologies and gain processes are also employed, including Raman, erbium-doped fibers and Brillouin amplification.

3.1. Fiber lasers in sensing applications

As it has been previously described in Chapter 1, fiber lasers can be formed by adding a feedback to an optical gain medium, achieving total loss inside the cavity lower than the total gain. Different amplification methods can be employed to achieve the stimulated emission, such as fiber doped with rare earths (erbium, praseodymium, ytterbium, neodymium and thulium among others). Each type of doping induces amplification at different wavelength bands, being this is an important factor to be considered in the design of the laser. In addition, non linearities of the fiber can be exploited to generate amplification; typically stimulated Raman or Brillouin scattering. In this case the wavelength of the amplification is related to the wavelength of the pump laser. More information about amplification types can be found in Chapter 1.

The type of feedback is also a crucial factor in the laser development. If the feedback is wavelength-selective, it can *force* the laser emission at certain wavelengths. Furthermore, the bandwidth of the wavelength-selective reflector (together with the cavity length) has a decisive impact in the longitudinal-mode behavior of the laser. In this manner, using highly selective reflectors can stimulate the single-longitudinal mode operation of the laser. This is highly preferred in some applications such as interferometry with coherent sensors due to the narrow linewidth (few kilohertz) and hence very long coherence lengths of the lasers. To obtain single-longitudinal mode operation, a long free spectral range (FSR) is required, which implies that the cavity length should be short. Additional techniques can be used to increase the FSR such as employing composed cavities. Moreover, stable multi-wavelength single-longitudinal mode fiber lasers are especially interesting for their potential use in optical fiber sensing, sensor network multiplexing schemes, microwave photonics systems and instrument testing among others [1]-[3].

The topology used in the laser design also influences the final behavior of the laser; for example, half FSR is obtained by using a ring cavity instead of linear (supposing equal cavity length). Furthermore, each type of topology favors the use of different spectral filters inside the

cavity. E.g. ring topologies can easily integrate FBG filters in transmission, while reflecting filters would require including complementary devices such as circulators or couplers.

Taking all those main aspects into account, fiber lasers present a very flexible design, with notably different properties depending on the type of amplification, cavity, longitudinal-mode behavior and number of emission lines. For example, very short cavities (a few centimeters) can be formed to achieve SLM operation but if remote sensing is desired, ultra-long cavities (more than one hundred kilometers) can be formed. In this manner, those main features define and should be considered to describe a fiber laser:

- *Amplification*: Raman, Brillouin, erbium-doped fiber, etc.
- *Cavity:* Ring, linear (Fabry-Pérot), hybrid.
- *Longitudinal-mode behavior*: Single-longitudinal mode, multi-longitudinal mode fiber lasers.
- *Number of emission lines*: Single, dual or multiwavelength fiber lasers.
- *Band of operation*: C-band, L-band, etc.

Those are the key aspects used to describe fiber lasers such as the presented in this Ph.D. work. However, there are many other remarkable aspects such as pulsed or continuous-wave (CW) operation, multi-mode or single-traverse mode operation but these aspects are not considered here since every laser presented is single-traverse mode and operates in CW regime. More information about fiber lasers can be found in Chapter 1.

Fiber lasers present significant advantages over other lasers such as robustness, compactness, reliability, all-fiber setup, flexible design and potential low cost. As a consequence, fiber lasers are interesting for many applications such as material processing, telecommunications, optical metrology, surgery and optical sensing [4].

It is evident the wide applicability of fiber lasers as light sources in optical sensing. However, instead of using fiber lasers as light sources to monitor sensors, this chapter is focused on fiber lasers as sensing systems themselves. I.e. the sensors are an active part of the fiber laser so the properties of the laser will be modified with the sensor variations. This approach presents some advantages such as the high compatibility with wavelength multiplexing techniques. In this manner, a single fiber laser can generate multiple emission lines, each one encoding the sensing information from a sensor (or even more). A second important advantage of fiber lasers employed in sensing applications is that the active operation of the sensor generally results in higher signal-to-noise ratio [5]. This is particularly evident in the case of using FBGs as wavelength selector in a laser. Even using a low reflectivity FBG, a laser line with an optical signal-to-noise ratio higher than 40 dB can be attained. In addition, the linewidth of the laser line can be orders of magnitude narrower than the bandwidth of the sensor itself.

There are several laser properties that can be used to encode the sensing information. The most common are the wavelength, amplitude, polarization, free-spectral range between longitudinal modes, polarization mode beating and wavelength spacing between emission lines among others. Thus, multiple sensing principles can be exploited in combination with fiber lasers. The most significant for this Ph.D. work are described in the next subsections. It should be noticed that the application of random distributed feedback fiber lasers for optical sensing is addressed in Chapter 4. Consequently they are not considered in this chapter.

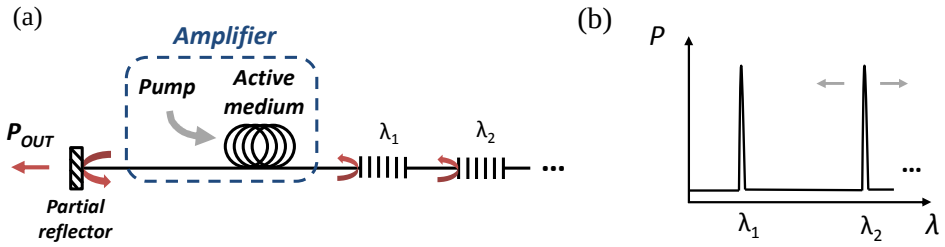

Fig. 3.1. Basic scheme of a linear fiber laser for FBG multiplexing and (b) its characteristic optical spectrum

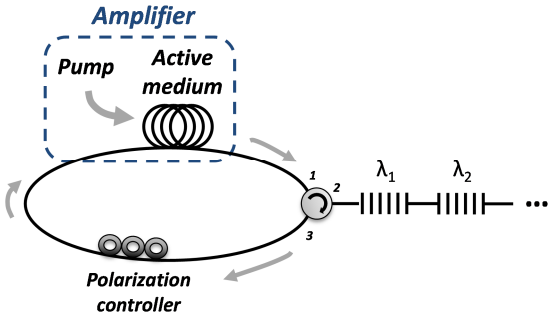

Fig. 3.2. Basic scheme of a ring fiber laser for FBG multiplexing.

3.1.1. Fiber lasers for fiber Bragg gratings interrogation

One of the key advantages of fiber lasers for optical sensing is the possibility of using fiber Bragg gratings simultaneously as transducers and as filtering element in the cavity. Many interrogation techniques use a broadband source with a low power (under 100 μW), to monitor the wavelength shift of the fiber Bragg gratings. However, output power higher than 1 mW can be attained using a FBG in the laser cavity, with the consequent benefit in the signal-to-noise ratio [6].

The most basic implementation of a fiber laser for temperature or strain measuring can be seen in Fig. 3.1(a). It consists of a linear cavity with a reflector placed at one end of the cavity and FBGs at the other. The amplification process takes place inside the cavity; being in the most basic scheme given by a type of rare-earth doped fiber amplification. Therefore, the emission lines are selected by the FBGs [Fig. 3.1(b)], reflecting the changes in temperature and strain suffered by the sensors. Due to the wavelength selectivity of FBGs, they are very well suited for wavelength-division multiplexing as stated in Chapter 1. The most straightforward FBG multiplexing technique is based on including multiple sensors located is series at different spectral bands.

Some of the different topologies presented in the Section 4 of Chapter 1 can be adapted for including FBGs and consequently operate as sensor devices. For example, ring cavities can be used in the same manner as linear, just by including an optical circulator (or even a coupler) as shown in Fig. 3.2 for wavelength division sensor multiplexing.

Regarding the detection method, the previous examples require an optical spectrum analyzer but simpler devices can be utilized. Additionally, simultaneous lasing of multiple lines can be limited in multi-wavelength architectures by the available pump power or by adverse effects

such as gain competition. To overcome this restraint, a tunable filter can be inserted into the cavity so it performs a wavelength shift as depicted in Fig 3.3 [7]. If the bandwidth of the filter is narrower than the wavelength distance between sensors, one FBG can be selected at a time [8]. As a consequence, only one laser line emits so there is not gain competition or limitation by the pump power. Furthermore, if the wavelength of the tunable laser is known, a simple power detector can be employed to reconstruct the optical spectrum, considerably reducing the cost of the system.

Another fiber laser that can be exploited for interrogating FBGs is the mode locked type. The principle of operation of this fiber laser is based on generating a fixed phase between the longitudinal modes of the laser. The interference between modes causes the generation of a train of pulses, being this effect known as *phase-locked* or *mode-locked*. There are many methods to mode-lock a fiber laser. In [9], a modulator is inserted into the cavity as depicted in Fig. 3.4. When the frequency of the modulation matches with a multiple of the cavity mode spacing, a train of pulses is generated. Since the longitudinal mode spacing is proportional to the length of the cavity, two FBGs can be identified by their different lock frequencies. As a result, when the frequency of one of those gratings is selected it will lase, while the other cavity will suffer higher losses (not lasing if the pump power is set close to the threshold). A more advanced setup is proposed in [10] where a tunable filter is inserted in the cavity, so each FBG can be identified by its locking frequency and by its wavelength, achieving hybrid TDM/WDM multiplexing.

Those are the most basic schemes to interrogate FBGs using fiber lasers but numerous approaches have been published up to date to monitor different classes of FBGs and using multiple topologies, detection systems, multiplexing techniques, bands of operation, amplification, etc. In this chapter, four fiber lasers are designed in combination with fiber Bragg gratings for varied sensing applications: striving for remote long-range operation, single-longitudinal mode operation or multi-parameter monitoring.

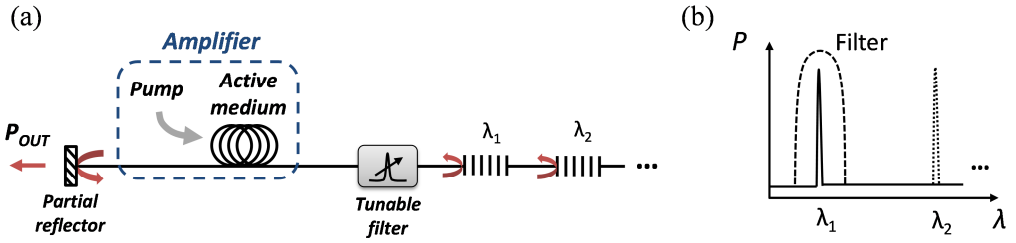

Fig. 3.3. Scheme of a linear fiber laser for FBG multiplexing using a tunable filter to select the emission line and (b) characteristic optical spectrum when the tunable filter is set in λ_1.

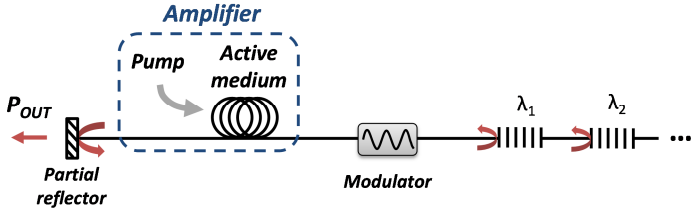

Fig. 3.4. Basic scheme of a linear fiber laser for FBG multiplexing using mode-locking [7].

3.1.2. Fiber lasers for interferometers/resonators interrogation

It is evident that the resonant properties of the laser, like longitudinal mode spacing, will change if the cavity length is modified. This effect can be exploited for measuring displacements/axial strain. Besides using the properties of the laser resonator as transducers, compound cavities can be formed to select the wavelength operation like in [11]. In that work, a ring resonator is included in the laser cavity to generate multiple laser lines which total power varies with a micro-bending sensor placed inside the ring. The results using a laser setup are compared with the obtained employing a passive interrogation, showing a stability increase from 12 to 0.1 dB.

Combining interferometers with fiber lasers is of special interest for monitoring PCF-based sensors. For example, HiBi fiber loop mirrors (FLM) are frequently used in the cavity as a reflectors in order to select the wavelength of operation of multi-wavelength lasers. If the HiBi fiber is employed as micro-bending sensor, the total power of the multi-wavelength laser will be modified [12]. Additionally, the wavelength shift of each of the laser emission reflects the physical changes in the HiBi fiber section (such as strain or temperature). Other interferometers can be equivalently employed as in [13], where a Fabry-Pérot cavity based sensor using a section of microstructured suspended core fiber is used as temperature sensor. However, the interrogation technique is this time based on the relationship between the power of the emission lines calculated by means of a quadrature phase-shift method. A simpler manner to monitor interferometric sensors placed inside a laser cavity is presented in [14]. In this case the wavelength selection is achieved by a FBG, with different wavelength for each interferometer (up to six were interrogated). Thus, each interferometer is employed to modulate the amplitude of its corresponding laser line.

As mentioned in Chapter 2, fiber optic gyroscopes based on Sagnac interferometers are one of the most successful fiber optic sensors up to date. This field of application has been object of intensive investigation the last decades, creating numerous solutions that also include fiber optic lasers. Some of these approaches include Brillouin ring fiber lasers [15], mode-locked fiber optic gyroscopes [16] or fiber lasers that combine a Sagnac with a Fabry-Pérot interferometer [17].

3.1.3. Fiber lasers for remote sensing applications

Fiber optic sensors are a dominant technology for ultra-long remote measurements, achieving interrogation distances as far as 253 km [18]. Fiber lasers are a critical part of those schemes, serving in some of them only as light sources. However, in other systems, including the sensor as an active part of the laser itself present important advantages.

The basis of remote sensing is to interrogate sensors located tens or hundreds of kilometers away from the monitoring station. This is a key factor in some applications where the measurand is in a hostile environment. The main challenge of such methods is to reach the longest possible distance, overcoming limitations given not only by the fiber attenuation, but also by the Rayleigh scattering and non-linear effects such as Brillouin scattering broadening [19]. It is also of particular interest the multiplexing capability of the system, in order to reduce the potential cost of the network.

In this respect, it is considered remote operation the absence of energy supply at the sensor location. Moreover, active elements are only present at the monitoring station from which the distance to the sensor is considered.

Table 3.1 summarizes the most significant remote sensor schemes for distances over 75 km [20], presenting the maximum distance attained, the type of amplification employed, the number of sensors multiplexed and the influence of the sensor in the laser. In this manner, fiber sensors that are an active part of the laser itself are labeled as intrinsic while sensors monitored by an external laser source are considered extrinsic.

It is evident the importance of fiber laser in remote interrogation since every most of the schemes require a fiber laser to operate; additionally, most of the schemes are fiber lasers themselves. Four of the remote systems presented in Table 3.1 are contributions related to this Ph.D. work, being two of them included in this chapter [PAPER F], [PAPER G] while the third is presented in Chapter 4 [PAPER J].

REMOTE SENSOR SYSTEMS				
Distance	**Sensor type***	**Amplification type**	**Sensors multiplexed**	**REF**
253 km	Extrinsic	-	1	[18]
250 km	Extrinsic	Raman	4	[21]
230 km	Extrinsic	EDFA	1	[22]
200 km	Extrinsic	Raman	9	[PAPER J]
200 km	Intrinsic	Raman	11	[23]
200 km	Extrinsic	Raman	4	[21]
155 km	Intrinsic	Raman+EDFA+Brillouin	2	[PAPER G]
150 km	Intrinsic	Raman	3	[24]
120 km	Extrinsic	-	1	[25]
100 km	Intrinsic	Raman	4	[PAPER F]
100 km	Intrinsic	EDFA	4	[26]
100 km	Extrinsic	-	1	[27]
100 km	Intrinsic	Raman+Brillouin	4	[CONF 9]
100 km	Intrinsic	Raman+EDFA	1	[28]

Table 3.1. Summary of remote sensor systems (**Intrinsic* type refers to sensors that are active part of the laser itself while *extrinsic* refers to sensors interrogated by an external laser source).

3.2. [PAPER D] Simultaneous measurement of strain and temperature using a single emission line

In optical sensing, the fact that many sensors suffer crosstalk between temperature and axial strain measurements is an issue that has been subject to an intense research. This is the case of some of the most successful optical sensors such as photonic crystal fibers, systems based on Brillouin scattering as optical time-domain reflectometers (BOTDAs) or fiber Bragg gratings. A simple reading of one of those sensing systems is simultaneously affected by both temperature and strain. As a consequence, one cannot identify if a sensor change is induced by variations in temperature, axial strain or both. Regarding temperature monitoring an easy solution is to isolate the sensor from strain variations which is feasible in the case of point sensors. However, for axial strain monitoring, it is not straightforward to isolate sensors from temperature changes. Many solutions have been proposed to overcome this effect but only a few combine simultaneous measurements of strain and temperature with the advantages of a laser design.

The aim of this work was to design a fiber laser for simultaneous temperature and strain monitoring using a single laser emission. In this manner, the main contributions of the work are the following:

- *Independent strain and temperature sensing:* Independent temperature and strain measurements were attained by monitoring the wavelength and amplitude of a single laser emission. Two types of fiber Bragg gratings were used in the setup: a simple FBG selects the wavelength of the emission line and a long-period grating modulates its amplitude.
- *Fiber laser:* The setup is based on a linear cavity fiber laser with erbium doped fiber amplification. A narrow emission line with high stability and high signal-to-noise ratio (55 dB) is achieved.
- *Economic bandwidth usage:* The temperature and strain information of two fiber Bragg gratings was multiplexed in a single emission line (in the wavelength and amplitude). As a result, the system allows an economic usage of the optical spectrum, which is of special interest in wavelength-division multiplexing sensor networks.

PAPER D

Journal of Lightwave Technology ***33****(12), 2426 (2015)*

http://dx.doi.org/10.1109/JLT.2014.2374531

Simultaneous Measurement of Strain and Temperature Using a Single Emission Line

Daniel Leandro, Martin Ams, Manuel López-Amo, Tong Sun and Kenneth V. Grattan

3.3. [PAPER E] L-band multi-wavelength single-longitudinal mode fiber laser for sensing applications

Single-longitudinal mode fiber lasers for optical sensing are typically designed in the conventional-band (C-band: 1530-1565 nm) mainly due to the reduced cost of the equipment (greatly developed by the telecommunication industry), lower loss of the optical fiber and frequency coincidence with the erbium-doped fiber amplification. The operating band of the laser is not a decisive factor in the development of many sensing setups. However, in order to improve the multiplexing capability of laser-based systems using wavelength-division multiplexing, broadening the band of operation is especially interesting. Additionally, in some sensing applications, like in direct absorption spectroscopy, the wavelength of the laser is critical but also the stability and the linewidth of the emission line. In the case of some gases, their absorption lines are located at higher wavelengths than the included in the C-band, which is known as the long-wavelength band (L-band).

Taking all this into account, the main objective in this work was to design a fiber laser in the L-band with a narrow line-width (in single-longitudinal mode operation) for multi-wavelength operation, taking also into account the stability of the system and the wavelength tunability. As a result, the main findings of the work are:

- *L-band operation:* The device was designed to operate in the long-wavelength band (1565 to 1625 nm), with emission lines located at 1587.7 nm, 1591.9 nm, 1599.9 nm and 1610.2 nm. The wavelength of operation can be tuned by temperature/strain changes on the FBGs used for the laser selection.
- *Four-wavelength single-longitudinal mode laser:* Simultaneous operation in single-longitudinal mode regime of up to four emission lines was achieved by using a hybrid topology and the adequate power equalization of each emission line.
- *Enhanced stability:* The measured power instability of the system was 1.2 dB, against the 2.1 dB measured for a conventional multi-longitudinal mode emission.
- *Temperature verification:* The appropriate behavior of the system was verified for temperature measurements. This effect also demonstrates the ability of the emission lines to be wavelength-tuned.

PAPER E

Journal of Lightwave Technology ***30****(8), 1173 (2012)*

http://dx.doi.org/10.1109/JLT.2011.2174138

L-Band Multiwavelength Single-Longitudinal Mode Fiber Laser for Sensing Applications

Rosa Ana Pérez, Angel Ullán, Daniel Leandro,
Montserrat Fernandez, María Ángeles Quintela, Alayn Loayssa,
Jose Miguel López Higuera and Manuel Lopez-Amo

3.4. [PAPER F] Experimental study of the SLM behavior and remote sensing applications of a multi-wavelength fiber laser topology based on DWDMs

As mentioned in Chapter 1, there are many different approaches used in the development of multi-wavelength fiber lasers. Some of them use periodic filters like fiber loop mirrors, Fabry-Pérot or Lyot-Sagnac filters, etc. Others are based on individual wavelength selectors like fiber Bragg gratins. In the case of sensing applications, the main purpose of multi-wavelength fiber lasers is to be used in wavelength-division multiplexing schemes. Accordingly, the FBG-based approach is generally the most extended since FBGs can be simultaneously used as wavelength-selectors and sensors. In addition, in schemes that do not use FBGs for sensing, the use of FBGs for the wavelength selection also offers more versatility because each emission line can be individually wavelength-tuned (which is not possible using periodic filters). As it has been shown in previous works, not only regular fiber Bragg gratings (which usually work in reflection) are used in the sensing schemes, but also long-period or phase-shifted fiber Bragg gratings, which usually operate in transmission.

In this manner, efficient multiplexing of fiber Bragg gratings in a single scheme is an important aspect of the laser's design. Depending on the filter characteristics and the aim of the structure different approaches are used, being the most straightforward the serial and the parallel configurations. However, serial multiplexing filters increases the length of the cavity which is crucial in single-longitudinal mode lasers. Additionally, it does not generally allow the independent and efficient attenuation control of each emission line. On the other hand, parallel multiplexing allows the independent loss control but highly increase the loss of the cavity if optical couplers are used. In this regard, the main motivation of this work was to present wavelength-division demultiplexers and multiplexers (DMUX/MUX) as versatile elements in the laser design and explore their advantages for different laser schemes. The main contributions of this work are:

- *DMUX/MUX versatility:* They allow the independent attenuation control of each channel independently without excessively increasing the loss in the laser cavity. To show their applicability, two antagonistic laser schemes were validated: One using EDF amplification and striving for narrow emission lines and a second based on Raman amplification for remote sensing applications.
- *Single-longitudinal mode operation:* The SLM operation of four emission lines was attained by using phase-shifted FBGs as filtering elements in combination with regular FBGs. Line-widths as narrow as 2.2 KHz were measured.
- *Remote sensing applicability:* A second version of the topology was verified for remote long-range measurements. Four emission lines were generated and validated for temperature monitoring using FBGs sensors located as far as 100 km. This system offers two main advantages over other long-range sensing setups:
    - Higher versatility in the position of the sensors along the cavity (each emission line can equalized from the monitoring station to achieve similar power levels).
    - The sensing information of the sensors can be retrieved simultaneously, instead of using tunable filters to interrogate one sensor at a time.

PAPER F

Applied Physics B ***118****(3), 497 (2015)*

http://dx.doi.org/10.1007/s00340-015-6020-5

Experimental Study of the SLM Behavior and Remote Sensing Applications of a Multi-wavelength Fiber Laser Topology Based on DWDMs

Daniel Leandro, Rosa Ana Pérez, Ion Iturri
and Manuel López-Amo

3.5. [PAPER G] Remote (155 km) fiber Bragg grating interrogation technique combining Raman, Brillouin, and erbium gain in a fiber laser

The capability of fiber optic devices for remote long-range interrogation is far superior to other technologies due to the low loss of optical fiber. As described in Section 3.1, the concept remote refers to the absence of energy supply with exception to the monitoring station. The maximum range of the network is a crucial aspect, but also the multiplexing capability has to be considered. Several works have been reported striving for ultra-long range sensor monitoring by means of different approaches. Some solutions consist of fiber lasers in which FBGs are used as sensors and wavelength-selecting devices. However, in such long cavities the feedback provided by the amplified Rayleigh scattering can act as a distributed mirror. As a result, lasing might initiate without the FBG contribution. A solution is using an external laser source to perform a wavelength sweep and interrogate the sensors but conventional narrow fiber lasers generate stimulated Brillouin scattering that degenerate the probe wave.

Considering these aspects, the main motivation of this work was to design a fiber laser for remote long-range monitoring of FBGs avoiding limitations imposed by Rayleigh and Brillouin scattering. In this manner, the commonly undesired stimulated Brillouin scattering was employed as gain medium for the laser generation. The contributions of this work can be summarized as follows:

- *Long-range:* Two fiber Bragg gratings were interrogated 155 km away from the monitoring station. That was the longest distance achieved for a multiplexing system at that time.
- *Laser:* The pump power is adjusted so the Brillouin-induced Stokes wave is just under the lasing threshold. When the tunable laser reaches the FBG, the laser emission is initiated due to the Raman, EDF and Brillouin amplification.
- *Improved OSNR:* Heterodyne detection of the generated laser with the pump laser is performed. Consequently, the power increase of the laser line is translated in a power increment in the heterodyne signal located at the Brillouin frequency.
- *Pump economy:* After the first 55 km, the Raman amplification is negligible. Nevertheless, the remaining pump is able to induce strong amplification in a section of erbium doped fiber, limiting the total required pump to 0.6 W.

PAPER G

IEEE Photonics Technology Letters ***23****(10), 621(2011)*

Remote (155 km) Fiber Bragg Grating Interrogation Technique Combining Raman, Brillouin, and Erbium Gain in a Fiber Laser

http://dx.doi.org/10.1109/LPT.2011.2119298

Daniel Leandro, Angel Ullán, Alayn Loayssa,
Jose Miguel López Higuera and Manuel López-Amo

3.6. References

[1] Bellemare, A. (2003). Continuous-wave silica-based erbium-doped fibre lasers. *Progress in Quantum Electronics*, *27*(4), 211-266.

[2] Sun, J., & Huang, L. (2007). Single-longitudinal-mode fiber ring laser using internal lasing injection and self-injection feedback. *Optical Engineering*, *46*(7), 074201-074201.

[3] Pan, S., & Yao, J. (2009). A wavelength-switchable single-longitudinal-mode dual-wavelength erbium-doped fiber laser for switchable microwave generation. *Optics express*, *17*(7), 5414-5419.

[4] Paschotta, R. (2008). *Field Guide to Lasers* (Vol. 12). SPIE press..

[5] Cranch, G. A. (2014). 15. Fiber-Optic Sensor Multiplexing Principles. In *Handbook of Optical Sensors*, 377.

[6] Langford. (1998). Optical fiber lasers. In *Optical Fiber Sensor Technology* (pp. 37-98). Springer US.

[7] Kim, B. Y. (1998). Fiber lasers in optical sensors. In *Optical Fiber Sensor Technology* (pp. 99-115). Springer US.

[8] Kersey, A. D., & Morey, W. W. (1993). Multi-element Bragg-grating based fibre-laser strain sensor. *Electronics Letters*, *29*(11), 964-966

[9] Kersey, A. D., & Morey, W. W. (1993). Multiplexed Bragg grating fibre-laser strain sensor system with mode-locked interrogation. *Electronics Letters*, *29*(1), 112.

[10] Fernandez-Vallejo, M., Ardanaz, D., & López-Amo, M. (2015). Optimization of the Available Spectrum of a WDM Sensors Network Using a Mode-Locked Laser. *Journal of Lightwave Technology*, *33*(22), 4627-4631.

[11] Rota-Rodrigo, S., González-Herráez, M., & López-Amo, M. (2015). Compound Lasing Fiber Optic Ring Resonators for Sensor Sensitivity Enhancement. *Journal of Lightwave Technology*, *33*(12), 2690-2696.

[12] Pinto, A. M. R., Bravo, M., Fernandez-Vallejo, M., Lopez-Amo, M., Kobelke, J., & Schuster, K. (2011). Suspended-core fiber Sagnac combined dual-random mirror Raman fiber laser. *Optics express*, *19*(12), 11906-11915.

[13] Pinto, A. M. R., Lopez-Amo, M., Kobelke, J., & Schuster, K. (2012). Temperature fiber laser sensor based on a hybrid cavity and a random mirror. *Journal of Lightwave Technology*, *30*(8), 1168-1172.

[14] Bravo, M., Fernández-Vallejo, M., Echapare, M., López-Amo, M., Kobelke, J., & Schuster, K. (2013). Multiplexing of six micro-displacement suspended-core Sagnac interferometer sensors with a Raman-Erbium fiber laser. *Optics express*, *21*(3), 2971-2977.

[15] Zarinetchi, F., Smith, S. P., & Ezekiel, S. (1991). Stimulated Brillouin fiber-optic laser gyroscope. *Optics letters*, *16*(4), 229-231.

[16] Jeon, M. Y., Jeong, H. J., & Kim, B. Y. (1993). Mode-locked fiber laser gyroscope. *Optics letters*, *18*(4), 320-322.

[17] Kim, H. S., & Kim, B. Y. (1996, May). New fiber laser interferometer for rotation sensing. In *Optical Fiber Sensors* (p. Tu34). Optical Society of America.

[18] Bravo, M., Baptista, J. M., Santos, J. L., Lopez-Amo, M., & Frazão, O. (2011). Ultralong 250 km remote sensor system based on a fiber loop mirror interrogated by an optical time-domain reflectometer. *Optics letters*, *36*(20), 4059-4061.

[19] Jenkins, R. B., Sova, R. M., & Joseph, R. I. (2007). Steady-state noise analysis of spontaneous and stimulated Brillouin scattering in optical fibers. *Journal of lightwave technology*, *25*(3), 763-770.

[20] Rota Rodrigo, S. (2015). *Development of advanced structures for optical fiber lasers and sensors*. (Doctoral dissertation, Universidad Publica de Navarra).

[21] Fernandez-Vallejo, M., Rota-Rodrigo, S., & Lopez-Amo, M. (2011). Remote (250 km) fiber Bragg grating multiplexing system. *Sensors*, *11*(9), 8711-8720.

[22] Saitoh, T., Nakamura, K., Takahashi, Y., Iida, H., Iki, Y., & Miyagi, K. (2008, April). Ultra-long-distance (230 km) FBG sensor system. In *19th International Conference on Optical Fibre Sensors* (pp. 70046C-70046C). International Society for Optics and Photonics.

[23] Fernandez-Vallejo, M., Bravo, M., & Lopez-Amo, M. (2013). Ultra-long laser systems for remote fiber Bragg gratings arrays interrogation. *Photonics Technology Letters, IEEE*, *25*(14), 1362-1364.

[24] Hu, J., Chen, Z., & Yu, C. (2012). 150-km long distance FBG temperature and vibration sensor system based on stimulated Raman amplification. *Journal of Lightwave Technology*, *30*(8), 1237-1243.

[25] Saitoh, T., Nakamura, K., Takahashi, Y., Iida, H., Iki, Y., & Miyagi, K. (2007). Ultra-long-distance fiber Bragg grating sensor system. *IEEE Photonics Technology Letters*, *19*(17/20), 1616.

[26] Bravo, M., Candiani, A., Cucinotta, A., Selleri, S., Lopez-Amo, M., Kobelke, J., & Schuster, K. (2014). Remote PCF-based sensors multiplexing by using optical add–drop multiplexers. *Optics & Laser Technology*, *57*, 9-11.

[27] Yuan, J., Zhao, C. L., Ye, M., Zhang, Z., & Jin, S. (2013, December). Optical fiber sensor system for remote refractive index measurement based on Fresnel reflection using an OTDR. In *International Conference on Optical Instruments and Technology (OIT2013)* (pp. 904410-904410). International Society for Optics and Photonics.

[28] Hu, J., Chen, Z., Yang, X., Ng, J., & Yu, C. (2010). 100-km Long distance fiber bragg grating sensor system based on erbium-doped fiber and Raman amplification. *IEEE Photonics Technology Letters*, *19*(22), 1422-1424

Chapter 4

Investigation on random distributed feedback lasers for sensing applications

In this chapter, the concept of random distributed feedback fiber laser is presented and used in the design of new schemes for sensing applications. This is a relatively new type of fiber laser based on an open cavity which properties differ in many aspects from those of conventional fiber lasers. Initially, the theoretical concepts and basic properties of random fiber lasers are discussed, followed by three original research works on random fiber lasers, mainly focused on its applicability in optical sensing.

4.1. Introduction to random distributed feedback fiber lasers

4.1.1. Background

Light generation in a random active medium was firstly reported by Vladilen S. Letokhov in 1967 studying the scattering of particles with *negative absorption* in interstellar clouds [1]. Following this initial concept, the field of random lasers has been intensely investigated due to the particularities of random compared with conventional lasers. In classic lasers, the cavity defines the main properties of the laser, such as spectral and spatial modes, directionality, polarization, etc. However, in random lasers the cavity is defined in a different manner, and the generated light is characterized by the random scattering of photons in an active medium. Due to the random nature of the feedback used in the laser generation, the properties of random lasers might be radically different from other fiber lasers. As a result, the properties of the material used as random media finally define the performance of the random laser itself. Some examples of materials used in the design of random lasers are powders, plastics or polymers, granular structures, dye materials or porous glasses. However, defining the laser performance using these random scattering materials is in general challenging with some aspects that still need to be addressed. For instance, due to the randomness of the reflectors, some aspects should be improved such as the high lasing threshold, low directionality and the low signal-to-noise ratio, with spontaneous laser oscillations at different wavelengths. On the other hand, the properties of the random lasers can be completely different from the given by conventional lasers, presenting for instance a longitudinal modeless behavior.

Understanding lasing modes in random scattering active media is an attractive and complex research challenge that is still under study. Light scattered in a random manner exhibits very complicated paths along the active medium. Nowadays, it is assumed that the output features of random lasers are given by the randomly embedded localized spatial modes that can coexist with non-localized extended modes [2]-[4]. One of the most interesting properties of random lasers compared with the conventional ones is that the spatial distribution of modes is a fingerprint of the laser's randomness. However, the understanding and description of the spatial mode distribution is a scientific challenge due to its complexity.

In this manner, a lot of studies on random lasers are in progress, exploiting different lasing properties, finding new applications and exploring multiple random materials. Some of the main types of random lasers are specifically based on direct bandgap semiconductors, using mainly different forms of ZnO, but also GaAs or ZnSe powders for instance [5]-[12]. Another main class of random laser utilizes dye and polymer active materials like in [13] where a solution that contains TiO_2 is used as strongly scattering medium. Other approaches can use different types of micro and nano-particles [14]-[16] or liquid crystals [17]. The scattering efficiency of sub-wavelength size metal particles can be improved due to the presence of surface plasmons. As a consequence, many random laser schemes have been proposed exploiting the plasmon-enhanced scattering mechanism [18]-[19]. Those can be considered three classes of random lasers but an important number of different random laser schemes working in different gain and scattering media have been published up to date. As a result, some good reviews have been also presented [4], [20]-[23]; focusing on different aspects of random lasers, such as systems with non-resonant and resonant feedback or random fiber lasers based on distributed feedback. This chapter develops new approaches for fiber optic sensing using this last type of lasers. Consequently, the features of random distributed feedback fiber lasers are presented in the next subsections, stressing in particular their differences with conventional lasers and their applicability in fiber optic sensing.

4.1.2. Principle of operation

In random distributed feedback fiber lasers (RDFLs) the random reflection in the scattering medium is given by the Rayleigh scattering effect. In this manner, the light propagating along the fiber scatters on random variations of the fiber core following the Rayleigh distribution. Those variations are imperfections created during the fabrication of the fiber and are random in strength and location but they are constant over time. As represented in Fig. 4.1, the light interacts elastically with the density fluctuations which result in most part of the light being transmitted without changes and a small part of the light scattered at different angles. About a 1/1000 part of the scattered light is coupled back into the fiber and starts counter-propagating (the 1/1000 ratio is given by the numerical aperture of the fiber) [24]. The scattered light not coupled into the fiber is radiated out of the waveguide. Even though the distributed reflection along the fiber due to the Rayleigh scattering is weak, the effect generated in ultra-long systems (above 270 km) is comparable with the feedback given by point reflectors in conventional lasers [25]. In any case, the gain needed to reach the lasing threshold of a RDFL is typically high so a strong amplification method is needed.

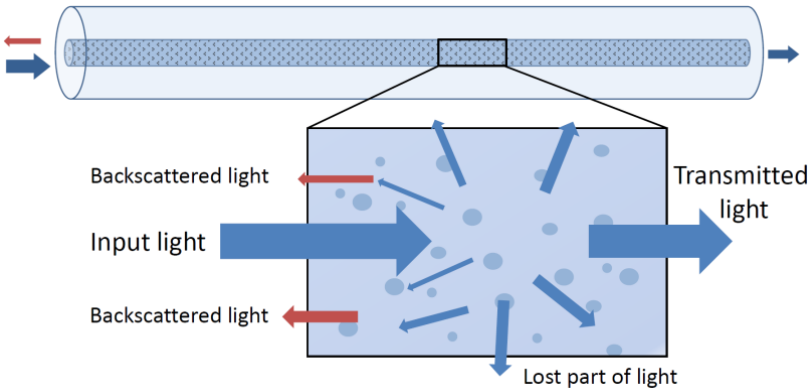

Fig. 4.1. Illustration of the Rayleigh scattering in an optical fiber.

Different random lasers based on Rayleigh scattering have been presented up to date but the most significant gain mechanism is the stimulated Raman scattering. As mentioned in Section 1.3.2, when pump light of frequency v enters a medium, it stimulates molecular vibrations in the material in an inelastic scattering process, losing part of its energy. As a consequence, a wave carrying the remaining energy is induced at a lower frequency (due to the lower energy) known as the Stokes wave. The shifted frequency is named Stokes shift, being this frequency drop defined by the vibration levels for the material. The rate amount of stimulated Raman scattering is defined by the Raman gain coefficient (which is frequency-dependent) and the power of the pump and Stokes waves. In contrast to other amplification systems, the gain in this case is distributed along tens of kilometers of fiber until the pump wave is depleted.

Therefore, a laser system can be formed using the Raman scattering as the amplifying process in a cavity where the feedback is provided by the distributed Rayleigh scattering along the fiber. As a result, the lasing threshold of such laser can be reached due to the high gain values obtained in the cavity. The first work that described the performance of a random distributed feedback fiber laser exploiting the weak scattering reflection given by the Rayleigh scattering was proposed by Turitsyn *et al*. in [26]. This initial scheme can be seen in Fig. 4.2, where the cavity is formed by two reels of standard single-mode fiber with a total length of 83 km and the fiber ends cleaved to avoid Fresnel reflections. Two pump lasers at 1455 nm provide stimulated Raman scattering amplification around 1550 nm. The measured lasing threshold is about 1.6 W of total pump power for a generated light emission with the shape of the classic Raman gain curve of amplified spontaneous emission overlapped with random spikes and dips, similar to classic random lasers. The emission line varies completely over 2 W of pump power, where the laser starts operating in continuous wave regime with suppressed power variations. In the optical spectrum two stable and narrow (< 1.5 nm) peaks appear at the wavelengths of the maximum Raman gain. The optical signal-to-noise ratio is above 35 dB and the radiation of the traverse mode showed a near-Gaussian profile. In this manner, it was demonstrated the stationary laser operation in an open cavity with a feedback provided by the Rayleigh scattering.

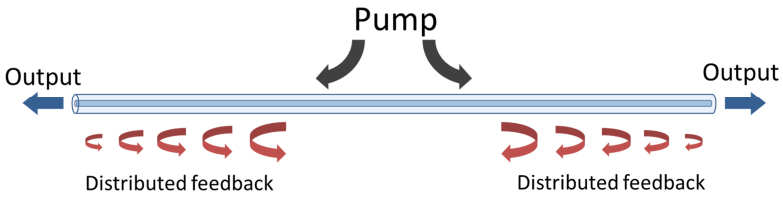

Fig. 4.2. Basic scheme of a random distributed feedback fiber laser.

The theoretical description of the system is based on the equation for the power evolution, taking into account the average Rayleigh backscattering [26]:

$$\frac{dP^{\pm}}{dz} = \mp\alpha P^{\pm} \pm g_R \left(P_P^{+} + P_P^{-}\right) P^{\pm} \pm \varepsilon P^{\mp} \tag{3.1}$$

Where $P^{\pm}(z)$ represent the generated Stokes waves and $P_P^{\pm}(z)$ are the pump waves, ε is the average Rayleigh backscattering coefficient, g_R is the Raman gain coefficient and $\pm$ corresponds to the forward and backward direction of propagation. The results of the simulations show that the laser power at 1550 nm increases due to the Raman gain until L_{RS} in which the gain provided by the pump wave do not overcome the loss level of the cavity (Fig. 4.3). The value of L_{RS} can be derived from:

$$L_{RS} = \frac{1}{\alpha_P} \ln \frac{g_R P_{th}}{\alpha_S} \tag{3.2}$$

Where α_S and α_P are the attenuation of the Stokes and pump wave, g_R represent the Raman gain coefficient and P_{th} is the lasing threshold power.

Equation (3.1) is a simplified description of the system but do not take into account effects that also have an impact on the laser like spontaneous emission, power depletion and backscattering of both pump and Stokes waves [26]. A more detailed modelling of RDFLs can be found in [4] and [23] where a set of differential equations have to be solved using specific boundary conditions depending on the laser scheme. For example, using the scheme shown in Fig. 4.2 the boundary conditions would be:

$$\begin{cases} P_s^{-}(L) = 0 \\ P_s^{-}(0) = P_s^{+}(0) \\ P_P^{+}(0) = P_0 \end{cases} \tag{3.3}$$

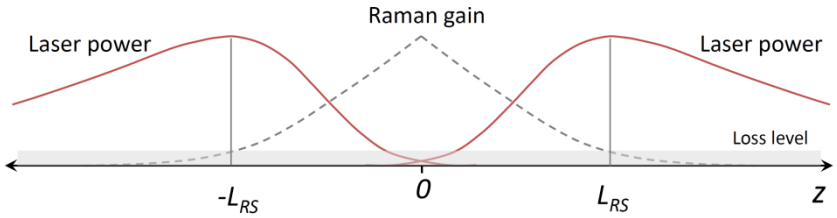

Fig. 4.3. Power distribution along the cavity in a RDFL.

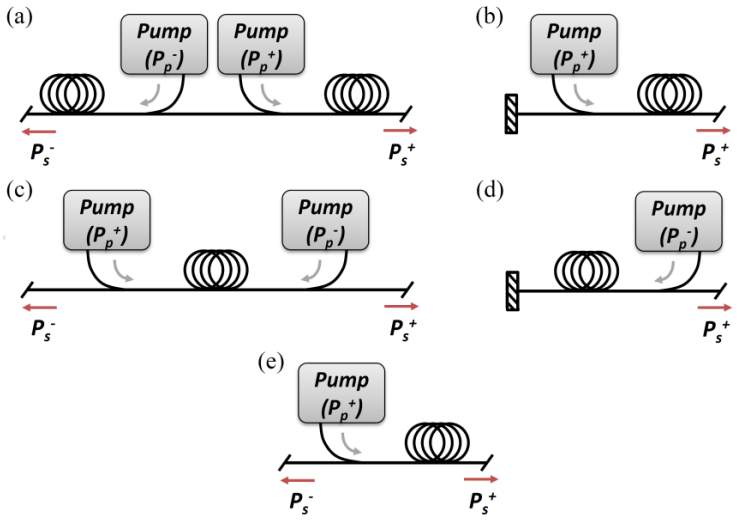

Fig. 4.4. RDFL configurations: (a) forward-pumped, (b) forward-pumped equivalent single-arm version, (c) backward-pumped, (d) backward-pumped equivalent single-arm version and (e) simple single-arm version.

In this case, there is not reflection at the end of the fiber so $P_s^-(L) = 0$, the pump power is injected at $z = 0$, and the Stokes waves in both directions are equal in $z = 0$. However, other laser designs can be also used, depending on the number of arms and the relative direction of the pump lasers to the output signal [27]. In this manner, ideally three main classes of laser configurations can be defined as depicted in Fig. 4.4: forward-pumped, backward-pumped and simple single-arm configuration. Forward and backward-pumped have also equivalent single-arm versions in which a mirror is located at $z = 0$, considerably simplifying the scheme (half of the fiber and only one pump are needed). In the works presented in this chapter, the single-arm versions are used due to equipment saving and the additional possibility of using the mirror at $z = 0$ for including filtering elements, modulators, etc. The last simple single arm scheme [Fig. 4.4 (e)] does not include a mirror, resulting in a higher pump power required in order to reach the lasing threshold given by the double scattering effect inside the cavity.

The lasing threshold of RDFLs can be described by the integral gain/loss balance equation in a roundtrip for a fiber with an effective distributed mirror given by the Rayleigh scattering. Thus, using a saddle-point approximation for an $L >> 2\,L_{RS}$ the lasing threshold for a single arm can be defined as [26]:

$$P_{th} = \frac{\alpha_S}{g_R}\left(1+\ln\left(\frac{g_R P_{th}}{\alpha_S}\right)\right)+\frac{\alpha_P}{2g_R}\ln\left(\frac{1}{\varepsilon}\sqrt{\frac{\alpha_S\alpha_P}{\pi}}\right) \qquad (3.4)$$

Where α_S and α_P represent the attenuation of the Stokes and pump wave respectively, ε is the average Rayleigh backscattering coefficient and g_R is the Raman gain coefficient. The result for a forward-pumped double-arm scheme with a Raman pump at 1455 nm ($g_R \approx 0.39$ km^{-1}W^{-1}) in a single mode fiber SMF28 with $\varepsilon = 4.5\times10^{-5}$ km^{-1} is 0.8 W per laser arm (1.6 W in total). In the same manner, 0.8 W of pump power are needed if the forward-pumped single arm version with a mirror is used. However, if the simple single-arm configuration without mirror is used, the lasing threshold is 1.75 W which is approximately two times the needed using a mirror. Detailed information about modelling RDFLs and comparatives between the different schemes can be found in [4], [26]-[27], being of especial interest the theoretical modelling included in the work published by Dmitry V. Churkin [23]. It should be noticed that the mirror's reflectivity in the single-arm scheme has an important effect in the lasing threshold (higher reflectivity

implies lower threshold), but also in other parameters of the laser such as the power distribution and output power [28].

4.1.3. Laser properties

As it has been mentioned previously, RDFLs present interesting properties and particularities, especially compared with conventional fiber lasers. Laser generation typically requires two key elements: an amplification medium and an optical cavity where the light is confined. In this manner, when the total gain overcomes the total loss of the cavity the lasing threshold is reached and the laser emission is initiated. The simplest case can be represented by a linear cavity with two mirrors like the depicted in Fig. 4.5(a). In this case only the longitudinal modes given by $\upsilon_k = k\,c/nL$ will propagate; where k is an integer number, L is the effective roundtrip of the cavity, c is the speed of light in vacuum and n is the refractive index of the medium. In this manner, in the spectral domain, the longitudinal modes that can propagate in the linear cavity exhibit an intermodal frequency given by $\Delta\upsilon = c/nL$ like displayed in Fig. 4.5(b). Consequently, if multiple longitudinal modes reach the lasing threshold in a linear cavity (the most common situation) the laser emission will present a multi-longitudinal mode emission like the depicted in Fig. 4.5(c).

However, if one of the cavity reflectors is replaced by a distributed mirror like in a random distributed feedback fiber laser [Fig. 4.6(a)], the cavity length will not be fixed and the light will be reflected along the fiber due to the Rayleigh scattering. In this case, the spectral response of the cavity is formed by the combination of numerous broad low-Q longitudinal modes in contrast to the narrow high-Q longitudinal modes of a conventional fiber laser (as in the linear-cavity based mentioned previously) [4]. Therefore, the cavity does not impose any spectral selectivity, being the feedback frequency-independent and non-resonant as represented in Fig. 4.6(b). When the lasing threshold is reached, a continuous collective mode formation located at the frequency of maximum gain can be seen in the optical spectrum [26] like schematically depicted in Fig. 4.6(c). However, typically this laser emission is several orders of magnitude broader than the generated for instance by a linear-cavity erbium doped fiber laser.

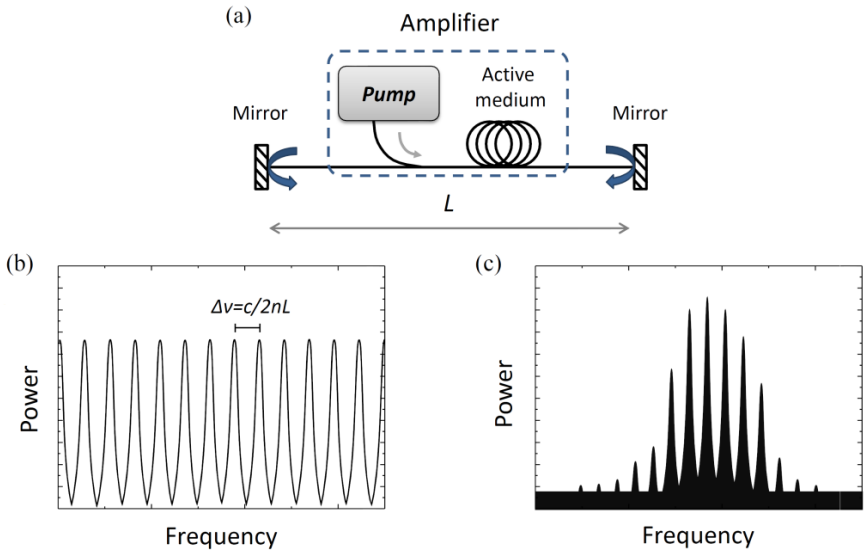

Fig. 4.5. (a) Schematic of a linear-cavity fiber laser. (b) Spectral response of a linear cavity and (b) Multi-longitudinal mode emission of a linear-cavity fiber laser.

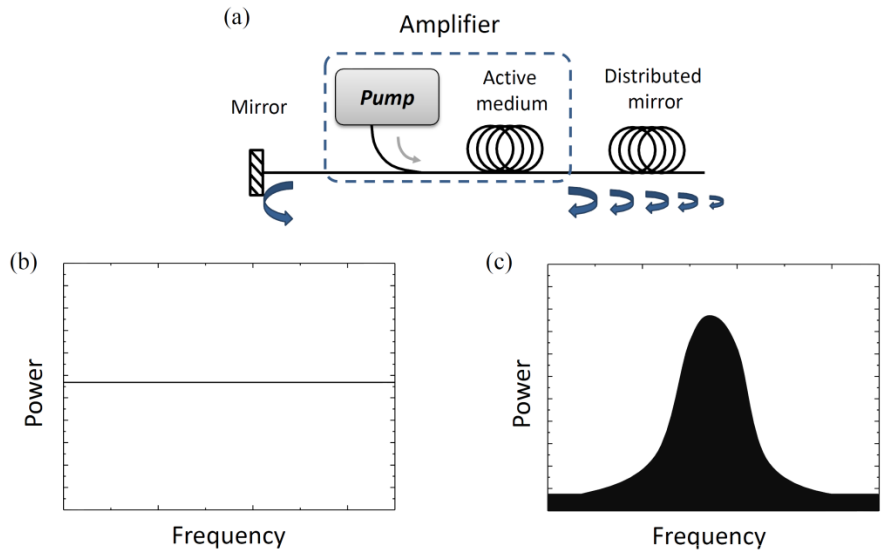

Fig. 4.6. (a) Schematic of an open-cavity fiber laser (RDFL). (b) Spectral longitudinal-mode distribution of an open-cavity and (c) *Modeless* emission of an open-cavity RDFL.

Besides the continuous spectrum of a RDFL, there are numerous implications of using an open cavity in the laser design. As it has been said, in contrast to conventional lasers, the spectral response of a RDFL cavity is constant. In this manner, it is feasible to internally modulate the laser without any frequency restriction typical in other fiber lasers [29].

Additionally, the modeless behavior of random distributed feedback lasers implies the *absence* of mode-hopping and mode competition. This effect is associated with the manifestation of self-organization that in a random feedback depends on the spatial-power distribution of the waves [30]. As a result, the stability attained by RDFLs in both frequency and power is higher than in most of conventional fiber lasers. This is especially noticeable in the case of multi-wavelength operation, where the lack of competition between lines makes RDFLs a promising solution for multi-wavelength devices. As a consequence, several works have been published up to date using random distributed cavities in combination with different spectral filters. For instance, a fiber loop mirror interferometer using PCF fiber is used in [31] to generate more than 150 emission lines spaced 0.09 nm in a wavelength range of 16 nm, with a power instability under 0.05 dB. All-fiber Lyot filters can be also utilized for the multi-wavelength operation as proposed in [32] where 10-20 emission lines are generated depending on the pump power. A classic solution for multi-wavelength emission based on Fiber Bragg gratings is presented in [30], using 22 FBGs to generate the same number of emission lines and reaching a total generation efficiency higher than the attained using a laser with conventional feedback. The outstanding performance of RDFLs in multi-wavelength operation is particularly evidenced in [33], where a fully-switchable multi-wavelength random fiber laser is presented. Multiple emission lines were attained (30 in the network demonstration) in a fully-switchable random laser combined with erbium-doped fiber amplification.

It is worth noticing that in practice, the type of fiber used for the distributed reflection has an important influence on the output properties of the laser. Dispersion-compensating fiber (DCF) like the used in [31] has a high Raman gain coefficient. Therefore, the output values attained using about 1.2 km of DCF fiber are comparable to the achieved with 50 km of standard SMF. Additionally, the DCF fiber allows a more compact design of the random laser. In this manner,

the type (or combination of types) of fiber used in the design of a RDFL is also an important factor to be taken into account. For instance, in [30] 11 km of SMF fiber where used together with 11 km of TrueWave (non-Zero dispersion) fiber.

The mentioned properties of RDFLs are the most significant with respect to conventional lasers. However, random distributed feedback lasers offer other capabilities like tunability, high power values inside the cavity, high efficiency and operation in spectral bands that cannot be reached by conventional lasers based in doped fibers. Two detailed reviews on random distributed feedback fiber lasers can be found in [4] and [23].

4.1.4. Random distributed feedback fiber laser in sensing applications

Due to the particular properties of RDFLs, one of the main fields of application is in optical sensing; nonetheless, up to date not many works have been published in this respect. The possibility of using tens of kilometers of fiber to generate the laser makes RDFLs a good candidate for remote long-range sensing devices. In [34] two fiber Bragg gratings (FBGs) were used as wavelength selector to monitor temperature in a 100 km system, taking advantage of both first and second Stokes waves. Also FBGs (up to eleven) were monitored using a single-arm 200 km-long random fiber laser [35]. Apart from FBGs, other sensing devices can be used as reflectors in a RDFL like optical interferometers. For instance, a Fabry-Pérot interferometer has been used for optical sensing in combination with random cavities in [36]. Also fiber loop mirror interferometers using a suspended-core fiber have been interrogated as displacement sensor [37]. Four different schemes using a double-pump 300 km backward RDFLs are presented in [38] to interrogate fiber loop mirrors or FBGs. Compound ring resonators can be used as well as filtering elements in a RDFL as demonstrated in [39] for displacement measurements, obtaining improved sensitivity (10 dB) and instability (0.04 dB). As commented previously, a fully switchable multi-wavelength laser is validated as sensor network by successfully monitoring 11 fiber Bragg gratings and 7 fiber loop mirror interferometers in [33]. On the other hand, an interesting approach to achieve temperature-independent strain measurements is presented in [40]. In this work, the four-wave mixing effect between two lines generated by FBGs is used to independently measure strain applied in one of the FBGs.

A few works have also combined RDFLs with distributed sensing. For example, a proof of concept of a Brillouin optical time-domain analysis (BOTDA) reflectometer that includes a random laser to increase the signal-to-noise (SNR) ratio was presented in [41]. A hybrid-pump scheme was validated in [42] to increase the SNR of the furthest point of the scheme, located 154.4 km away from the monitoring station. Almost an equivalent range was measured in [43] but with a single-pump scheme. On the other hand, other types of distributed sensing have made use of RDFLs. A phase-sensitive optical time-domain reflectometer (Φ-OTDR) was presented in [44], using a distributed cavity to increase the sensing range of the system to 175 km.

Summarizing, random distributed feedback fiber lasers have some aspects such as efficiency and performance that are comparable or that even exceed those of conventional fiber lasers. Some of the key properties of the generated laser emission in RDFLs include: a stationary continuous modeless spectrum that is free of mode competition, nonlinear power broadening, and an output beam with a Gaussian profile in the fundamental transverse mode. In the works presented in this chapter, the singularities of RDFLs are exploited with the aim of proposing new solutions for optical sensing.

4.2. [PAPER H] Narrow-linewidth multi-wavelength random distributed feedback laser

Due to the aforementioned particularities of random distributed feedback fiber lasers, especially when compared with their conventional counterparts, numerous studies have been conducted analyzing their properties. The modeless behavior, high stability (due to the lack of mode competition and mode-hopping), high peak power, open cavity, etc. allow the design of new fiber laser configurations that overcome limitations previously imposed by conventional linear or ring-cavity fiber lasers. However, in some other aspects, RDFLs present inferior performance with respect to other lasers such as erbium doped fiber lasers (EDFL) for instance. An important drawback is its broad bandwidth which typically surpasses one nanometer. This restricts the application of RDFLs in some systems, like in those based on dense wavelength division multiplexing. In addition, a wide linewidth imposes the use of filtering devices in the study of temporal and statistical properties of the laser. As a consequence, some authors have addressed this limitation, presenting narrow-linewidth RDFLs with a bandwidth as narrow as 50 pm.

The main motivation of this work was to continue the development of narrow-linewidth RDFLs and investigate its properties. In this manner, commercial fiber Bragg gratings have been used as optical filters in the development of a narrow-linewidth RDFL. Moreover, the multi-wavelength operation of the laser has been investigated due to the potential stability of RDFLs compared with other fiber lasers (EDFLs for example). As a result, the main findings of this publication are:

- *Narrowest RDFL:* The minimum linewidth achieved is 5.3 pm, which improves in almost ten times the narrowest RDFL reported up to date.
- *Laser analysis:* An investigation of the characteristics of the laser was also carried out. The influence of the loop mirror reflectivity in the linewidth, lasing threshold and peak power was investigated.
- *Multi-wavelength:* A multi-wavelength version of the setup was validated. Four emission lines were obtained with independent power control and wavelength tunability, in contrast with previous systems where the generated lines cannot be independently defined (in wavelength and power). High stability values were also attained.
- *New applications:* The study of the laser revealed that the wavelength stability of the system was given just by temperature changes in the phase-shifted FBG (even with temperature changes under 0.01°C). This led to the development of new high-resolution temperature, strain and transversal loading devices based on RDFLs [PAPER I], [CONF 1].

PAPER H

Journal of Lightwave Technology ***33****(17), 3591 (2015)*

http://dx.doi.org/10.1109/JLT.2015.2445377

Narrow-Linewidth Multi-Wavelength Random Distributed Feedback Laser

Daniel Leandro, Sergio Rota, Diego Ardanaz
and Manuel López-Amo

4.3. [PAPER I] High-resolution sensor system using a random distributed feedback fiber laser

Fiber Bragg gratings have been used extensively in optical sensing applications for years, being of particular interest in temperature and strain monitoring. There are different techniques to interrogate FBGs like using a broad spectrum source or a tunable laser to retrieve the reflected spectrum of the sensors, so the characteristic wavelength of each sensor can be tracked. Other schemes take advantage of fiber lasers to obtain higher signal-to-noise ratios, which is particularly important in long-range systems. However, the resolution of optical devices is limited, being typically around 10-5 pm in optical spectrum analyzers. In addition, systems based on fiber lasers have a maximum resolution restricted by the length of the cavity (related to the inter-longitudinal mode distance). Furthermore, even though conventional fiber lasers can have a few-kilohertz bandwidth (e.g. in the case of a single-longitudinal mode EDFL), effects like the mode hopping induce a frequency instability that degrade the sensing resolution of the system. Thus, most FBG-based sensor systems have a limited resolution around 0.1°C, typically. RDFLs do not have cavity-imposed limitations like other laser schemes and do not present mode hopping or mode competition. Therefore, despite having a wider linewidth than other lasers, the particular properties of RDFLs are promising for high-stability related applications, like high-resolution measurement.

The aim of this study was to investigate the capabilities of narrow RDFLs for high-resolution measurements in particular. Due to the narrow-linewidth of the laser (compared with other RDFL schemes) and high stability, the interrogation process was performed in the electrical domain, overcoming the maximum resolution given by the optical equipment. Initial results were presented as an oral contribution in the *24th Optical Fiber Sensors (OFS 24) conference* that took place in Curitiba (Brazil) in October 2015 [CONF 3]. Additionally, a modified version for transversal loading measurements will be presented in the *European Workshop on Optical Fibre Sensors* (EWOFS) that will take place in Limerick in June 2016 [CONF 1].The main findings of this work are:

- *High-resolution:* Temperature and strain resolutions under 0.01°C and 0.2 με respectively were attained in the electrical domain, reaching the resolution limit imposed by the equipment used as reference.
- *Heterodyne detection:* The use of a sub-gigahertz linewidth RDFL allowed the detection of the laser in the electrical domain where the equipment has higher accuracy.
- *Self-compensated strain monitoring:* Strain measurements were attained without indirect temperature-compensation techniques. The temperature influence on the strain measurements was directly compensated by beating two emission lines: one exposed to temperature and strain and other exposed just to temperature variations.
- *High stability:* The key factor of the system is the outstanding stability of the RDFL and its modeless behavior. Accurate results were obtained even using a relative broad emission line (compared with EDFL for instance) due to the far superior frequency stability of RDFLs.

PAPER I

Journal of Lightwave Technology

(In press: available online)

DOI: 10.1109/JLT.2016.2536650

http://dx.doi.org/10.1109/JLT.2016.2536650

High-Resolution Sensor System Using a Random Distributed Feedback Fiber Laser

Daniel Leandro, Verónica de Miguel and Manuel López-Amo

4.4. [PAPER J] Random DFB fiber laser for remote (200 km) sensor monitoring using hybrid WDM/TDM

Random distributed feedback fiber lasers have been intensely researched during the last five years but few works have focused on their applicability in optical sensing. However, there are many aspects where RDFLs outperform conventional laser schemes. One of these aspects is the possibility to be designed using a single-arm scheme with an open cavity. As a consequence, RDFLs can be internally modulated without frequency restrictions that are otherwise imposed by the cavity. In this manner, it is possible to use optical time domain reflectometry (OTDR) for measuring the reflected power along a fiber length. This can be of practical use in fiber fault detection and optical sensing for instance. A number of optical sensors can be measured using OTDR techniques, all inserted in a reflective configuration; however, wavelength-based sensors require the wavelength tuning of the light source.

Taking all these aspects into account the main motivation of this work was to explore the experimental performance of RDFLs in OTDR architectures for sensing applications. In this manner, the open cavity of the laser, together with the capability of being internally modulated and the high power inside the cavity make RDFLs a good candidate to ultra-long range sensing systems using reflectometry techniques. Preliminary results of this work were presented as an oral contribution in the *24th Optical Fiber Sensors (OFS 24) conference* that took place in Curitiba (Brazil) in October 2015 [CONF 4]. The main outcomes of this work are:

- *Long-range multiplexing scheme:* Several FBG sensors were monitored at different positions along the cavity in a 200 km-long sensor network.
- *Hybrid TDM-WDM:* The FBG sensors were identified by their wavelength and position in the network for a wavelength range of 10 nm and a spatial resolution of 45 m (maximum distance of 200 km).
- *Flexibility:* Compared with other ultra-long range sensor networks, this approach offers a higher flexibility in the position, wavelength and type of the sensors employed.
- *Laser cavity:* The main difference with other OTDR approaches is that part of the transmission channel is also the laser cavity. This implies that the maximum peak power is reached 50 km away from the heading which is an advantage for long-range monitoring. However, it also implies that variations in the cavity such as strong reflections can modify the behavior of the laser.
- *Further work*: This is the first time that a RDFL is adapted to be used as a time-domain reflectometer. Those initial results can be expanded by further analyzing different aspects of the system: multiplexing capability, noise effect, maximum range, spatial resolution, etc. In addition, variations of the setup can be used in the analysis and validation of RDFL's theory.

PAPER J

Journal of Lightwave Technology

(In press: available online)

DOI: 10.1109/JLT.2016.2547868

http://dx.doi.org/10.1109/JLT.2016.2547868

Random DFB Fiber Laser for Remote (200 km) Sensor Monitoring Using Hybrid WDM/TDM

Daniel Leandro, Verónica de Miguel, Rosa Ana Pérez,
Mikel Bravo and Manuel López-Amo

4.5. References

[1] Letokhov, V. S. (1967). Stimulated emission of an ensemble of scattering particles with negative absorption. *ZhETF Pisma Redaktsiiu*, *5*, 262.

[2] Cao, H. (2003). Lasing in random media. *Waves in random media*, *13*(3), R1-R39.

[3] Andreasen, J., Asatryan, A. A., Botten, L. C., Byrne, M. A., Cao, H., Ge, L., ... & Vanneste, C. (2011). Modes of random lasers. *Advances in Optics and Photonics*, *3*(1), 88-127.

[4] Turitsyn, S. K., Babin, S. A., Churkin, D. V., Vatnik, I. D., Nikulin, M., & Podivilov, E. V. (2014). Random distributed feedback fibre lasers. *Physics reports*, *542*(2), 133-193.

[5] Cao, H., Zhao, Y. G., Ho, S. T., Seelig, E. W., Wang, Q. H., & Chang, R. P. H. (1999). Random laser action in semiconductor powder. *Physical Review Letters*, *82*(11), 2278.

[6] Cao, H., Zhao, Y. G., Liu, X., Seelig, E. W., & Chang, R. P. H. (1999). Effect of external feedback on lasing in random media. *Applied physics letters*, *75*(9), 1213-1215.

[7] Thareja, R. K., & Mitra, A. (2000). Random laser action in ZnO. *Applied Physics B*, *71*(2), 181-184.

[8] Cao, H., Xu, J. Y., Zhang, D. Z., Chang, S. H., Ho, S. T., Seelig, E. W., ... & Chang, R. P. H. (2000). Spatial confinement of laser light in active random media. *Physical review letters*, *84*(24), 5584.

[9] Cao, H., Ling, Y., Xu, J. Y., Cao, C. Q., & Kumar, P. (2001). Photon statistics of random lasers with resonant feedback. *Physical Review Letters*, *86*(20), 4524.

[10] Noginov, M. A., Zhu, G., Fowlkes, I., & Bahoura, M. (2004). GaAs random laser. *Laser Physics Letters*, *1*(6), 291.

[11] Nakamura, T., Takahashi, T., & Adachi, S. (2010). Temperature dependence of GaAs random laser characteristics. *Physical Review B*, *81*(12), 125324.

[12] Takahashi, T., Nakamura, T., & Adachi, S. (2009). Blue-light-emitting ZnSe random laser. *Optics letters*, *34*(24), 3923-3925.

[13] Lawandy, N. M., Balachandran, R. M., Gomes, A. S. L., & Sauvain, E. (1994). Laser action in strongly scattering media. *Nature*, *368*(6470), 436-438.

[14] Sha, W. L., Liu, C. H., & Alfano, R. R. (1994). Spectral and temporal measurements of laser action of Rhodamine 640 dye in strongly scattering media. *Optics letters*, *19*(23), 1922-1924.

[15] Noginov, M. A., Caulfield, H. J., Noginova, N. E., & Venkateswarlu, P. (1995). Line narrowing in the dye solution with scattering centers. *Optics communications*, *118*(3), 430-437.

[16] Siddique, M., Berger, G. A., Kempe, M., Alfano, R. R., & Genack, A. Z. (1996). Time-resolved studies of stimulated emission from colloidal dye solutions. *Optics letters*, *21*(7), 450-452.

[17] Wiersma, D. S., & Cavalieri, S. (2001). Light emission: A temperature-tunable random laser. *Nature*, *414*(6865), 708-709.

[18] Dice, G. D., Mujumdar, S., & Elezzabi, A. Y. (2005). Plasmonically enhanced diffusive and subdiffusive metal nanoparticle-dye random laser. *Applied Physics Letters*, *86*(13), 131105.

[19] Popov, O., Zilbershtein, A., & Davidov, D. (2006). Random lasing from dye-gold nanoparticles in polymer films: enhanced gain at the surface-plasmon-resonance wavelength. *Applied physics letters*, *89*(19), 191116.

[20] Cao, H. (2005). Review on latest developments in random lasers with coherent feedback. *Journal of Physics A: Mathematical and General*, *38*(49), 10497.

[21] Wiersma, D. S. (2008). The physics and applications of random lasers. *Nature physics*, *4*(5), 359-367.

[22] Andreasen, J., Asatryan, A. A., Botten, L. C., Byrne, M. A., Cao, H., Ge, L., ... & Vanneste, C. (2011). Modes of random lasers. *Advances in Optics and Photonics*, *3*(1), 88-127.

[23] Churkin, D. V., Sugavanam, S., Vatnik, I. D., Wang, Z., Podivilov, E. V., Babin, S. A., ... & Turitsyn, S. K. (2015). Recent advances in fundamentals and applications of random fiber lasers. *Advances in Optics and Photonics*, *7*(3), 516-569.

[24] Nakazawa, M. (1983). Rayleigh backscattering theory for single-mode optical fibers. *JOSA*, *73*(9), 1175-1180.

[25] Turitsyn, S. K., Ania-Castañón, J. D., Babin, S. A., Karalekas, V., Harper, P., Churkin, D., ... & Mezentsev, V. K. (2009). 270-km ultralong Raman fiber laser. *Physical review letters*, *103*(13), 133901.

[26] Turitsyn, S. K., Babin, S. A., El-Taher, A. E., Harper, P., Churkin, D. V., Kablukov, S. I., ... & Podivilov, E. V. (2010). Random distributed feedback fibre laser. *Nature Photonics*, *4*(4), 231-235.

[27] Churkin, D. V., Babin, S. A., El-Taher, A. E., Harper, P., Kablukov, S. I., Karalekas, V., ... & Turitsyn, S. K. (2010). Raman fiber lasers with a random distributed feedback based on Rayleigh scattering. *Physical Review A*, *82*(3), 033828.
[28] Wu, H., Wang, Z., Fan, M., Zhang, L., Zhang, W., & Rao, Y. (2015). Role of the mirror's reflectivity in forward-pumped random fiber laser. *Optics Express*, *23*(2), 1421-1427.
[29] Bravo, M., Fernandez-Vallejo, M., & Lopez-Amo, M. (2013). Internal modulation of a random fiber laser. *Optics letters*, *38*(9), 1542-1544.
[30] El-Taher, A. E., Harper, P., Babin, S. A., Churkin, D. V., Podivilov, E. V., Ania-Castanon, J. D., & Turitsyn, S. K. (2011). Effect of Rayleigh-scattering distributed feedback on multiwavelength Raman fiber laser generation. *Optics letters*, *36*(2), 130-132.
[31] Pinto, A. M. R., Frazão, O., Santos, J. L., & Lopez-Amo, M. (2011). Multiwavelength Raman fiber lasers using Hi-Bi photonic crystal fiber loop mirrors combined with random cavities. *Journal of Lightwave Technology*, *29*(10), 1482-1488.
[32] Sugavanam, S., Yan, Z., Kamynin, V., Kurkov, A. S., Zhang, L., & Churkin, D. V. (2014). Multiwavelength generation in a random distributed feedback fiber laser using an all fiber Lyot filter. *Optics express*, *22*(3), 2839-2844.
[33] Bravo, M., de Miguel Soto, V., Cayetano, A. O., & Sainz, M. L. A. (2015). Fully Switchable Multi-Wavelength Fiber Lasers Based on Random Distributed Feedback for Sensors Interrogation. *Journal of Lightwave Technology*, *33*(12), 2598-2604.
[34] Wang, Z. N., Rao, Y. J., Wu, H., Li, P. Y., Jiang, Y., Jia, X. H., & Zhang, W. L. (2012). Long-distance fiber-optic point-sensing systems based on random fiber lasers. *Optics express*, *20*(16), 17695-17700.
[35] Fernandez-Vallejo, M., Bravo, M., & Lopez-Amo, M. (2013). Ultra-long laser systems for remote fiber Bragg gratings arrays interrogation. *Photonics Technology Letters, IEEE*, *25*(14), 1362-1364.
[36] Pinto, A. M. R., Lopez-Amo, M., Kobelke, J., & Schuster, K. (2012). Temperature fiber laser sensor based on a hybrid cavity and a random mirror. *Journal of Lightwave Technology*, *30*(8), 1168-1172.
[37] Pinto, A. M. R., Bravo, M., Fernandez-Vallejo, M., Lopez-Amo, M., Kobelke, J., & Schuster, K. (2011). Suspended-core fiber Sagnac combined dual-random mirror Raman fiber laser. *Optics express*, *19*(12), 11906-11915.
[38] Martins, H., Marques, M. B., & Frazão, O. (2011). 300 km-ultralong Raman fiber lasers using a distributed mirror for sensing applications. *Optics express*, *19*(19), 18149-18154.
[39] Rota-Rodrigo, S., González-Herráez, M., & Lopez-Amo, M. (2015, September). Fiber laser sensor system based on a random mirror and a compound ring resonator for displacement measurements. In *International Conference on Optical Fibre Sensors (OFS24)* (pp. 96344A-96344A). International Society for Optics and Photonics.
[40] Martins, H. F., Marques, M. B., & Frazão, O. (2011). Temperature-insensitive strain sensor based on four-wave mixing using Raman fiber Bragg grating laser sensor with cooperative Rayleigh scattering. *Applied Physics B*, *104*(4), 957-960.
[41] Jia, X. H., Rao, Y. J., Wang, Z. N., Zhang, W. L., Jiang, Y., Zhu, J. M., & Yang, Z. X. (2012, October). Towards fully distributed amplification and high-performance long-range distributed sensing based on random fiber laser. In *OFS2012 22nd International Conference on Optical Fiber Sensor* (pp. 842127-842127). International Society for Optics and Photonics.
[42] Jia, X. H., Rao, Y. J., Yuan, C. X., Li, J., Yan, X. D., Wang, Z. N., ... & Peng, F. (2013). Hybrid distributed Raman amplification combining random fiber laser based 2nd-order and low-noise LD based 1st-order pumping. *Optics express*, *21*(21), 24611-24619.
[43] Jia, X. H., Rao, Y. J., Wang, Z. N., Zhang, W. L., Yuan, C. X., Yan, X. D., ... & Peng, F. (2013). Distributed Raman amplification using ultra-long fiber laser with a ring cavity: characteristics and sensing application. *Optics express*, *21*(18), 21208-21217.
[44] Wang, Z. N., Zeng, J. J., Li, J., Fan, M. Q., Wu, H., Peng, F., ... & Rao, Y. J. (2014). Ultra-long phase-sensitive OTDR with hybrid distributed amplification. *Optics letters*, *39*(20), 5866-5869.

Conclusion and future research lines

Conclusions

Fiber optic technology has suffered a rapid evolution during the last decades due to its outstanding capabilities in telecommunication applications. Taking advantage of this scientific and technical advance, fiber optic sensors have emerged as a flexible solution to overcome some of the main limitations of conventional sensors. In this regard, many sensing approaches have been presented, using different transducer mechanisms, interrogation or multiplexing techniques, etc. Fiber optic sensor technology has been successfully exploited in some specific applications, but there are still some aspects to be improved. Possibly the most important weakness of optical sensors is the relatively high cost compared with well stablished technologies. Taking this into account, multiplexing techniques are of special interest due to the inherent cost reduction per sensing element.

In this framework, the results presented in this thesis propose new solutions based on fiber optic sensors, particularly focusing on their multiplexing capability. In accordance, three original contributions have been presented in chapter 2 related to interferometric sensor multiplexing:

- Initially, the multiplexing capability of HiBi fiber loop mirror (HiBi FLM) interferometric sensors have been analyzed and enhanced. A commercial optical fiber Bragg grating (FBG) sensor interrogator has been simply adapted to efficiently monitor interferometric sensor networks using the fast Fourier transform. This interrogation technique allows individually identifying the contribution of different sensing elements, also showing superior performance compared with conventional techniques. Additionally, two multiplexing architectures have been validated as crosstalk-free sensor networks both experimentally and theoretically.
- The understanding of the principles of multi-section fiber loop mirrors allowed the implementation of full all-polarization maintaining fiber loop mirror interferometers. In this manner, polarization-maintaining versions of their conventional SMF counterparts are validated. They present an outstanding stability and do not require polarization controllers, easing the measurement process. Simulations have been also performed, agreeing well with the experimental results. Additionally, high resolution temperature measurements (under 0.001 °C) were attained as a consequence of the better isolation of the all-PM system to externally-induced birefringence changes.
- Finally, the multi-section analysis of a three sensing-fiber FLM interferometer was performed. In this work, the study of three and four-section FLMs was carried out both theoretically and experimentally. Simulations were computed, matching with the experimental results and validating the three-section FLM as sensor multiplexing scheme. Additionally, the four-section theory was developed to design an all-PM version of the setup, which was confirmed as a crosstalk-free sensor network. It should also be mentioned that further increasing the number of sensing fibers would be experimentally challenging due to the high number of secondary interference contributions.

The third chapter of this Ph.D work focuses on the application of fiber lasers as sensing systems. Accordingly, the advantages of such devices have been exploited in four different setups:

- In the first work, an erbium doped-fiber laser is designed to multiplex the sensing information related to strain and temperature measurements in the amplitude and wavelength of a single laser line. This implies an economic bandwidth usage, which is especially important in wavelength-division multiplexing systems.
- A completely different approach is presented in the second work, which is focused in single-longitudinal mode operation in an alternative wavelength band. A multiwavelength L-band erbium-doped fiber laser is validated as sensor scheme using a hybrid topology with enhanced power stability.
- In the next contribution it is also achieved the single-longitudinal operation of four emission lines using a dense wavelength-division multiplexer (DWDM) for sensing applications. In addition, the flexibility of DWDMs for designing fiber lasers is shown by adapting the system to remote long-range applications (100 km). The main advantage of using DWDMs in the setup is that the spectral bands can be attenuated independently allowing the sensors to be located at any position of the fiber.
- In the same manner, the last work focuses on remote sensing applications. In this case the maximum distance attained is 155 km using a combination of Raman, Brillouin and erbium-doped fiber amplification. A tunable laser is inserted in the cavity so the Stokes wave generated by Brillouin scattering reaches the lasing threshold when the wavelength of the tunable laser meets the FBG sensors. Since the Stokes line is generated at a fixed frequency shift from the tunable laser, the detection system can take place in the electrical domain by monitoring the power detected at the Brillouin frequency.

Finally, in the fourth chapter of the manuscript, the particularities of random distributed feedback fiber lasers have been studied, emphasizing on their capabilities for sensing applications. In this manner, the main conclusions of this chapter can be summarized as follows:

- One of the main drawbacks of RDFL is their wide linewidth (a few nanometers) compared to other conventional fiber lasers such as erbium-doped fiber lasers. In an initial work, a random fiber laser with narrow linewidth (5.3 pm) was achieved, improving in almost ten times the narrowest RDFL reported up to date. A deep analysis of the setup was carried out, also adapting the system for multiwavelength operation.
- As a consequence of that initial work, it was observed a high applicability of the system for high resolution temperature and strain measurements. Due to the outstanding frequency and power stability of RDFLs and its wavelength dependence with the Bragg wavelength of a fiber grating, temperature and strain resolutions under 0.01°C and 0.2 με were attained respectively. As a result of the narrow linewidth of the laser, the detection could be done in the electrical domain were more accurate equipment is available. The inclusion of a second emission line allowed the design of a self-compensating setup for independent strain monitoring.
- A different approach for exploiting the properties of RDFL in sensing applications was also performed. In this last work, the capability of RDFL to be internally modulated was employed to achieve hybrid TDM/WDM sensor multiplexing in a 200 km-long sensor network. It is based on optical time domain reflectometry in a lasing cavity, identifying fiber Bragg grating sensors by their position in the fiber (with a spatial resolution of

45m in 200 km) and by their wavelength (in a range of 10 nm). This scheme offers much superior multiplexing flexibility than other long-range measurement systems in terms of position, wavelength and type of sensors employed.

Summarizing, different fiber optic sensing solutions have been presented, which can be divided in two main groups: based on FLM interferometers and based on fiber lasers. In the case of interferometric sensors, the work has been focused on the multiplexing capability and adaptation of the devices to all-polarization maintaining fiber. The second main group of contributions, based on fiber lasers, can be subsequently divided in two parts: in the first, single-longitudinal mode operating and remote long range laser schemes have been designed; in the second, the particular random distributed feedback fiber lasers have been studied, focusing on their capabilities for sensing applications.

Conclusiones

El campo de la fibra óptica ha sufrido una rápida evolución las últimas décadas debido a sus excepcionales cualidades para aplicaciones de telecomunicaciones. Aprovechando este avance científico y técnico, los sensores de fibra óptica suponen una solución flexible, capaz de superar algunas de las limitaciones sufridas por los sensores convencionales. En esta línea, han surgido múltiples planteamientos utilizando diferentes mecanismos de transducción, técnicas de multiplexación o interrogación, etc. La tecnología de sensores de fibra óptica ha sido utilizada con éxito en algunas aplicaciones específicas, pero todavía tiene margen de mejora. Una de las debilidades más importantes de los sensores de fibra óptica es posiblemente el coste, que es relativamente alto comparado con otras tecnologías ya establecidas. Teniendo esto en cuenta, las técnicas de multiplexación son especialmente interesantes debido a la inherente disminución de coste que suponen por cada elemento sensor.

En este contexto, los resultados que se presentan en esta tesis pretenden contribuir al campo de los sensores de fibra óptica, incidiendo en su capacidad de multiplexación. Teniendo esto en cuenta, se presentan en el capítulo 2 tres contribuciones originales relacionadas con la multiplexación de sensores interferométricos:

- Inicialmente, se ha estudiado y mejorado la capacidad de multiplexación de configuraciones en espejo (*fiber loop mirrors*) basados en fibra altamente birrefringente (HiBi FLMs por sus siglas en inglés). Se ha adaptado un interrogador comercial de redes de difracción Bragg ha sido adaptado de manera sencilla para interrogar sensores interferométricos por medio de la transformada rápida de Fourier. Esta técnica de interrogación permite identificar individualmente y en tiempo real las contribuciones de los diferentes elementos sensores, mostrando asimismo un mejor rendimiento que técnicas convencionales. Además, se han validado teórica y experimentalmente dos esquemas de multiplexación que interrogan redes de sensores que no tienen diafonía entre sí.
- El conocimiento del funcionamiento de los interferómetros FLM multi-secciones ha permitido el desarrollo de HiBi FLMs totalmente formados por fibra mantenedora de polarización. De esta manera, se han validado versiones totalmente mantenedoras de polarización de interferómetros clásicos, sin la necesidad de utilizar controladores de polarización. También se han realizado simulaciones que han coincidido con los resultados experimentales. Además, como consecuencia del mejor aislamiento del sistema ante

cambios de birrefringencia inducidos externamente, se han realizado medidas de temperatura de alta resolución (menor que 0.001 °C).

- Por último, se ha llevado a cabo el análisis de un interferómetro FLM formado por tres secciones de fibra sensoras. En este trabajo se ha efectuado el estudio teórico y experimental de interferómetros formados por tres y cuatro secciones de fibra altamente birrefringente. De nuevo se han realizado simulaciones que han coincidido con los resultados experimentales, validando el FLM de tres secciones como red de multiplexación de sensores. Adicionalmente, se ha formulado el modelo teórico para el interferómetro de cuatro secciones. Dicho modelo se ha utilizado para diseñar y validar como red de sensores sin diafonía una versión realizada con fibra mantenedora de polarización del primer esquema. Conviene mencionar que aumentar más el número de fibras sensoras multiplexadas sería complicado en la práctica debido al gran número de contribuciones secundarias en la interferencia.

El tercer capítulo de la tesis se centra en la utilización de láseres de fibra como elementos sensores. Las ventajas de estos dispositivos se han aprovechado en cuatro montajes diferentes de la siguiente manera:

- En el primer trabajo se ha diseñado un láser de fibra dopada con erbio para multiplexar la información de temperatura y deformación en la amplitud y en la longitud de onda de una única línea de emisión. Esto supone un uso económico del ancho de banda disponible, lo cual es especialmente importante en sistemas con multiplexación en longitud de onda.
- El segundo trabajo presenta un enfoque totalmente diferente, centrado en el funcionamiento del láser en régimen mono-frecuencia para su operación en una banda de trabajo alternativa. De esta manera, se ha validado un láser multi-longitud de onda de fibra dopada con erbio como esquema sensor, utilizando una topología híbrida que presenta una estabilidad mejorada en potencia.
- También en la siguiente contribución se ha logrado la operación como sensor de un láser mono-frecuencia de cuatro líneas de emisión gracias al uso de un multiplexor en longitud de onda (WDM por sus siglas en inglés). Además, se ha mostrado la flexibilidad de los WDMs para el diseño de láseres de fibra mediante la adaptación del sistema para monitorización remota de señores (100 km). La mayor ventaja de utilizar WDMs en el esquema es que las diferentes bandas espectrales pueden atenuarse independientemente. Esto permite colocar los sensores en cualquier posición de la fibra.
- De la misma manera, el último trabajo se centra en aplicaciones de interrogación remota. En este caso la distancia máxima conseguida es 155 km utilizando una combinación de amplificación Raman, Brillouin y de fibra dopada con erbio. Se inyecta en la cavidad un láser sintonizable generando una onda de Stokes debido a la dispersión Brillouin. Esta onda alcanza el umbral de emisión láser cuando el láser sintonizable alcanza la longitud de onda del sensor FBG. Ya que la onda de Stokes se genera con una diferencia en frecuencia fija respecto del láser sintonizable, la detección puede llevarse a cabo en el dominio eléctrico. De esta manera simplemente deben medirse las variaciones en potencia detectadas a la frecuencia Brillouin.

Por último, en el cuarto capítulo de la tesis se han estudiado las particularidades de los láseres de fibra *random* de cavidad distribuida (RDFL por sus siglas en inglés: *random distributed feedback fiber lasers*). Este análisis está especialmente enfocado hacia sus capacidades para aplicaciones en interrogación de sensores ópticos. Las principales conclusiones de este capítulo pueden resumirse de la siguiente manera:

- Una de las mayores desventajas de los RDFLs es su gran ancho de línea (varios nanómetros) comparado con otros láseres convencionales como los que utilizan fibra dopada con erbio. En un primer trabajo se ha diseñado un láser *random* de fibra con un ancho de línea estrecho (5.3 pm), mejorando en casi diez veces el láser *random* más fino conseguido hasta la fecha. Se ha estudiado en profundidad el esquema, incluyendo su adaptación para operación multi-línea.
- Como consecuencia de este trabajo inicial se observó la alta aplicabilidad del láser para medidas de temperatura y deformación de alta resolución. Gracias a la destacada estabilidad de este tipo de láseres tanto en potencia como en longitud de onda, se obtuvieron medidas de temperatura y tensión con resoluciones menores de 0.01°C y 0.2 με respectivamente. Debido a la reducida anchura de línea del láser, la medida del sistema sensor puede realizarse en el dominio eléctrico, donde el equipamiento es más preciso. La inclusión de una segunda línea de emisión permite el diseño de un esquema autocompensado para la medida independiente de la deformación.
- Otro enfoque diferente para utilizar las propiedades de RDFLs en aplicaciones de interrogación de señores se ha llevado a cabo en el último trabajo. En este, la capacidad del láser para ser modulado internamente se ha utilizado para lograr multiplexación híbrida en tiempo y longitud de onda en una red de sensores de 200 km. Se basa en reflectometría óptica temporal en una cavidad láser, identificándose sensores FBG por su posición en la fibra (con una resolución de 45 m en 200 km) y por su longitud de onda (en un rango de 10 nm). Este esquema ofrece una capacidad de multiplexación de sensores muy superior a otros sistemas de medida remotos para larga distancia en términos de posición, longitud de onda y tipo de sensores.

En resumen, se han presentado diferentes soluciones para interrogación óptica de sensores, que pueden dividirse en dos grandes grupos: basadas en interferómetros FLM y basadas en láseres de fibra. En el caso de sensores interferométricos, el trabajo se ha centrado en la capacidad de multiplexación de estos y su adaptación a esquemas totalmente formados por fibra mantenedora de polarización. El segundo grupo de contribuciones basadas en láseres de fibra puede dividirse a su vez en dos partes. En la primera se han diseñado láseres para operación mono-frecuencia e interrogación remota. En la segunda parte sin embargo se han analizado las particularidades de los láseres *random* de fibra, enfocando especialmente su posible uso en aplicaciones de interrogación de sensores.

Future research lines

The development of new fiber optic sensing solutions will undoubtedly continue the following years due to the continuous advance in the optical technology and the reduction of the equipment costs. Additionally, it is expected that fiber optic sensors increase their weight in industrial applications if the reliability and cost-competitiveness of the technology keeps growing. Moreover, besides reliability or cost reduction, effort should be made to improve the capabilities of optical sensing schemes, such as resolution, multiplexing capability, noise immunity, remote operation, etc.

Regarding the systems related to this work, new multiplexing architectures could be designed and analyzed using the FFT method. Moreover, full polarization-maintaining interferometers should be also investigated, since their sensing capabilities are expected to greatly overcome the classic SMF versions. In addition, the FFT technique is commonly used as a tool in some particular cases where the contributions of a compound interference have to be identified. However, even in simple interferometers, the results of this method are much superior to the obtained using other conventional approaches. Consequently, a study in depth of the capabilities and limitations of the FFT-based interrogation technique would be highly valuable.

Fiber laser-based sensing systems can also improve their applicability. Narrower and more stable single-longitudinal fiber lasers should be investigated not only for their application in sensing schemes, but also for microwave signal generation. In addition, longer remote sensor networks might be achieved by using assisted pumping setups and by avoiding spontaneous Raman noise at the detector.

Finally, completely new approaches should also be explored. This is the case of random distributed feedback lasers, which properties are being intensely investigated at this moment. Their particular properties compared to conventional lasers open an exciting new range of opportunities, not only in sensing applications. The design of time domain reflectometers based on RDFLs seems to be promising due to the high energy of the laser and its capability to be internally modulated. Additionally, ultra-narrow linewidth RDFLs would be highly desired in numerous applications due to their inherent power and frequency stability.

Appendix I: Author's contributions

International journals

[PAPER A] **Leandro, D.**, Bravo, M., Ortigosa, A., & Lopez-Amo, M. (2015). Real-time FFT analysis for interferometric sensors multiplexing. *Journal of Lightwave Technology*, *33*(2), 354-360.

[PAPER B] **Leandro, D.**, Bravo, M., & Lopez-Amo, M. (2015). High resolution polarization-independent high-birefringence fiber loop mirror sensor. *Optics express*, *23*(24), 30985-30990.

[PAPER C] **Leandro, D.**, Lopez-Aldaba, A., Bravo Acha, M., & Lopez-Amo, M. (2016). Monitoring Multiple Hi-Bi Sensing Fibers in a Single Fiber Loop Mirror. *Journal of Lightwave Technology*, (In press). doi: 10.1109/JLT.2016.2523880.

[PAPER D] **Leandro, D.**, Ams, M., López-Amo, M., Sun, T., & Grattan, K. T. (2015). Simultaneous Measurement of Strain and Temperature Using a Single Emission Line. *Journal of Lightwave Technology*, *33*(12), 2426-2431.

[PAPER E] Perez-Herrera, R. A., Ullan, A., **Leandro, D.**, Fernandez-Vallejo, M., Quintela, M. A., Loayssa, A., ... & Lopez-Amo, M. (2012). L-band multiwavelength single-longitudinal mode fiber laser for sensing applications. *Journal of Lightwave Technology*, *30*(8), 1173-1177.

[PAPER F] **Leandro, D.**, Perez-Herrera, R. A., Iturri, I., & Lopez-Amo, M. (2015). Experimental study of the SLM behavior and remote sensing applications of a multiwavelength fiber laser topology based on DWDMs. *Applied Physics B*, *118*(3), 497-503.

[PAPER G] **Leandro, D.**, Ullan, A., Loayssa, A., López-Higuera, J. M., & López-Amo, M. (2011). Remote (155 km) fiber bragg grating interrogation technique combining Raman, Brillouin, and erbium gain in a fiber laser. *Photonics Technology Letters, IEEE*, *23*(10), 621-623.

[PAPER H] **Leandro, D.**, Rota-Rodrigo, S., Ardanaz, D., & Lopez-Amo, M. (2015). Narrow-Linewidth Multi-Wavelength Random Distributed Feedback Laser. *Journal of Lightwave Technology*, *33*(17), 3591-3596.

[PAPER I] **Leandro, D.**, deMiguel-Soto, V., & López-Amo, M. (2016). High-resolution Sensor System Using a Random Distributed Feedback Fiber Laser. *Journal of Lightwave Technology*, (In press). doi: 10.1109/JLT.2016.2536650.

[PAPER J] **Leandro, D.**, deMiguel-Soto, V., Perez-Herrera, R.A., Bravo, M., & Lopez-Amo, M. (2016). Random DFB Fiber Laser for Remote (200 km) Sensor Monitoring Using Hybrid WDM/TDM. *Journal of Lightwave Technology* (In press). doi: 10.1109/JLT.2016.2547868

[JOUR 11] Diaz, S., **Leandro, D.**, & Lopez-Amo, M. (2015). Stable Multiwavelength Erbium Fiber Ring Laser With Optical Feedback for Remote Sensing. *Journal of Lightwave Technology*, *33*(12), 2439-2444.

[JOUR 12] Lopez-Amo, M., Fernandez-Vallejo, M., & **Leandro, D.** (2011). Bidirectional dual-wavelength Raman fiber ring laser. *Photonics Technology Letters, IEEE*, *23*(7), 399-401.

Conferences

International conferences

[CONF 1] DeMiguel-Soto, V., **Leandro, D.**, & López-Amo, M. (2016, June). High-resolution transversal load sensor using a random distributed feedback fiber laser. In *European Workshop on Optical Fibre Sensors (EWOFS16).* Accepted. PAPER NUMBER: 9916-30.

[CONF 2] **Leandro, D.**, Bravo, M., Ortigosa, A., & Lopez-Amo, M. (2015, September). Monitoring multiple interferometric sensors multiplexed in a single fiber loop mirror. In *International Conference on Optical Fibre Sensors (OFS24)* (pp. 963418-963418). International Society for Optics and Photonics.

[CONF 3] **Leandro, D.**, Ardanaz, D., & Lopez-Amo, M. (2015, September). High resolution fiber Bragg grating interrogation using a random distributed feedback fiber laser. In *International Conference on Optical Fibre Sensors (OFS24)* (pp. 96340O-96340O). International Society for Optics and Photonics.

[CONF 4] **Leandro, D.**, Perez-Herrera, R., Bravo, M., & Lopez-Amo, M. (2015, September). Time and wavelength division multiplexing scheme for ultra-long sensing based on a cavity-modulated random DFB fiber laser. In *International Conference on Optical Fibre Sensors (OFS24)* (pp. 963415-963415). International Society for Optics and Photonics.

[CONF 5] **Leandro, D.**, Ams, M., López-Amo, M., Sun, T., & Grattan, K. T. (2014, June). Simultaneous measurement of strain and temperature using a unique LPG-coupled fibre laser scheme. In *OFS2014 23rd International Conference on Optical Fiber Sensors* (pp. 9157AB-9157AB). International Society for Optics and Photonics.

[CONF 6] Perez-Herrera, R. A**., Leandro, D**., & Lopez-Amo, M. (2014, June). High sensitive micro-displacement intensity fiber sensor by using a multiwavelength erbium doped fiber ring laser based on optical add-drop multiplexers. In *OFS2014 23rd International Conference on Optical Fiber Sensors* (pp. 915762-915762). International Society for Optics and Photonics.

[CONF 7] Diaz, S., **Leandro, D.**, & Lopez-Amo, M. (2014, June). Multi-wavelength erbium fiber ring laser with optical feedback for temperature measurements. In *OFS2014 23rd International Conference on Optical Fiber Sensors* (pp. 91575Y-91575Y). International Society for Optics and Photonics.

[CONF 8] Perez-Herrera, R. A., **Leandro, D.**, Urquhart, P., Schlüter, M., & Lopez-Amo, M. (2012, October). Resilient optical fiber ladder network with OADMs to multiplex sensors: experimental validation of binary state connectivity analysis. In *OFS2012 22nd International Conference on Optical Fiber Sensor* (pp. 84218C-84218C). International Society for Optics and Photonics.

[CONF 9] Fernandez-Vallejo, M., **Leandro, D.**, Loayssa, A., & Lopez-Amo, M. (2011, May). Fiber Bragg Grating interrogation technique for remote sensing (100km) using a hybrid Brillouin-Raman fiber laser. In *21st International Conference on Optical Fibre Sensors (OFS21)* (pp. 77537I-77537I). International Society for Optics and Photonics.

[CONF 10] Perez-Herrera, R. A., Ullán, A., **Leandro, D.**, Fernández-Vallejo, M., Quintela, M. A., Loayssa, A., ... & Lopez-Amo, M. (2011, May). L-band multiwavelength erbium-doped fiber ring laser for sensing applications. In *21st International Conference on Optical Fibre Sensors (OFS21)* (pp. 77533C-77533C). International Society for Optics and Photonics.

[CONF 11] **Leandro, D.**, Perez-Herrera, R.A., Rota, S., & Lopez-Amo, M. (2013, July). Multi-wavelength fiber laser in single-longitudinal mode operation based on DWDMs for sensing applications. In *RIAO/OPTILAS 2013 VIII Iberoamerican Conference on Optics and XI Latinamerican meeting on Optics, Lasers and Applications.* (Invited talk).

National conferences

[CONF 12] **Leandro, D.**, Perez-Herrera, R.A., Bravo, M., & Lopez-Amo, M. (2015, July). Sistema para interrogación de sensores a larga distancia con multiplexación en tiempo y en longitud de onda basado en un láser DFB random. In *IX Reunión Española de Optoelectrónica, OPTOEL 2015*.

[CONF 13] Bravo, M., **Leandro, D.**, Ortigosa, A., & Lopez-Amo, M. (2015, July). Multiplexación de sensores interferométricos de fibra óptica mediante análisis FFT. In *IX Reunión Española de Optoelectrónica, OPTOEL 2015*.

[CONF 14] **Leandro, D.**, Perez-Herrera, R.A., Rota, S., & Lopez-Amo, M. (2013, July). Láser monomodo multilínea utilizando DWDMs para sensores de fibra óptica. In *VIII Reunión Española de Optoelectrónica, OPTOEL 2013*.

[CONF 15] Fernandez-Vallejo, M., **Leandro, D.**, Loayssa, A. & Lopez-Amo, M. (2011, July). Interrogación remota (100km) de sensores de fibra óptica mediante un láser de fibra híbrido Brillouin-Raman. In *VII Reunión Española de Optoelectrónica, OPTOEL 2011*.